Decision Support for Operational Plantation Forest Inventories through Auxiliary Information and Simulation

Patrick Corey Green

Dissertation submitted to the faculty of the Virginia Polytechnic Institute and State University in partial fulfillment of the requirements for the degree of

Doctor of Philosophy
In
Forest Resources and Environmental Conservation

Harold E. Burkhart
John W. Coulston
Philip J. Radtke
Valerie A. Thomas
Randolph H. Wynne

October 1, 2019
Blacksburg, Virginia

Keywords: Loblolly pine, UAS, Small area estimation, auxiliary data, projection

Copyright 2019, Patrick Corey Green

Decision Support for Operational Plantation Forest Inventories through Auxiliary Information and Simulation

Patrick Corey Green

ABSTRACT

Informed forest management requires accurate, up-to-date information. Ground-based forest inventory is commonly conducted to generate estimates of forest characteristics with a predetermined level of statistical confidence. As the importance of monitoring forest resources has increased, budgetary and logistical constraints often limit the resources needed for precise estimates. In this research, the incorporation of ancillary information in planted loblolly pine (*Pinus taeda* L.) forest inventory was investigated. Additionally, a simulation study using synthetic populations provided the basis for investigating the effects of plot and stand-level inventory aggregations on predictions and projections of future forest conditions.

Forest regeneration surveys are important for assessing conditions immediately after plantation establishment. An unmanned aircraft system was evaluated for its ability to capture imagery that could be used to automate seedling counting using two computer vision approaches. The imagery was found to be unreliable for consistent detection in the conditions evaluated. Following establishment, conditions are assessed throughout the lifespan of forest plantations. Using small area estimation (SAE) methods, the incorporation of light detection and ranging (lidar) and thinning status improved the precision of inventory estimates compared with ground data alone. Further investigation found that reduced density lidar point clouds and lower resolution elevation models could be used to generate estimates with similar increases in precision. Individual tree detection estimates of stand density were found to provide minimal improvements in estimation precision when incorporated into the SAE models.

Plot and stand level inventory aggregations were found to provide similar estimates of future conditions in simulated stands without high levels of spatial heterogeneity. Significant differences were noted when spatial heterogeneity was high.

Model form was found to have a more significant effect on the observed differences than plot size or thinning status.

The results of this research are of interest to forest managers who regularly conduct forest inventories and generate estimates of future stand conditions. The incorporation of auxiliary data in mid-rotation stands using SAE techniques improved estimate precision in most cases. Further, guidance on strategies for using this information for predicting future conditions is provided.

Decision Support for Operational Plantation Forest Inventories through Auxiliary Information and Simulation

Patrick Corey Green

GENERAL AUDIENCE ABSTRACT

Informed forest management requires accurate, up-to-date information. Ground-based sampling (inventory) is commonly used to generate estimates of forest characteristics such as total wood volume, stem density per unit area, heights, and regeneration survival. As the importance of assessing forest resources has increased, resources are often not available to conduct proper assessments. In this research, the incorporation of ancillary information in planted loblolly pine (*Pinus taeda* L.) forest inventory was investigated. Additionally, a simulation study investigated the effects of two forest inventory data aggregation methods on predictions and projections of future forest conditions.

Forest regeneration surveys are important for assessing conditions immediately after tree planting. An unmanned aircraft system was evaluated for its ability to capture imagery that could be used to automate seedling counting. The imagery was found to be unreliable for use in accurately detecting seedlings in the conditions evaluated. Following establishment, forest conditions are assessed at additional points in forest development. Using a class of statistical estimators known as small-area estimation, a combination of ground and light detection and ranging data generated more confident estimates of forest conditions. Further investigation found that more coarse ancillary information can be used with similar confidence in the conditions evaluated.

Forest inventory data are used to generate estimates of future conditions needed for management decisions. The final component of this research found that there are significant differences between two inventory data aggregation strategies when forest conditions are highly spatially variable.

The results of this research are of interest to forest managers who regularly assess forest resources with inventories and models. The incorporation of ancillary information has potential to enhance forest resource assessments. Further, managers have guidance on strategies for using this information for estimating future conditions.

Acknowledgements

There are so many people who have supported me throughout my studies at Virginia Tech. I want to first thank my wife, Lisa. She has supported me through good days and bad. Without her love and support, my doctoral studies wouldn't have been possible. My graduate advisor, Dr. Harold Burkhart is a mentor without peer. I cannot thank him enough for his patience and dedication to helping me learn and succeed. He provided me with opportunities and guidance that have enhanced my program in so many ways.

My parents, Christine Franklin and Dale Green inspired my love of learning from an early age. Thank you for everything over the years. I would not be here without you both. Additionally, thank you to my brother, Cody Green, for his love and support.

I would like to thank my graduate committee: John Coulston, Phil Radtke, Val Thomas, and Randy Wynne for their advice and guidance. You were all instrumental to my success. Additionally, I would like to thank Ralph Amateis for his sage advice and support. The Department of Forest Resources and Environmental Conservation, the Forest Management Research Cooperative, the Edna Bailey Sussman Fund, the Robert S. Burruss Fellowship, and the United States Forest Service are all gratefully acknowledged for their support throughout my time at Virginia Tech. The Virginia Department of Forestry is thanked for the invaluable assistance on so many aspects of this work.

A special thanks to Sheng-I Yang for his friendship and collaboration during our time at Virginia Tech together. Sheng-I is an amazing friend and inspired me to be better in so many ways. A tremendous thank you to John Peterson for his help in the field, often in less than ideal conditions. Additionally, thank you to Matthew Fields and Daniel Cross at the Conservation Management Institute for their assistance on the seedling survival study.

Finally, to my family, friends, and peers far and wide. I owe a special thanks to all of you.

Table of Contents

List of Figures

List of Tables

List of Supplemental Figures

Chapter 1 Introduction

Forest management requires accurate, reliable, up-to-date information for informed decisions. Forest resources are generally assessed using ground-based forest inventory and predictive models. Forest inventory with fixed or variable radius sample plots, has been traditionally used at certain points in stand development to collect information needed for planning, management decisions, and fiduciary reporting responsibilities. Inventory is rarely conducted annually and estimates of future conditions are often required. Growth and yield models are commonly used to predict future conditions and project current conditions to a future date (Burkhart et al. 2019). Southern pines account for approximately 16% of global commercial wood production. Of these species, loblolly pine is the most widely planted and intensively managed species (Zhao et al. 2016). In recent years, timberland ownership in the southeastern United States has undergone significant changes (Fox et al. 2007). The emergence of the timberland investment organization following the divestiture of timberlands by vertically integrated forest products companies have led to frequent land exchanges and increased fragmentation. A combination of rapid acquisitions and dispositions and fiduciary reporting requirements have strained the ability of managers to reliably assess their forest resources. Additionally, interest in plantation pine carbon cycles has increased. As productivity and markets change, the implications on carbon storage are being actively explored.

The need for reliable estimates of stand characteristics has inspired managers to seek alternate sources of information for use in resource assessments. In this research, the incorporation of auxiliary information in operational loblolly pine forest inventory was investigated at multiple points of stand development. It is common to first conduct a forest inventory soon after plantation establishment to assess survival and possible recruitment (Ezell 2011). The incorporation of unmanned aircraft system (UAS) imagery was investigated for its potential to be used for forest regeneration surveys. Following stand establishment, forest inventory is conducted around the time of canopy closure (9-12 years old), immediately prior to and following a first thinning (13-20), and around the time of additional thinning and final harvests. Using light detection and ranging (lidar)

and thinning status as auxiliary information, small area estimation (SAE) methods were investigated for their potential to improve the precision of total volume estimates. Further, the effects of SAE estimates using auxiliary data with lower resolution were investigated.

Forest inventory is expensive and time consuming making yearly inventory impractical. Additionally, future estimates of stand characteristics are often needed for planning and management purposes. A simulation study using synthetic loblolly pine populations with four levels of spatial heterogeneity was conducted to assess inventory data aggregation effects on predicted and projected stand characteristics.

The overall objective of this research was to provide decision support to forest inventory managers through the incorporation of auxiliary data and simulation. Specific topics investigated in each chapter include the following:

1) Assess the potential for UAS imagery and computer vision techniques for use in forest regeneration surveys.
2) Investigate the incorporation of auxiliary data in SAE methods for improving the precision of inventory estimates.
3) Investigate additional topics related to using SAE methods including: lidar point cloud density, elevation model resolution, incorporation of lidar individual tree detection counts, and the reliability of the observed patterns of improved precision with SAE.
4) Compare the differences between plot-level and stand-level inventory predictions and projections on common characteristics of interest including density, basal area and volume under varying levels of spatial heterogeneity.

The second chapter in this work has been submitted for publication and the final chapter was published prior to the completion of the dissertation. The remaining chapters will be prepared and submitted for publication. In addition to the chapters relating to the research objectives, an overall introduction and conclusion are included for context and general conclusions.

1.1. References

Burkhart, H.E., Avery, T.E. and Bullock, B.P., 2019. Forest measurements 6th ed. Waveland Press, Long Grove, IL. pp 434.

Ezell, A.W., 2011. Planting southern pines: a guide to species selection and planting techniques. Starkeville, MS: Mississippi State University Extension; Publication P1776. 16 p.

Fox, T.R., Jokela, E.J., Allen, H.L., 2007. The development of pine plantation silviculture in the southern United States. J. For. 105(7), 337-347.

Zhao, D., Kane, M., Teskey R., Fox, T.R., Albaugh, T.J., Allen, H.L., and Rubilar, R., 2016. Maximum response of loblolly pine plantations to silvicultural management in the southern United States. For. Ecol. Manage. 375, 105-111.

Chapter 2 Plantation loblolly pine (*Pinus taeda* L.) seedling counts with unmanned aerial vehicle imagery: opportunities and challenges

2.1. Abstract

An unmanned aircraft system (UAS) was evaluated for its potential to capture imagery for use in plantation loblolly pine (*Pinus taeda* L.) regeneration surveys. Five stands located in the Virginia Piedmont were evaluated in which one had completed a single growing season and four had completed two. Imagery was collected using a recreational grade unmanned aerial vehicle (UAV) at three flight altitudes ~200 ft, ~260 ft, and ~360 ft using a camera capable of capturing red-green-blue imagery. Two computer vision approaches were evaluated for their potential to automatically detect seedlings in the imagery. The results of the study indicated that the proposed methods were not capable of generating accurate, reliable counts of seedlings in the conditions evaluated. Due to the presence of significant natural pine regeneration amongst the planted trees and the small size of many planted seedlings, the imagery was not capable of capturing enough detail for consistent detection. In conditions without a large natural component and planted seedlings large enough to be captured in imagery, the automated detection methods performed with high levels of accuracy in individual cases. Challenges including global positioning system locational errors and image distortion made comparisons between ground sample locations and imagery difficult. In summary, UAS have potential for use in plantation loblolly pine regeneration surveys if the challenges observed in this study can be addressed.

2.2. Introduction

Plantation forests occupy approximately 35 million acres (14 million ha) in the southeastern United States (Zhao et al. 2016). Loblolly pine (*Pinus taeda* L.) is the most extensively planted and intensively managed species in the region. Extensive artificial regeneration of loblolly pine began in the 1930's when the Civilian Conservation Corps planted approximately 1.5 million acres (607,000 ha) on degraded agriculture land across the Southeast. Following WWII, planting continued through the Soil Bank Program (Fox et al. 2007). The results of early plantings using a combination of native seed sources and establishment practices were inconsistent and set the stage for widespread efforts of producing and deploying higher quality seedlings (Fox et al. 2007). Much like many agricultural crops, tree breeding programs are commonplace and produce almost all the seedlings currently planted across the region (McKeand et al. 2006). Genetic improvement has greatly enhanced both the quantity and quantity of volume production from previous generations of seedlings (McKeand et al. 2006).

Artificial regeneration affords many benefits when establishing a new forest. Stand density is one of the most important aspects affecting the development of pine plantations (Amateis and Burkhart 2012). Initial planting density has been extensively shown to affect diameter at breast height (DBH), crown characteristics, mortality, stem quality, and in some cases, height (e.g. Sharma et al. 2002; Amatais and Burkhart 2012; Akers et al. 2013). It is common for significant coniferous natural regeneration to develop in young plantations. This can alter the desired stand density, genetics, and species composition. Pre-commercial thinning (PCT) is an option often used to control unintended volunteer pines. PCT has been shown to increase DBH and volume growth in overstocked loblolly pine stands (Lohrey 1977; Haywood 2005). Controlling hardwood and herbaceous competition has also been shown to improve growth in young pine plantations. In a regionwide study, Creighton et al. (1987) found significant increases in height and DBH growth at every site evaluated after chemical control of herbaceous competition. Controlling both herbaceous and hardwood competitors was found to significantly increase the mean annual increment of volume growth in a region wide, loblolly pine site preparation study (Zhao et al. 2009).

With proper planting procedures and high-quality seedlings, loblolly pine survival can be higher than 80% following establishment (Shiver et al. 1990). Despite this, poor nursery practices, untrained planting crews, or natural climate variation can reduce survival. In addition, natural pine regeneration can be significant leading to overly dense conditions. Common practice is to assess survival one growing season after plantation establishment (Ezell 2011); however, two years is acceptable in some cases. An accurate count of stems per unit area early in the rotation is important for management decisions. If poor survival or high natural regeneration is found, interplanting, precommercial thinning, or stand re-establishment may be recommended. Models have been developed to predict early stand survival (Hitch et al. 1996); however, they assume ideal planting conditions and require inputs that may not be available in all cases. Further, they do not account for the possibility of recruitment of natural stems. The importance of an accurate stem count leads many forest managers to install small fixed-radius plots throughout plantations to assess survival. Usually, every living stem is counted, and planted trees are distinguished from natural trees if possible. Additional data regarding competing vegetation and seedling size are often collected.

Statistically valid, well-executed ground samples will produce unbiased estimates of tree counts over the long run. In some cases, however, stands exhibit large amounts of variability leading to an inventory that does not reliably estimate density. Even in the case of an accurate seedling count, inventory data are just one component of a forest regeneration survey. Spatial patterns of characteristics such as survival, competing vegetation, site wetness, and site productivity are generally not fully captured with common inventory practice. Field inventories are often expensive and time consuming leading to estimates that may not be reliable due to restrictions on sample intensity.

Unmanned aircraft systems (UAS) have recently emerged as a promising technology for rapid natural resource assessments. The UAS is a combination of an unmanned aircraft and any other systems needed for its operation (FAA 2016). UAS aircraft, often referred to as unmanned aerial vehicles (UAVs), generally operate in either fixed-wing or rotary configurations. Fixed-wing aircraft benefit from longer battery life; however, they suffer from the requirement of a larger take-off and landing area. Rotary models have minimal take-off and landing restrictions, but battery life is limited

compared with fixed-wing models. Both forms can be outfitted with a variety of sensors including cameras and light detection and ranging (lidar). In addition, a global positioning unit (GPS), an inertial measurement unit (IMU), and communication equipment facilitate data collection and flight control. The use of UAS in the United States are regulated by the Federal Aviation Administration (FAA) under regulations outlined in the Small Unmanned Aircraft Rule (Part 107) Summary (FAA 2016). Restrictions imposed by the FAA include, but are not limited to the following: 1) The aircraft must always remain in visual line-of-site (VLOS) , 2) a maximum flight altitude of 400 ft (122 m), 3) a minimum of 3 miles (4.8 km) of visibility, 4) operation in certain controlled airspace is restricted, 5) all other aircraft have right of way, 6) for non-recreational use, a Part 107 certified pilot must be present for all flights, and 7) the aircraft may weigh no more than 55 lbs (25 kg).

UAS have seen extensive application in precision agriculture (Zhang and Kovacs 2012; Adão et al. 2017) and in forest resource assessments (Adão et al. 2017; Torresan et al. 2017). Despite high levels of interest in use of unmanned aerial systems, very few studies have examined the suitability of UAS technology for forest regeneration surveys. Using a UAS-based sampling approach, Feduck et al. (2018) were able to detect 76% of coniferous seedlings in mixed pine-spruce planted stands using red-green-blue (RGB) imagery. With a combination of photogrammetrically derived point clouds and hyperspectral imagery from UAS, Imangholiloo et al. (2019) underestimated stand density by 20.8% and 7.4% under leaf-off and leaf-on conditions, respectively. There are no known published examples of reliably using UAS in plantation loblolly pine regeneration surveys.

2.2.1. Research Objectives

The overall objective of this work was to investigate the potential for using UAS for operational forest regeneration surveys in loblolly pine plantations. Specific research objectives/questions include:

1. Can a recreational grade UAS effectively capture useful wall-to-wall forest regeneration survey imagery?
2. What are the effects of flight altitude on tree detection?

3. Can a reliable, broadly applicable workflow be established for automating seedling detection using the imagery collected?
4. What recommendations for future research studies and applications can be offered?

2.3. Data and Methods

2.3.1. Study Locations

State forests in Virginia are managed by the Virginia Department of Forestry (VDOF) for multiple use objectives including timber management, wildlife, and recreation. Two state forests, Appomattox-Buckingham (ABSF), and Cumberland (CUSF) were selected for this study (Figure 2-1a). These forests are in the Piedmont physiographic region and are characterized by a mixture of rolling hills, flat land, and a diverse species composition. Loblolly pine is native to this area and is widely planted and managed with practices common for the Piedmont region. On ABSF and CUSF, VDOF hand plants Elite open pollenated 1-0 genetically improved seedlings at a target density of 538 $trees\ ac^{-1}$ (1329 $trees\ ha^{-1}$). Typical site preparation consists of chemical competition control followed by burning if necessary. Significant natural regeneration of Virginia pine (*Pinus virginia*) and loblolly pine is common for the area.

This study focused on loblolly pine plantations that have completed either one or two growing seasons. Five stands were selected for this study, three located on ABSF and two on CUSF (Figure 2-1b and 2-1c). One stand had completed a single growing season and the remainder completed two. An examination from preliminary UAV flights and field visits on other non-sampled age 1 stands revealed the seedling size was insufficient for reliable detection. The seedlings in these stands were characterized by heights and crown widths of less than 1 ft (0.3 m) and dull, thin crowns (Figure 2-2a). Only a single age 1 stand was investigated further. Trees that had completed two growing seasons were generally larger and had fuller crowns (Figure 2-2b). In total, 46.9 ac (19 ha.) age 1 and 166.8 ac (67.5 ha) of age 2 plantings were surveyed.

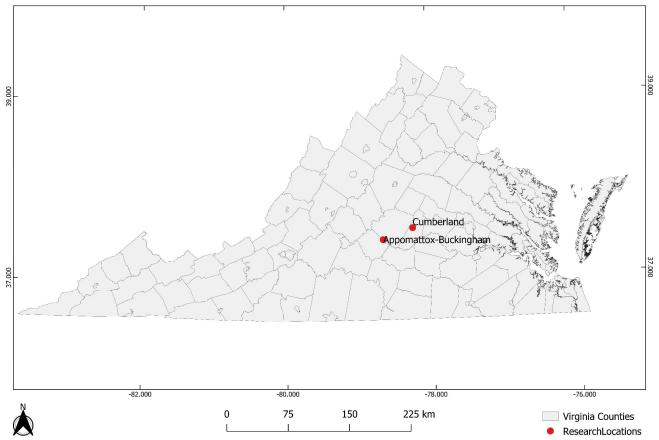

(a)

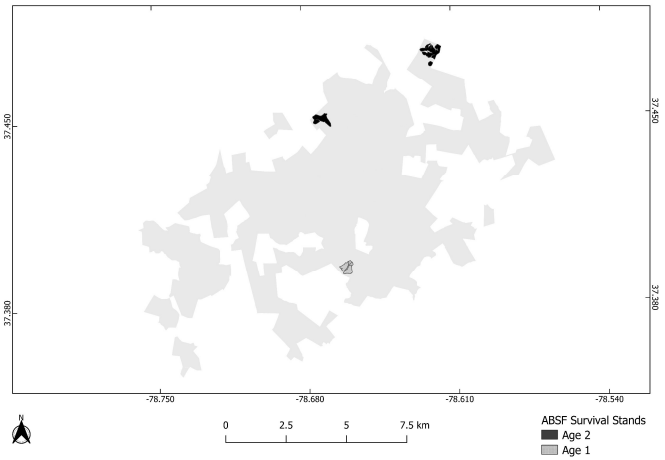

(b)

(c)

Figure 2-1. (a) Locations of State Forests used for study, (b) stand locations evaluated at Appomattox-Buckingham State Forest, and (c) stand locations evaluated at Cumberland State Forest.

(a) (b)

Figure 2-2. (a) Age 1 seedling example and (b) age 2 seedling example

2.3.2. Ground Data

In the dormant season of 2019, temporary, 1/30th acre (0.013 ha) fixed radius plots were installed in the five stands evaluated at an intensity of one plot per 3 acres (1.2 ha) with a minimum distance of approximately 3.5 - 4 chains (70 - 80 m) between plot centers. This sampling scheme was assumed to generate an unbiased sample design that ensured spatial coverage across the stands. On each sample location, all living pine stems were counted and average seedling heights and crown widths were estimated. Information regarding competing vegetation and other notes were recorded. Distinguishing planted and natural stems was not attempted due to size and spacing variation in planted and natural trees. Plot center locations were captured with a Trimble Geo7x GPS capable of submeter accuracy. At each plot center, a minimum of 50 GPS points were recorded followed by differential correction using the nearest available continuously referencing base stations. Due to logistical constraints with flight timing, visible plot center targets were not installed on these plots prior to UAV flights. These plots will be referred to as the “general plots”. Immediately before flights, temporary

1/30th acre fixed radius plots were installed with large, visible plot centers. The same information was collected on these locations and will be referred to as the "validation plots". A total of 16 validation plots were installed across the five stands evaluated.

2.3.3. UAV Imagery

During the winter of 2019, imagery was captured for the areas of interest. Dormant season flights were chosen to limit the amount of green foliage from woody and herbaceous competition that would interfere with seedling detection. The Solo 3DR rotary style aircraft with a gimble mounted GoPro Hero Black 3.0 RGB camera was used for all flights. The Solo was equipped with a Blox-Neo-7N-002 GPS. Weather conditions varied; however, no flights occurred during limited visibility, high wind, or rain. Three flight altitudes were evaluated, ~200 ft (60 m), ~260 ft (80 m), and ~360 ft (110 m). Due to the maximum allowed flight height of 400 ft, 360 ft was chosen to provide allowance for error in the automated UAV height control. For all flights, a flight speed of 25 mph (11 m/s) was targeted. Sidelap and frontlap between images was approximately 75% and 90% respectively. The ArduPilot Mission Planning software (ArduPilot 2019) was used for flight planning and autopilot controls.

2.3.3.1. Processing UAV Flight Data

Prior to analysis, the raw imagery was processed using the UAV specific photogrammetry software Pix4Dmapper version 4.3.31. Using photogrammetric techniques, a single, three-band orthomosaic was generated for the areas of interest. Processing options used in Pix4Dmapper follow in table 2-1.

Table 2-1. Processing options used for raw image processing in Pix4Dmapper.

Processing Options	Setting
Image Scale	Multiscale, ½ (half image size, default)
Point Density	Optimal
Minimum Number of Matches	3
3D Textured Mesh Generation	Yes
3D Textured Mesh Settings	Resolution: High Color Balancing: no
LOD	Generated: no
Advanced: 3D Textured Mesh Settings	Sample Density Divider: 1
Advanced: Image Groups	Group1
Advanced: Use Processing Area	Yes
Advanced: Use Annotations	Yes

Validation plots were located on imagery and exact plot centers were stored in a geospatial layer. In some cases, targets could not be located resulting in 15 validation plots for 200 ft flying height imagery, 13 validation plots for 260 ft imagery, and 12 validation plots for 360 ft imagery. The distance from the plot center observed in the imagery and the plot center collected during the field visit was measured in QGIS (QGIS Development Team 2019).

The plot locations sampled with both general and validation plots were subset from the overall flight orthomosaic images for further processing and analysis. To facilitate automated seedling detection, the Green Leaf Index (GLI) was calculated for each image subset (equation 2-1)

$$GLI = \frac{(G-R)+(G-B)}{(2G+R+B)} \quad \text{Equation 2-1}$$

where R, G, and B are the red, green, and blue bands from the imagery respectively. The GLI was first described by Louhaichi et al. (2001) and is effective for enhancing green vegetation in RGB imagery when it is contrasted by non-green soil, rocks, and other dead organic matter.

Following calculation of the GLI, each image was subjected to a binary classification. Based on preliminary investigations, it was determined that a GLI pixel value > 0.04 was a strong indication of coniferous foliage and was reclassified to 1. In cases where the maximum GLI value in an image was < 0.05, a threshold of 0.02 was used to better highlight faint foliage. All other pixels were classified as 0. Seedlings in the reclassified images were then counted with two automated, computer vision approaches. A "blob-detection" procedure, using the determinant of the hessian matrix method outlined in the R imager package (Barthelme 2017), was evaluated using image blur standard deviations from 4.5 to 6 by increments of 0.1. These values were chosen after preliminary analysis determined any value below 4.5 generally resulted in a large overcount. A fixed percentage of 98.9% was used for the required threshold function in the blob-detection workflow. The blob detection method aims to detect and label local maxima in an image based on changes in brightness and color. Readers are directed to Marsh et al. (2018) for a more complete description of the blob detection method applied to locating biomolecules in microscopy imagery. In addition, an image segmentation procedure described in the imager package (Barthelme 2017) was evaluated. This method

aims to segment objects of interest by first correcting image illumination variation followed by morphological erosion and dilation procedures to segment the objects from the background. All processing of the orthomosaic was conducted using R (R Core Team 2018) with additional packages including the raster package (Hijmans 2019), the sp package (Pebesma and Riband 2005; Bivand et al. 2013), and the rgdal package (Bivand et al. 2019).

2.4. Results and Discussion

The ground survey data indicated that the plantations evaluated exceeded the targeted planting density of 538 trees per acre in four out of five cases. Average seedling counts per plot ranged from approximately 11 to 46 (Table 2-2), leading to estimates of approximately 330 – 1380 trees per acre.

Table 2-2. Summary of stands evaluated, and ground survey general-plot counts

StandID	Age	Acres (ha)	$\bar{x}$	sd	min	max
AB04	2	68.1 (27.6)	46.3	26.4	9	104
AB07	2	47.5 (19.2)	28.4	10.2	8	45
AB18	1	46.9 (19.0)	11.1	4.6	5	18
CU04	2	30.2 (12.2)	22.3	17.8	7	73
CU11	2	21.0 (8.5)	21.1	8.0	11	34

2.4.1. Impact of Flight Altitude

In both the validation and general plots, a decrease in flight altitude resulted in automated detections falling closer to the 1-1 relationship with the observed counts (Figures 2-3 and 2-4). Despite the improvements in detection accuracy, none of the flight heights evaluated reliably captured imagery that could be used to accurately count seedlings. The distributions of counts often differed greatly from the observed average with a general tendency to undercount (Figure 2-5, Table 2-3). An exception is the age 1 stand “AB18” where the automated methods generally overcounted seedlings. However, many of these overcounts were due to image artifacts not representative of seedlings. Significant differences in image resolution were observed. The average pixel size for 200 ft flying height imagery was ~1.7 in (4.2 cm), for 260 ft imagery was ~2.2 in (5.6 cm) and for 360 ft imagery 2.9 in (7.4 cm). This increase in pixel size was likely a major contributor to the decrease in accuracy for higher flight altitudes.

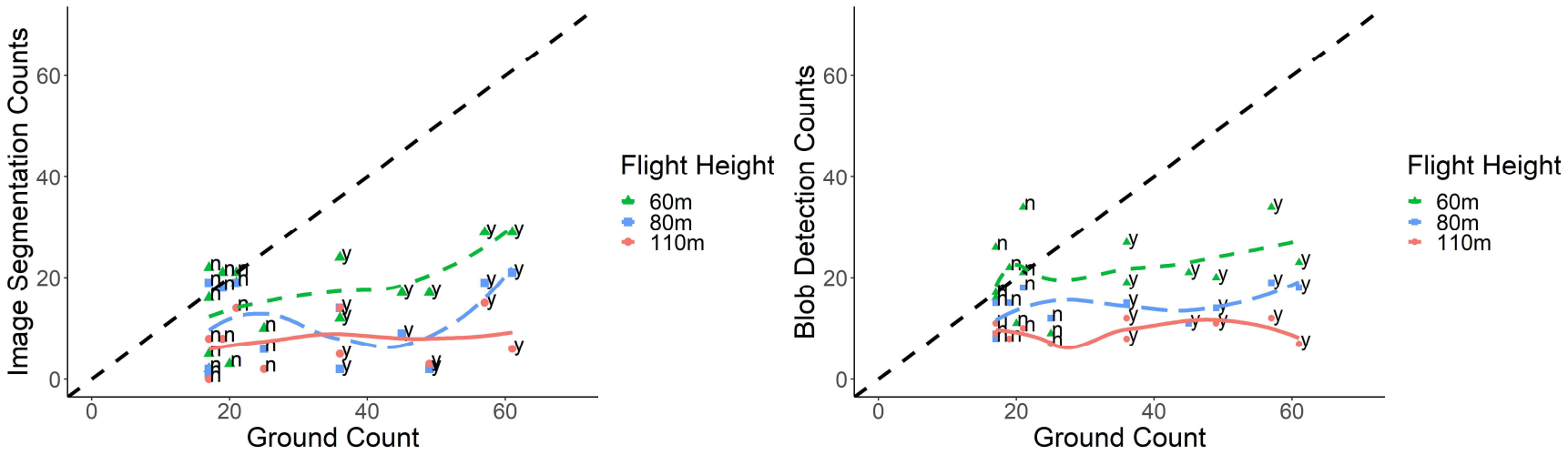

(a) (b)

Figure 2-3. Validation 1-1 plots between ground counts and automated detection methods. (a) Image segmentation method and (b) determinant of hessian blob detection method plotted with all the isoblur coefficients evaluated. Points are labeled by the presence or absence of significant natural regeneration observed during the field counts (y = yes, n = no). Smoothing curves are for visual interpretation of the trends between flight heights.

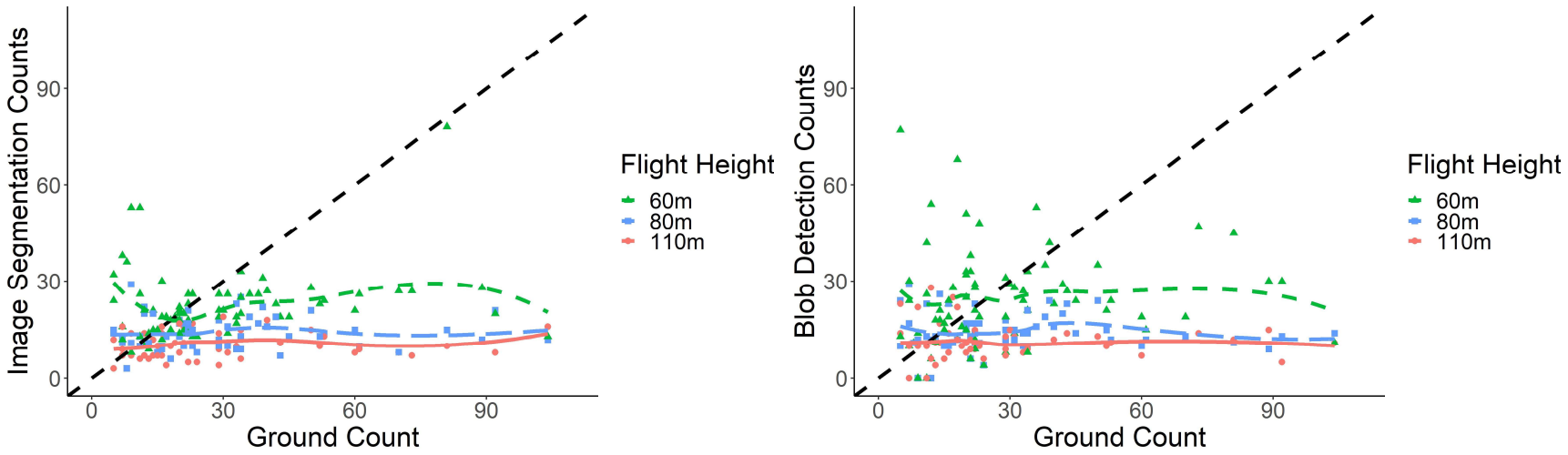

(a) (b)

Figure 2-4. General 1-1 plots between ground counts and automated detection methods. (a) Image segmentation method and (b) determinant of hessian blob detection method plotted single isoblur coefficient of 4.8. Smoothing curves are for visual interpretation of the trends between flight heights.

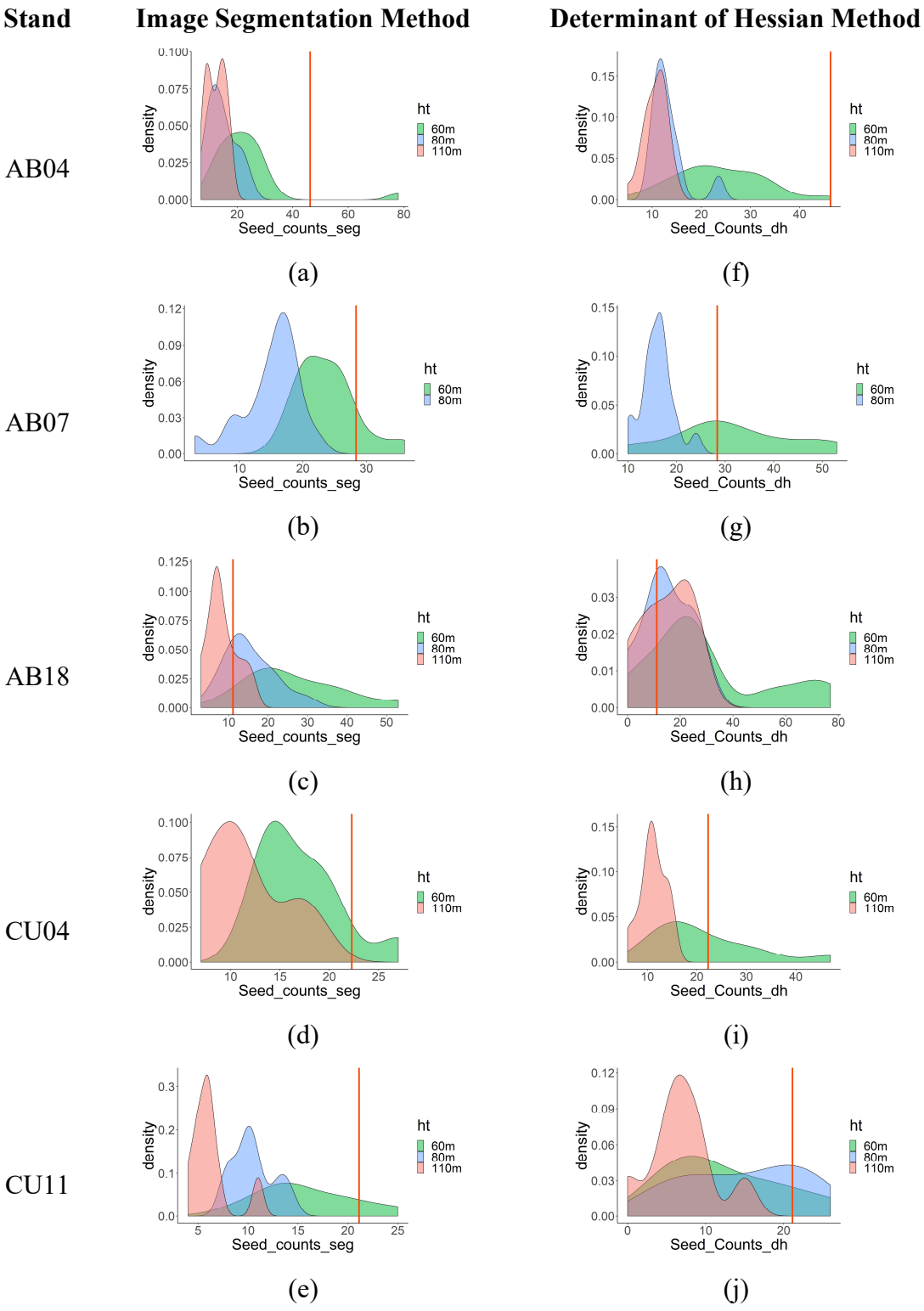

Figure 2-5. (a-e) Distributions of automated image segmentation general-plot counts for each stand evaluated and (f-j) distributions of automated determinant of hessian general-plot counts for each stand evaluated. Vertical line indicates the mean count from the general ground plots.

Table 2-3. Summary of automated counting methods compared with ground counts for the stands evaluated. Not all stands have summaries for each flying height due to image processing limitations.

StandID	Age	Acres (ha)	Height ft (m)	Method	Mean	Sd	Min	max
AB04	2	68.1 (27.6)	-	Ground	46.3	26.4	9	104
			200 (60)	Blob Detection (isoblur 4.8)	23.6	8.8	8	45
				Image Segmentation	23	13.6	8	78
			260 (80)	Blob Detection (isoblur 4.8)	13.2	3.7	9	24
				Image Segmentation	15.1	4.7	8	25
			360 (110)	Blob Detection (isoblur 4.8)	10.7	2.4	5	15
				Image Segmentation	12.5	3.3	8	18
AB07	2	47.5 (19.2)	-	Ground	28.4	10.2	8	45
			200 (60)	Blob Detection (isoblur 4.8)	31.6	12.5	11	53
				Image Segmentation	23.8	4.6	17	35
			260 (80)	Blob Detection (isoblur 4.8)	16.1	3.4	10	24
				Image Segmentation	15.0	4.8	3	23
			360 (110)	Blob Detection (isoblur 4.8)	-	-	-	-
				Image Segmentation	-	-	-	-
AB18	1	46.9 (19.0)	-	Ground	11.1	4.6	5	18
			200 (60)	Blob Detection (isoblur 4.8)	29.5	24.6	0	77
				Image Segmentation	25.7	14.5	9	54
			260 (80)	Blob Detection (isoblur 4.8)	14.8	9.4	0	29
				Image Segmentation	15.4	6.5	6	30
			360 (110)	Blob Detection (isoblur 4.8)	14.8	9.6	0	28
				Image Segmentation	9.3	3.7	4	16
CU04	2	30.2 (12.2)	-	Ground	22.3	17.8	7	73
			200 (60)	Blob Detection (isoblur 4.8)	21.8	10.9	10	47
				Image Segmentation	17.0	4.4	11	27
			260 (80)	Blob Detection (isoblur 4.8)	-	-	-	-
				Image Segmentation	-	-	-	-
			360 (110)	Blob Detection (isoblur 4.8)	11.1	2.7	6	15
				Image Segmentation	11.8	4.1	7	19
CU11	2	21.0 (8.5)	-	Ground	21.1	8.0	11	34
			200 (60)	Blob Detection (isoblur 4.8)	12.5	7.5	4	26
				Image Segmentation	14.1	3.2	9	19
			260 (80)	Blob Detection (isoblur 4.8)	14.8	7.6	4	23
				Image Segmentation	10.6	3.1	8	16
			360 (110)	Blob Detection (isoblur 4.8)	7	4.3	0	15
				Image Segmentation	6.4	2.2	4	11

2.4.2. Impact of Detection Algorithm

The two detection algorithms were comparable in their ability to detect seedlings (Figure 2-5). The blob-detection approach using the determinant of the hessian matrix was found to be more flexible and appeared to segment seedlings with overlapping crowns more reliably. A downside with this method was the failure to detect visibly apparent trees due to the threshold and isoblur parameters chosen. In these cases, the local maxima for some seedlings would not meet the threshold set to prevent a large overcount. The image segmentation approach appeared to outperform the hessian method where seedlings did not commonly overlap. Tree crowns that grew in close proximity were often not segmented as they were treated as a single "object". The segmentation approach suffers from the necessity of imagery with at least two distinct classes of pixel values. In cases with no pixels that meet the GLI reclassification rules, an image with 1 class will fail in the image segmentation function. Removing the GLI reclassification was used to overcome this limitation; however, there were potential impacts with detecting non-tree objects. Harvest debris and other non-vegetative features resembled seedlings if the reclassification threshold was set too low.

2.4.3. Further Discussion

There were many challenges in this study that complicated an evaluation of the methods. First, significant aircraft GPS error caused registration error between the imagery and the GPS locations collected at each plot center. From measurements taken on validation imagery, average GPS error was approximately 12.5 ft (3.8 m) for the 200 ft flights, 9.2 ft (2.8 m) for the 260 ft flights, and 30.4 ft (9.3 m) for the 360 ft flights. This error made exact comparisons between ground and imagery counts impossible on the general plots. Future studies should use large, visible targets at every plot center to ensure precise matching between ground and imagery data. An additional significant source of error was image distortion and loss of radiometric properties due to the orthomosaic process. The exact causes of individual errors are intractable; however, shadows, inconsistent lighting, and GPS error can all contribute to losses of image quality. The camera used in this study captured imagery that was not sufficient for the reliable detection of small seedlings at the flying heights evaluated. The lack of a near

infrared (NIR) channel limited the vegetation indices that could be used for detecting vegetation. While the GLI was effective in many cases, the addition of NIR may have been beneficial for evaluating vegetation indices that highlight coniferous foliage in some cases. This was particularly true in the age 1 stand. Visual observation revealed most of the automated counts were due to image artifacts and not reflection from seedling foliage. The largest challenge in the study was the significant amount of natural pine regeneration present on many sample plots. The natural seedlings were often indistinguishable from planted seedlings and commonly grew in clusters making identifying individual trees challenging. An example of the difficulties faced with detecting small, often clumped, seedlings is shown in figure 2-6. In cases where no natural seedlings were present, the detection workflow accurately identified the seedlings present on the validation plot (figure 2-6a – 2-6d). In contrast, many natural seedlings were not detected in the validation plot shown in figure 2-6e – 2-6h. In both cases, however, the GLI and classification methods successfully highlighted and identified tree canopies with enough foliage to produce reflection that could be captured by the camera. Due to the size and clustered spacing of seedlings, it is doubtful that any camera would be able to capture imagery that could be used to identify every seedling present. Seedlings on many plots were difficult to accurately count during ground visits due to tree size, overtopping, bunching, and competing vegetation. If wall-to-wall imagery is not needed, a sampling approach similar to Feduck et al. (2019) would likely perform better in areas with high amounts of natural regeneration. This approach eliminated many of the issues with image artifacts from the orthomosaic process and captured imagery with 0.12-inch resolution (3 mm) compared with the best resolution of 1.7 inches (43 mm) observed in this study.

There are practical issues other than FAA regulations that were encountered and should be considered when designing a similar study or implementing the proposed methods operationally. Weather, even if legal to fly in, can interfere with flights and data integrity. Rain, light winds, and inconsistent lighting due to clouds all negatively affect image quality. Generally, calm weather with consistent lighting are ideal conditions for photography. Battery performance was an additional limiting factor. With the aircraft evaluated, one battery would generally power a single flight. Multiple flights were required for the lowest evaluated flight height on large stands. As battery technology

progresses, flight and charge times will likely improve. While this was not a time and motion study, the use of UAS has the potential for significant time savings compared with traditional ground regeneration surveys. Future studies should carefully evaluate the efficiency of UAS compared with ground-based methods.

The classification and computer vision approaches evaluated in this study were chosen for their ability to detect seedlings with minimal human intervention. Further, they can be implemented in multiple open-source software including R and python. Supervised image classification techniques were intentionally avoided due to the need for manually generating training data. Future work should investigate the potential for machine learning and deep learning to detect and count tree seedlings. These are broad classes of artificial intelligence techniques that are effective for many computer vision applications (Goodfellow et al. 2016).

Despite the challenges encountered in this study with reliably detecting seedlings, UAS data provide valuable qualitative information. All stands have natural variation and wall-to-wall imagery highlights characteristics that may not be captured in traditional regeneration surveys. As an example, spatial patterns of competing vegetation may be present due to inconsistencies in site preparation. These patterns would be difficult to capture with traditional methods unless many additional sample plots were installed. In contrast, UAV imagery would quickly highlight this pattern potentially leading to more informed management decisions regarding a remedial treatment. Additionally, the process used to generate the orthomosaic imagery produces a photogrammetrically derived digital surface model and point cloud. These data were not evaluated in this study; however, they may prove useful in certain circumstances.

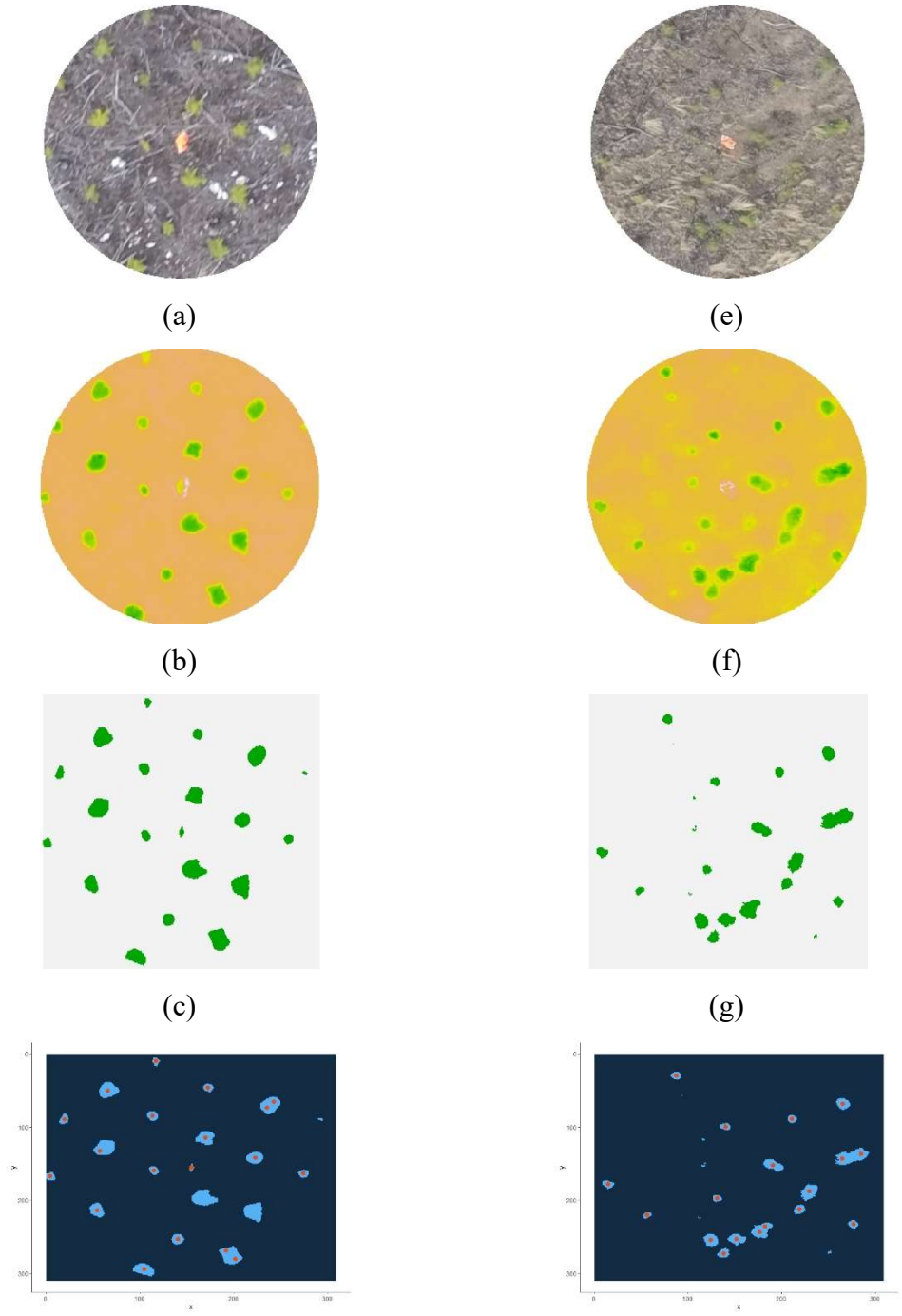

Figure 2-6. Examples of image classification and identification workflows. Figures a – d demonstrate an example of the successful use of Green Leaf Index and automated classification using blob detection (observed count: 19, predicted count: 20). Figures e – h is an example of the inability to capture small seedlings < 1.5 ft (~0.5 m) tall using the proposed workflow (observed count 49, predicted count: 18). Red points in figures d and h are the locations of the automatically detected seedlings.

2.5. Conclusions

The use of UAS for the detection of plantation loblolly pine seedlings was unreliable. More specific findings relevant to the research objectives and questions include: 1) The recreational grade UAS used in this study suffered from significant GPS error and used a camera not capable of capturing the imagery necessary for reliable detection in less than ideal conditions. 2) A decrease in flight altitude generally improved image quality and seedling detection; however, this was at the expense battery life. Users must balance the needs for higher resolution imagery with available battery resources. 3) The automated detection methods were successful considering the quality of imagery and the conditions evaluated. The blob detection and image segmentation methods both produced similar results to that possible by manual counting. 4) For those considering the incorporation of UAS into their forest regeneration surveys, it is recommended that an aircraft equipped with a highly accurate GPS, preferably capable of RTK, and a camera capable of capturing high spatial resolution imagery in both RGB and NIR, be used. For future research studies, large visible targets should be installed at all plot locations.

There are circumstances that will always limit the success of regeneration surveys with UAS including weather, legal restrictions, battery life, and significant competing vegetation. Despite the limitations, as aircraft, battery, and camera technology improve, UAS will have increased potential for providing wall-to-wall imagery for reliable seedling counts in favorable conditions. In addition to seedling counts, the imagery provides useful information regarding stand characteristics, such as spatial patterns of competing vegetation, not commonly captured in ground surveys. Based on the results of this study, UAS imagery will not likely replace traditional ground surveys; rather, it will serve as useful ancillary information for more informed forest regeneration surveys.

2.6. References

Adão, T., Hruška, J., Pádua, L., Bessa, J., Peres, E., Morais, R., Sousa, J., 2017. Hyperspectral imaging: A review on UAV-based sensors, data processing and applications for agriculture and forestry. Rem. Sens. 9(11), 1110.

Akers, M.K., Kane, M., Zhao, D., Teskey, R.O., Daniels, R.F., 2013. Effects of planting density and cultural intensity on stand and crown attributes of mid-rotation loblolly pine plantations. For. Ecol. Manage. 310, 468-475.

Amateis, R.L., Burkhart, H.E., 2012. Rotation-age results from a loblolly pine spacing trial. South. J. Appl. For. 36(1), 11-18.

ArduPilot, 2019. Available online at http://www.ardupilot.org/. Last accessed 09/07/2019.

Barthelme, S., 2017. imager: Image Processing Library Based on 'CImg'. R package version 0.40.2. https://CRAN.R-project.org/package=imager

Bivand, R., Keitt, T., Rowlingson, B., 2019. rgdal: Bindings for the 'Geospatial' Data Abstraction Library. R package version 1.4-3. https://CRAN.R-project.org/package=rgdal

Bivand, R.S., Pebesma, E., Gomez-Rubio, V., 2013. Applied spatial data analysis with R, Second edition. Springer, NY. http://www.asdar-book.org/

Creighton, J.L., Zutter, B.R., Glover, G.R., Gjerstad, D.H., 1987. Planted pine growth and survival responses to herbaceous vegetation control, treatment duration, and herbicide application technique. South. J. Appl. For. 11(4), 223-227.

Ezell, A.W., 2011. Planting southern pines: a guide to species selection and planting techniques. Starkeville, MS: Mississippi State University Extension; Publication P1776. 16 p.

Federal Aviation Administration. 2016. Summary of small unmanned aircraft rule (part 107). Available online at: https://www.faa.gov/uas/media/part_107_summary.pdf. Accessed 09/02/2019.

Feduck, C., McDermid, G.J., Castilla, G., 2018. Detection of coniferous seedlings in UAV imagery. Forests. 9, 432.

Fox, T.R., Jokela, E.J., Allen, H.L., 2007. The development of pine plantation silviculture in the southern United States. J. For. 105(7), 337-347.

Goodfellow, I., Bengio, Y., Courville, A., 2016. Deep Learning. MIT Press. Available online at: http://www.deeplearningbook.org/

Haywood, J.D., 2005. Influence of precommercial thinning and fertilization on total stem volume and lower stem form of loblolly pine. South. J. Appl. For. 29(4), 215-220.

Hijmans, R.J., 2019. raster: Geographic Data Analysis and Modeling. R package version 2.8-19. https://CRAN.R-project.org/package=raster

Hitch, K.L., Shiver, B.D., Borders, B.E., 1996. Mortality models for newly regenerated loblolly pine plantations in the Georgia Piedmont. South. J. Appl. For. 20(4), 197-202.

Imangholiloo, M., Saarinen, N., Markelin, L., Rosnell, T., Näsi, R., Hakala, T., Honkavaara, E., Holopainen, M., Hyyppä, J., Vastaranta, M., 2019. Characterizing seedling stands using leaf-off and leaf-on photogrammetric point clouds and hyperspectral imagery acquired from unmanned aerial vehicle. Forests, 10(5), 415.

Lohrey, R.E., 1977. Growth responses of loblolly pine to precommercial thinning. South. J. Appl. For. 1(3), 19-22.

Louhaichi, M., Borman, M.M., Johnson, D.E., 2001. Spatially located platform and aerial photography for documentation of grazing impacts on wheat. Geocarto Int. 16(1), 65-70.

Marsh, B.P., Chada, N., Gari, R.R.S., Sigdel, K.P., King, G.M., 2018. The Hessian blob algorithm: Precise particle detection in atomic force microscopy imagery. Scientific reports, 8(1), 978.

McKeand, S.E., Abt, Robert, C., Allen, H.L., Li, B., Catts, G.P., 2006. What are the best loblolly pine genotypes worth to landowners? J. For. 104(7), 352-358.

Pebesma, E.J., Bivand, R.S., 2005. Classes and methods for spatial data in R. R News 5 (2), https://cran.r-project.org/doc/Rnews/.

QGIS Development Team (2019). QGIS Geographic Information System. Open Source Geospatial Foundation Project. http://qgis.osgeo.org

R Core Team, 2018. R: a language and environment for statistical computing [online]. R Foundation for Statistical Computing, Vienna, Austria. Available from http://www.R-project.org/

Sharma, M., Burkhart, H.E., Amateis, R.L., 2002. Modeling the effect of density on the growth of loblolly pine trees. South. J. Appl. For. 26(3), 124-133.

Shiver, B.D., Borders, B.E., Page Jr., H.H., 1990. Effects of some seedling morphology and planting quality variables on seedling survival in the Georgia Piedmont. South. J. Appl. For. 14, 109-114.

Torresan, C., Berton, A., Carotenuto, F., Di Gennaro, S.F., Gioli, B., Matese, A., Miglietta, F., Vagnoli, C., Zaldei, A., Wallace, L., 2017. Forest applications of UAVs in Europe: a review. Int. J. Remote Sens. 38(8-10), 2427-2447.

Zhang, C., Kovacs, J.M., 2012. The application of small unmanned aerial systems for precision agriculture: a review. Precis. Agric. 13(6), 693-712.

Zhao, D., Kane, M., Borders, B.E., Harrison, M., Rheney, J.W., 2009. Site preparation and competing vegetation control affect loblolly pine long-term productivity in the southern Piedmont/Upper Coastal Plain of the United States. Ann. For. Sci. 66, 705.

Zhao, D., Kane, M., Teskey R., Fox, T.R., Albaugh, T.J., Allen, H.L., and Rubilar, R., 2016. Maximum response of loblolly pine plantations to silvicultural management in the southern United States. For. Ecol. Manage. 375, 105-111.

Chapter 3 Small area estimation in support of plantation loblolly pine (*Pinus taeda* L.) forest inventory

3.1. Abstract

Loblolly pine (*Pinus taeda* L.) is one of the most widely planted tree species globally. As the reliability of estimating forest characteristics such as volume, biomass, and carbon become more important, the necessary resources available for assessment are often insufficient to meet desired confidence levels. Small area estimation (SAE) methods were investigated for their potential to improve the precision of volume estimates in loblolly pine plantations aged 9 - 43. Area-level SAE models that included lidar height percentiles and stand thinning status as auxiliary information were developed to test whether precision gains could be achieved. Models that utilized both forms of auxiliary data provided larger gains in precision compared to using lidar alone. Unit-level SAE models were found to offer additional gains compared with area-level models in some cases; however, area-level models that incorporated both lidar and thinning status performed nearly as well or better. Despite their potential gains in precision, unit-level models are more difficult to apply in practice due to the need for highly accurate, spatially defined sample units and the inability to incorporate certain area-level covariates. The results of this study are of interest to those looking to reduce the uncertainty of stand parameter estimates. With improved estimate precision, managers, stakeholders, and policy makers can have more confidence in resource assessments for informed decisions.

3.2. Introduction

In the southern United States, managed pine plantations occupy approximately 14 million hectares of forest land (Zhao et al. 2016). Of the major pine species, loblolly pine (*Pinus taeda* L.) is the most widely planted and has seen large improvements in productivity beginning in the 1950's (Fox et al. 2007). Plantation loblolly pine is important not only as a productive timber species but also for multiple use forest management purposes (Schultz 1999). The extensive planting and intensive management of loblolly pine have significant implications for wildlife management (Andreu et al. 2008) and the global carbon cycle (Johnsen et al. 2001). In recent years, ownership patterns have seen changes resulting in frequent acquisitions and dispositions of timberlands (Fox et al. 2007; Jokela et al. 2010). Due to commercial and ecological implications, plantation forestry requires accurate, reliable, and expeditious information at the stand-level for informed management decisions. Forest inventory is a primary tool used to obtain estimates of stand parameters. Ground-based forest inventory is typically conducted using either fixed- or variable-radius plots as sample units established with a specific sampling intensity and spatial arrangement with the goal of achieving a certain targeted precision. Common sample measurements include species, diameter at breast height (DBH), total height (H), and stem quality assessments (Burkhart et al. 2019). In practice, it is common for design-based estimates (i.e. estimates derived only from the ground-based sample units) to lack the precision required for management purposes. This is often due to logistical and budgetary constraints which limit the planned sample intensity. In these cases, a class of model-assisted statistical estimation techniques known as small area estimation (SAE) is an option that can be used to reduce the uncertainty of inventory estimates. SAE models can be broadly classified as "area-level" and "unit-level". Area-level models relate area-based direct estimates to area-level covariates while unit-level models relate sample unit values to the corresponding sample unit covariates (Rao and Molina 2015). For many areas where loblolly pine is grown commercially, auxiliary data are available that can be leveraged for use in SAE models.

3.2.1. Light Detection and Ranging

Light detection and ranging, referred to as lidar, is a form of active remote sensing that includes a scanning laser, an inertial measurement unit, a global positioning system (GPS), and a computer containing timing systems and storage (Campbell and Wynne 2011). Generally, lidar systems are installed on fixed-wing aircraft or helicopters. In aerial lidar analysis, a "point cloud" contains three-dimensional data that include x-y-z coordinates representing both horizontal and vertical structure referenced above the Earth's ellipsoid. In many applications, the point cloud is normalized by subtracting the ground elevation from the heights above the ellipsoid. Starting in the 1980's with work such as Nelson et al. (1984) and Nelson et al. (1988), lidar has been extensively demonstrated to provide useful information in forestry applications. When utilized for forest inventory purposes, two general approaches have seen both research and application: 1) Area-based approaches and 2) Individual-tree detection approaches. Both methods have been demonstrated to be effective and are recommended for use in plantation forest inventory applications (Maltamo et al. 2014).

Area based approaches have been successfully applied to estimating mean dominant tree heights in a variety of forest conditions (e.g. Næsset 1997a; Means et al. 2000; Næsset 2004a; Næsset 2004b; and Næsset 2007). In addition to dominant height, the area-based approach has been used to predict total stand volume and biomass through regression approaches with lidar-derived height and canopy cover metrics as predictors (e.g. Næsset 1997b; Næsset 2002; Holmgren 2004; Næsset 2004a; Næsset 2004b; and Næsset 2007). Biomass and volume were estimated by van Aardt et al. (2006) through an object-oriented approach. Area-based methods have also been utilized to parameterize models that predict stem density, average diameter, and basal area (Means et al. 2000; Næsset 2002; Holmgren 2004; Næsset 2004a; Næsset 2004b and Næsset 2007).

All the studies mentioned up to this point have focused on estimating forest characteristics through area-based methods. These techniques do not rely on the detection and delineation of individual tree stems or crowns; rather, they rely on quantiles and distributional features of lidar data as predictors for a given area (Yu et al. 2010). The individual tree detection methods rely on algorithms to locate and measure trees in a point cloud. While they typically require higher pulse densities and greater computational

resources, individual tree detection requires less data from field measurements to calibrate (Yu et al. 2010). Successful examples of predicting stand characteristics using the individual tree approach include McCombs et al. (2003), Popescu and Wynne (2004), Popescu et al. (2003), and Yu et al. (2010).

3.2.2. Area-Level SAE

The area-level SAE approach was first proposed by Fay and Herriot (1979) for use in predicting income in low population areas. Using U.S. Census data and other auxiliary information, they were able to improve the estimation precision with their proposed composite estimators. The area-level approach has seen multiple forest research applications. Goerndt et al. (2011) used lidar-derived auxiliary information to improve the precision of stand-level estimates of density, quadratic mean diameter, total height, and total volume in a variety of cover types in coastal Oregon. Several area-level SAE composite estimators were found to provide comparable gains in precision with the aforementioned stand variables. In addition, Magnussen et al. (2017) presented three case studies using lidar and one case study using photogrammetrically derived point clouds as ancillary data in area-level analysis. In a variety of European locations including Spain, Germany, Switzerland, and Norway, both forms of auxiliary data provided increased precision of total volume estimates.

3.2.3. Unit-Level SAE

The unit-level approach was first introduced for the prediction of crop area in selected Iowa counties. Using Landsat imagery as auxiliary information, the standard errors for the estimates were reduced compared with the direct estimate alone (Battese et al. 1988). In addition, unit-level SAE models have seen application in the forestry literature. Weighted unit-level SAE models were used to estimate the total area occupied by olive trees in Navarra, Spain using Landsat imagery as auxiliary information (Militino et al. 2006). Using Norwegian National Forest Inventory data, Breidenbach and Astrup (2012) used a photogrammetrically derived point cloud as auxiliary information and found significant improvements in the precision of above-ground forest biomass estimates. Goerndt et al. (2013) utilized a variety of auxiliary data including Landsat

variables, land cover class, tree cover, and elevation to successfully improve the precision of a variety of county-level forest attributes in the Oregon Coast Range.

3.2.4. Unit vs. Area Comparisons

Several research studies have compared the effectiveness of the two SAE methods. Mauro et al. (2017) investigated area- and unit-level models in predominately coastal coniferous forests located in the Oregon Coast Range. Using auxiliary lidar data, unit-level approaches were found to produce more precise estimates compared with area-level and design-based approaches for all stand variables of interest. Area-level models, however, were found to produce more precise estimates when compared to the direct estimates. In addition to lidar, a comparison between area- and unit-level estimators using photogrammetrically derived point clouds found greater stand-level estimate precision with unit-level models compared with area-level models in most cases (Breidenbach et al. 2018).

3.2.5. Research Objectives and Questions

To our knowledge, no studies have focused on using SAE techniques specifically in intensively managed loblolly pine plantations. The overall objective of this work was to demonstrate the potential for using SAE techniques to improve the precision of stand-level estimates of total planted volume in operationally managed loblolly pine plantations across a range of common inventory entry points. Specific objectives/questions include:

1. Do lidar-derived auxiliary data improve total planted volume estimate precision with area-level SAE analysis?
2. Do lidar-derived auxiliary data improve total planted volume estimate precision with unit-level SAE analysis?
3. How do area- and unit-level SAE approaches compare in plantation pine forest inventory?
4. What other sources of auxiliary data improve estimates with area- and/or unit-level SAE analysis?

3.3. Data and Methods

3.3.1. Study Location and Ground Data

3.3.1.1. Locations

State forests in the Commonwealth of Virginia are under the administration of the Virginia Department of Forestry (VDOF) and are managed with multiple use objectives including timber management. Three state forests, Appomattox-Buckingham (ABSF), Cumberland (CUSF), and Prince Edward-Gallion (PESF), were selected for this study (Figure 3-1).

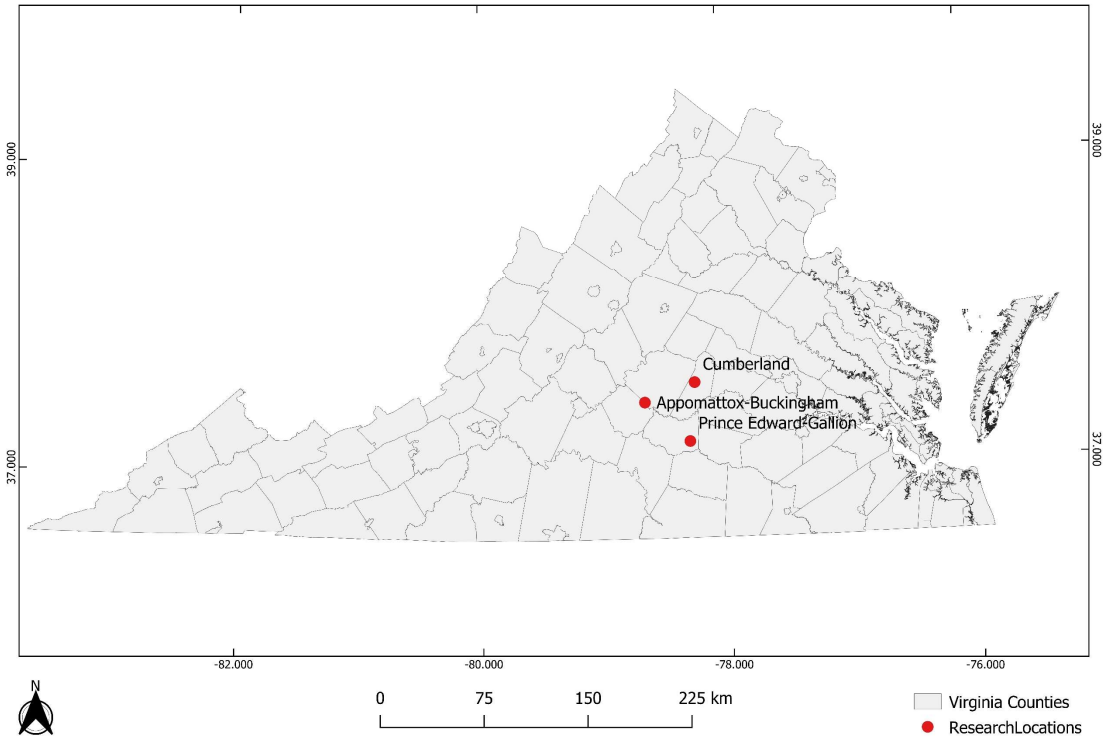

Figure 3-1. Locations of State Forests used in study

These forests are located in the central portion of the state and are representative of a variety of Piedmont physiographic conditions. ABSF is representative of the upper Piedmont with significantly higher elevations than typical Piedmont sites and is on the edge of the natural range of loblolly pine. CUSF exhibited great topographic diversity with many areas that resembled upper Coastal Plain topography. PESF was generally

representative of common Piedmont conditions. Managed loblolly pine plantations are prevalent throughout this area and the VDOF generally follows management strategies common throughout the Piedmont region of the Southeast (e.g. site preparation, planting densities, planting stock, and thinning type).

Forty stands were selected within the state forests to cover the range of forest inventory entry points typical of managed pine in the Southeast. Specifically, stages of development that commonly require inventory information for planning decisions include: Canopy closure, immediate pre-first thinning, immediate post thinning, and pre-final harvest. Both unthinned and thinned stands established from 1976 – 2010 were considered for study (Figure 3-2). Stands selected varied in initial planting density, genetic origin, and silviculture treatments. Apart from three stands nearing rotation age, all thinned stands were thinned within the past two years prior to ground measurements in the winter and early spring of 2019.

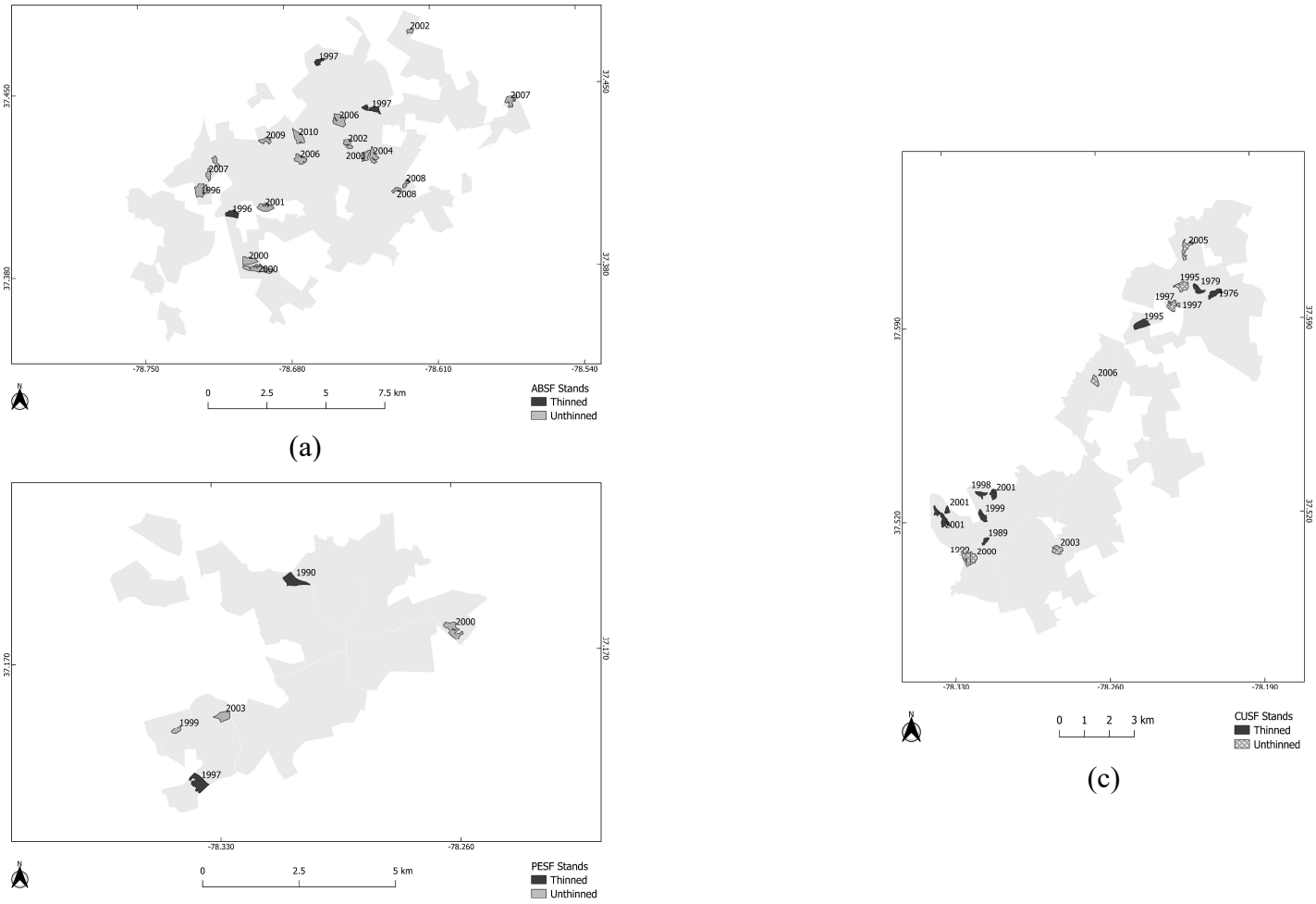

Figure 3-2. (a) Stands at Appomattox-Buckingham (a), Prince Edward-Gallion (b), and Cumberland (c) State Forests inventoried for study. Each stand is labeled with the year it was established (all ground measurements taken in the winter/early spring of 2019). The fill of the polygons indicates thinning status.

3.3.1.2. Sample Design and Ground Data

Stands selected for inventory in the winter and early spring of 2019 were allocated sample units using QGIS (QGIS Development Team 2019). Approximately 1 sample plot per 1.2 hectares were arranged at random with a minimum distance of approximately 70-80 meters between plot centers. This was assumed to produce an equal probability sample. Due to time constraints, the full sample intensity was measured for only 22 stands of 40. In stands that did not receive the full sample intensity, measurement plots were randomly chosen while still maintaining spatial coverage. Unthinned stands were inventoried with 0.013 hectare fixed-radius plots. In cases where excessive natural regeneration was present, 0.01 hectare fixed-radius plots were used instead. Thinned stands were all inventoried with 0.02 hectare fixed-radius plots. Plot center locations were established with a Trimble Geo7x GPS capable of submeter accuracy. A minimum of 50 GPS points were collected at each plot center and were differentially post processed based on the nearest continuously referenced base stations. A total of 267 plot locations were measured and 260 locations were collected using the Trimble Geo7x. Missing plot centers were due to a combination of missed field collections and GPS data post-processing limitations.

On each sample unit, all living planted stems were recorded and measured for diameter at breast height (DBH). Only living natural stems DBH >= 7.62 cm were recorded and measured for DBH. A subset of planted trees was measured for total height. With few exceptions, a minimum of 25 planted tree heights across the diameter distribution were measured in each stand with at least one height measured per plot (except for plots with no trees). For natural loblolly pine, Virginia pine (*Pinus virginiana*), and shortleaf pine (*Pinus echinata*), a subset of heights was measured across the diameter distribution. Planted pine heights not measured were predicted with heights measured at the stand level using equation 1. Natural pine heights measured were pooled region-wide and used to fit the regression model for predicting unmeasured heights, also using the model form in equation 3-1.

$$ln(HT) = b_0 + b_1 DBH^{-1} \qquad \text{Equation 3-1}$$

In addition to all coniferous species, hardwood trees (DBH >= 7.62 cm) were measured for DBH and a subset of heights was measured. Following definitions of dominant height given by Gyawali and Burkhart (2015), the top 80% of planted pine heights per plot were used in place of mean dominant height. For all trees, volumes were estimated using allometric equations presented in Table 3-1.

Table 3-1. Sources of allometric equations used to estimate total stem volume.

Species / Species Group	Source
Planted loblolly pine	Tasissa et al. 1997 (unthinned coefficients)
Natural loblolly, Virginia, and shortleaf >= 12.7 cm DBH	Tasissa et al. 1997 (unthinned coefficients)
Natural loblolly, Virginia, and shortleaf < 12.7 cm DBH	Warner and Goebel 1963
Hardwoods with no measured total height	Clark et al. 1986 (table 10 coefficients)
Hardwoods with measured total height	Clark et al. 1986 (table 14 coefficients)

All field data were processed using R (R Core Team 2018). Additional R packages used for graphics and data processing include the following: ggplot2 (Wickham 2016), xlsx (Dragulescu and Arendt 2018) and reshape2 (Wickham 2007).

3.3.2. Auxiliary Information

For the entire study area, 1-meter digital elevation models (DEM) and the associated lidar point clouds used to generate them were obtained from publicly available data maintained by the United States Geological Survey (USGS). ABSF and CUSF were part of the 2015 “Chesapeake Bay” lidar campaign while PESF was part of the 2014 “Sandy” campaign. Details of these two lidar collections are found in Table 3-2. The DEMs and the associated lidar point clouds are available from the USGS National Map (USGS 2017a; USGS 2017b).

Table 3-2. Lidar specifications for the Chesapeake Bay and Sandy projects.

	Chesapeake Bay	Sandy
Collection Dates	Nov. 15, 2015 – Mar. 30, 2016	Mar. 24, 2014 – Apr. 21, 2014
Sensor	Riegl 680i	Leica ALS60 or Leica ALS70
Scan Angle (degrees)	60	unreported
Point Density (pnts*m^-2)	2.3	unreported
Nominal Pulse Spacing (m)	0.66	0.7
Flight Line Overlap	55%	30% (ALS60) or 20% (ALS70)
Pulse Rate (kHz)	200	154.3 (ALS60) or 301.6 (ALS70)

Additionally, stand thinning status was used as auxiliary information for both area- and unit-level analysis. Stands and plots that had received at least one thinning treatment (not including pre-commercial thinning) were classified as thinned. No distinction was made between plots and stands that had one thinning treatment and those that had received multiple. Thinning status was obtained from stand attribute information and confirmed during the field inventory.

3.3.2.1. Processing Auxiliary Information

USGS delivers elevation data in tiles that were smaller than the areas of interest for this study. Stand boundaries often overlapped into multiple tiles. To facilitate and simplify analysis, the individual DEM tiles were merged and mosaicked using QGIS to produce a single 1-meter DEM for each state forest. The lasmerge tool in the LAStools suite (LAStools 2018) was used to combine the individual lidar tiles into a single lidar dataset for each state forest. The merged lidar dataset was clipped to each area of interest (stands for area-level analysis and plots for unit-level analysis) using lasclip in the LAStools suite. The DEMs were converted from ascii to DTM format using the ASCII2DTM tool in FUSION needed for further analysis with other FUSION tools (McGaughey 2018). For all lidar analyses, an area-based approach was utilized due to its relatively low computational demands and ability to accurately estimate stand parameters of interest. Lidar metrics were generated using the FUSION GridMetrics and Cloudmetrics tools. For area-level analysis, each stand was tessellated into a regular grid where the grid size was set to approximately the same size as the sample units used for the specific stand. Unit-level analysis used the Clipdata tool to normalize the lidar point clouds followed by Cloudmetrics to generate plot-level metrics. Lidar metrics were summarized using R. Returns >= 30.5 m above ground were excluded as all measured heights were lower than this value. Following this subset, any heights > third quantile + 1.5*(Interquartile range) were removed in the gridded metrics for area-level analysis. The subsets were to account for overlapping, large canopies from remnant trees and adjacent stands that may have caused an overestimation of height percentiles. Filtered grid cell percentiles were averaged to produce stand-level lidar attributes (e.g. a stand level 80^{th} percentile lidar height). A variety of R packages were used for geospatial processing

tasks such as reprojecting and subsetting spatial layers throughout the workflow. These packages include the raster package (Hijmans 2019), the sp package (Pebesma and Riband 2005; Bivand et al. 2013), and the rgdal package (Bivand et al. 2019).

3.3.3. Direct Estimators

Under the assumption of an equal probability simple random sample in stand i for the parameter of interest θ_i, the direct estimate of the mean is

$$\hat{\theta}_i = \bar{y}_i = n_i^{-1} \sum_{j=1}^{n_i} y_{ij} \quad \text{Equation 3-2}$$

and the variance of the estimate is

$$\widehat{\Psi}_i = Var(\hat{\theta}_i) = n_i^{-1} \frac{\sum(y_{ij} - \bar{y}_i)^2}{n_i - 1} \quad \text{Equation 3-3}$$

where y_{ij} is sample plot j in small area i and n_i is the sample size for area i.

3.3.4. Small Area Estimators

3.3.4.1. Area-level[1]

Given a properly designed sample in area i, a direct estimator for parameter of interest θ_i is available (eq. 3-4):

$$\hat{\theta}_i + e_i \quad \text{Equation 3-4}$$

where e_i in eq. 4 are individual random errors iid $N(0, \Psi_i)$. In many cases, however, an insufficient sample intensity leads to a direct estimate that is not reliable enough for a given management objective, (i.e. an inflated variance Ψ_i leading to an unacceptably wide confidence interval). In cases where auxiliary information is available for area i, we assume the parameter of interest θ_i can be linearly related to a set of covariates $\boldsymbol{z}$ through eq. 3-5:

$$\theta_i = \boldsymbol{z_i^T \beta} + b_i v_i \quad \text{Equation 3-5}$$

where $\boldsymbol{z}_i$ is a vector of area-specific covariates, $\boldsymbol{\beta}$ is the vector of regression coefficients, b_i are positive constants (often assumed to equal 1), and v_i are area-specific random effects that are assumed iid $N(0, \sigma_v^2)$. Combining eq. 4 and 5 leads to the following mixed model:

[1] *The proceeding descriptions of area-level small area estimators incorporates a combination of notation used in Goerndt et al. 2011 and Rao and Molina 2015.*

$$\hat{\theta}_i = \boldsymbol{z_i^T \beta} + b_i v_i + e_i$$ Equation 3-6

where all terms are as previously described in eq. 3-4 and 3-5.

Prior to estimation, sampling error variance (Ψ_i) and random error variance (σ_v^2) must be estimated and partitioned. In this study, variances calculated directly from the sample units were used as an estimate for Ψ_i. The estimated sample variance ($\widehat{\Psi}_i$) was utilized to estimate $\widehat{\sigma_v^2}$ using the restricted maximum likelihood (REML) method as implemented in the R SAE package (Molina and Marhuenda 2015).

The empirical best linear unbiased predictor (EBLUP) was then obtained with the composite estimator in equation 3-7:

$$\hat{\theta}_i^H = \hat{\gamma}_i \widehat{\theta}_\iota + (1 - \hat{\gamma}_i) \boldsymbol{z_i^T} \hat{\beta}$$ Equation 3-7

where γ is a weight using both sources of error accounted for previously and is defined in equation 3-8.

$$\gamma_i = \widehat{\sigma_v^2} / (\widehat{\sigma_v^2} + \widehat{\Psi}_i)$$ Equation 3-8

Final EBLUP and MSE estimates were obtained through the "mseFH" function in the R SAE package. The default REML method was used as were the default maximum iterations (100), and the default precision (0.0001). The MSE estimation involves three components:

$$\mathrm{g}_{i1}(\widehat{\sigma_v^2}) = \hat{\gamma}_i v(\hat{\theta}_i)$$ Equation 3-9

$$\mathrm{g}_{i2}(\widehat{\sigma_v^2}) = (1 - \hat{\gamma}_i)^2 \boldsymbol{z_i^T} ((\frac{\hat{\gamma}}{\widehat{\sigma_v^2}} \boldsymbol{Z})^T \boldsymbol{Z})^{-1} \boldsymbol{z}_d$$ Equation 3-10

$$\mathrm{g}_{\mathrm{i}3}(\widehat{\sigma_v^2}) = (1 - \hat{\gamma}_i)^2 \frac{2}{\sum_{\mathrm{i}}^{\mathrm{l}} \left(\frac{\hat{\gamma}}{\widehat{\sigma_v^2}}\right)^2} \left(\widehat{\sigma_v^2}\, \mathrm{v}(\hat{\theta}_i)\right)^{-1}$$ Equation 3-11

Where $\boldsymbol{Z}$ is an *I x m* matrix of $\boldsymbol{z_i^T}$ for each domain and $\hat{\boldsymbol{\gamma}}$ is an *I x 1* vector of $\hat{\gamma}_i$ for each domain. The combination of the components leads to the final MSE estimate:

$$MSE(\hat{\theta}_i^H) = \mathrm{g}_{i1}(\widehat{\sigma_v^2}) + \mathrm{g}_{i2}(\widehat{\sigma_v^2}) + 2\mathrm{g}_{\mathrm{i}3}(\widehat{\sigma_v^2})$$ Equation 3-12

For details of REML fitting to obtain EBLUP estimates, readers are directed to Rao and Molina (2015); Datta and Lahiri (2000) provide additional details of the MSE estimation.

3.3.4.2. Unit-level[2]

When data are available at the unit-level (individual sample plots in this study), unit-level SAE methods can be utilized. The nested error unit-level model specifies the observed attribute Y on plot j in area i as:

$$Y_{ij} = \boldsymbol{x_{ij}^T \beta} + u_i + e_{ij} \quad \text{Equation 3-13}$$

where u_i are iid $N(0, \sigma_u^2)$ and e_{ij} are iid $N(0, \sigma_e^2)$.

The EBLUP for a particular small area i is expressed in equation 3-14:

$$\hat{\bar{Y}}_i^{EBLUP} = f_i \bar{y}_{is} + (\bar{\boldsymbol{X}}_{\boldsymbol{i}} - f_i \bar{\boldsymbol{x}}_{\boldsymbol{is}})^T \hat{\boldsymbol{\beta}} + (1 - f_i)\hat{u}_i \quad \text{Equation 3-14}$$

where:

$$f_i = {}^{n_i}/_{N_i} \quad \text{Equation 3-15}$$

$$\bar{y}_{is} = n_i^{-1} \sum_{j \in s_i} Y_{ij} \quad \text{Equation 3-16}$$

$$\bar{\boldsymbol{x}}_{\boldsymbol{is}} = n_i^{-1} \sum_{j \in s_i} \boldsymbol{x_{ij}} \quad \text{Equation 3-17}$$

$$\hat{u}_i = \hat{\gamma}_i (\bar{y}_{is} - \bar{\boldsymbol{x}}_{\boldsymbol{is}}^{\boldsymbol{T}} \hat{\boldsymbol{\beta}}) \quad \text{Equation 3-18}$$

$$\hat{\gamma}_i = \hat{\sigma}_u^2 \Big/ (\hat{\sigma}_u^2 + \tfrac{\hat{\sigma}_e^2}{n_i}) \quad \text{Equation 3-19}$$

Final unit-level EBLUP estimates and the associated MSE values were obtained with the "pbmseBHF" function in the R SAE package. This function uses a REML procedure for fitting and a parametric bootstrap approach for estimating MSE values. The default value of 200 bootstrap samples was utilized. The parametric bootstrap method was utilized to relax some of the restrictions encountered with analytical error estimation methods. For details regarding EBLUP fitting using the REML method, readers are directed to Rao and Molina (2015); González-Manteiga et al. (2008) outline further details regarding the MSE estimation using the bootstrap procedure.

3.4. Results

Stand-level summaries of trees per hectare, basal area per hectare, total volume per hectare, and dominant height are presented in Figure 3-3. Density, basal area, and volume are partitioned into planted, natural, and total (the sum of planted and natural). Dominant height was not considered for natural trees; thus, dominant height is presented

[2] *The proceeding descriptions of unit-level small area estimators incorporates a combination of notation used in Molina and Marhuenda 2015 and Rao and Molina 2015.*

by stand thinning status. A goal of this work was to cover the full range of common entry points in loblolly pine plantation forest inventory. The distributions of stand variables capture a wide range of commonly encountered conditions from canopy closure to final harvest. A common condition encountered was significant natural Virginia pine regeneration which made up a large amount of the natural component as seen Figure 3-3. This is common throughout areas on the periphery of the loblolly pine range including the Piedmont of Virginia. A noted limitation in coverage was the small number of stands that received first thinning in the "typical" window of 12-19 years common in managed pine plantations (Figure 3-2).

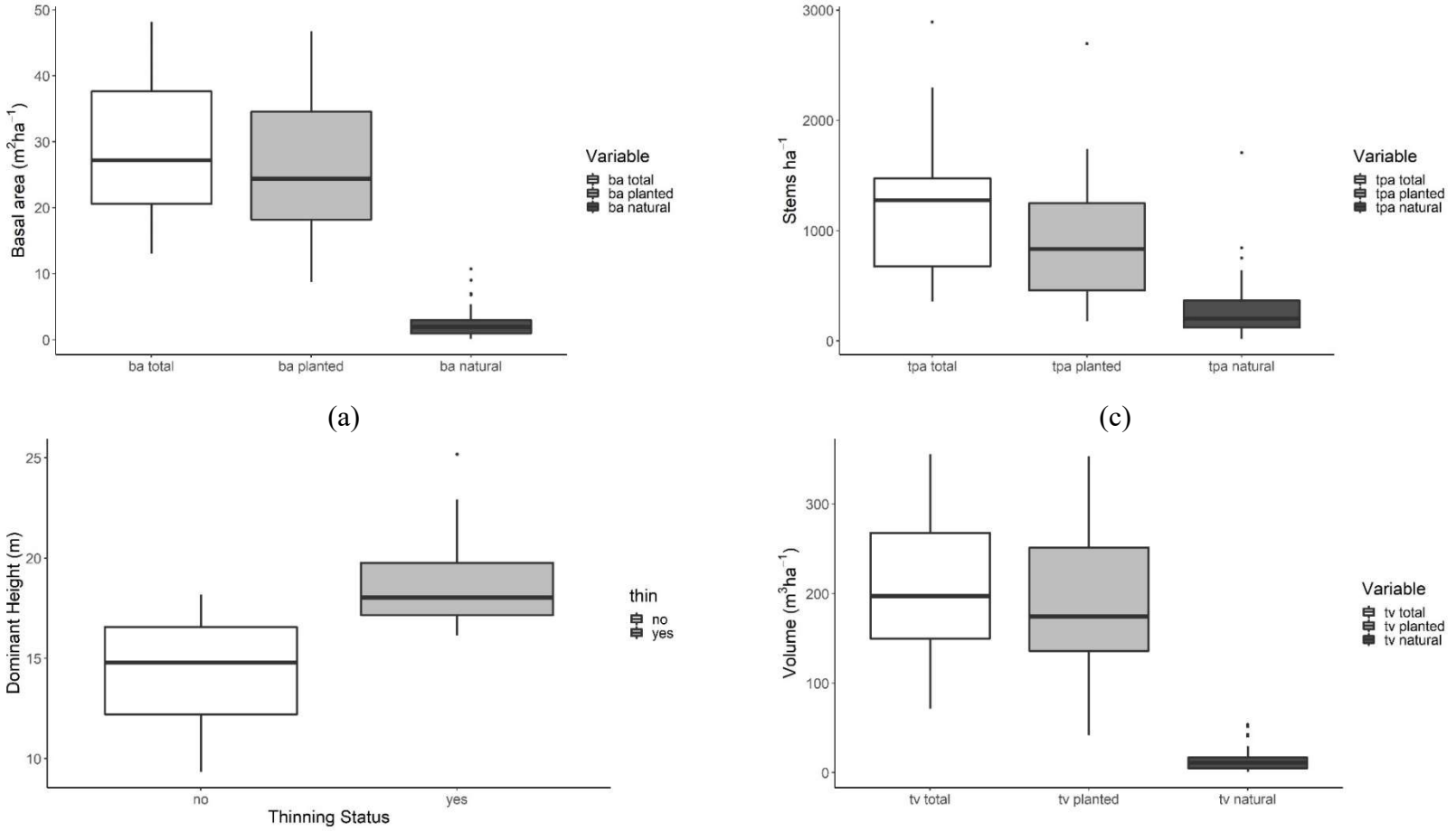

Figure 3-3. Boxplots (Tukey 1977) of stand variables for basal area per hectare (a), dominant height (b), live stems per hectare (c), and volume per hectare (d). Note: Dominant height was not considered for natural trees.

All SAE methods evaluated assume a linear relationship between the parameter of interest and the auxiliary information. The relationship between the auxiliary information (lidar-derived 80th percentile and thinning status) and total planted volume is confirmed in Figure 3-4. The remaining lidar height metrics (90th, 95th, and 99th percentiles) had very similar relationships thus the figures are not presented.

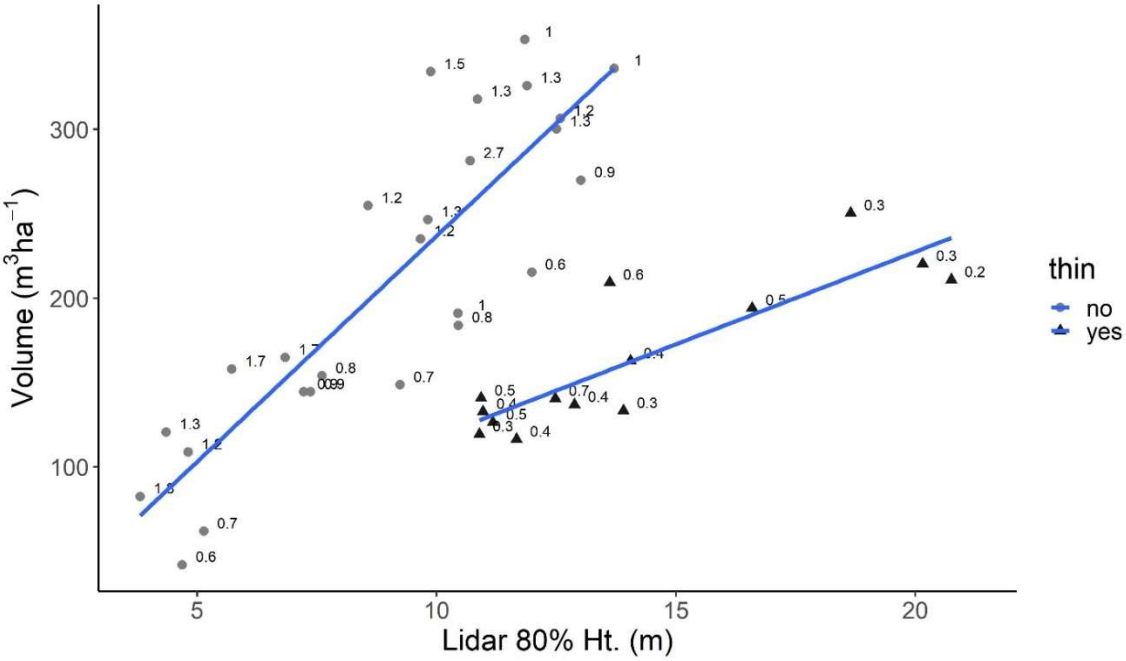

Figure 3-4. Linear relationship between auxiliary information (80th height percentile from lidar), with dependent variable of interest (total cubic volume per hectare) by thinning status (light gray round points are unthinned and dark gray triangular points are thinned). Points are labeled with direct estimate of surviving planted stem density in thousands of trees per hectare at the time of inventory. Linear fit by thinning status indicates the importance of including thinning status as explanatory variable.

For the following results and discussion, relative error ratios (RER), were constructed for comparisons between the precision of the model EBLUP and direct estimates. For SAE models the RER for small area i is

$$RER_i\ (\%) = \frac{\sqrt{MSE(eblup_i)}}{EBLUP_i} * 100 \qquad \text{Equation 3-20}$$

and the RER for the direct estimate is

$$RER_i\ (\%) = \frac{\sqrt{Var(\hat{\theta}_i)}}{\bar{y}_i} * 100 \qquad \text{Equation 3-21}$$

where $\bar{y}_i$ and $Var(\hat{\theta}_i)$ are as defined in equations 3-2 and 3-3 respectively.

A RER is similar to a coefficient of variation in that it standardizes the variation of the estimate to the estimate itself. The RERs were visually compared for each stand

using 1-1 scatterplots. In the following figures, any point falling below the 1-1 line indicated a smaller model RER for the estimate type on the y-axis. In addition, 1-1 scatterplots were used to compare direct estimates to SAE estimates.

3.4.1. Area-level SAE

Area-level SAE models that utilized only a lidar height percentile resulted in small gains in precision for some stands (Figure 3-5a). The incorporation of both a lidar height percentile and thinning status resulted in larger gains in precision (Figure 3-5b). Modeled total volume estimates generally followed the 1-1 relationship with the direct estimates for both model forms (Figure 3-5c and 3-5d). Additional lidar height percentiles were evaluated (90^{th}, 95^{th}, and 99^{th}) resulting in similar goodness of fit statistics (Table 3-3). The Akaike information criterion (AIC) and Bayesian information criterion (BIC), two forms of a penalized likelihood criteria, were calculated for model performance. Models that used the lidar 80^{th} height percentile exhibited the lowest AIC and BIC values. For consistency, models that use the 80^{th} percentile was used for all figures and further discussion.

Table 3-3. Goodness of fit summaries for area-level models considered for estimating total volume.

Model Fit	AIC	BIC
TV_Planted ~ P80	675.80	680.87
TV_Planted ~ P90	675.91	680.97
TV_Planted ~ P95	675.86	680.93
TV_Planted ~ P99	675.46	680.53
TV_Planted ~ P80 + thin_status	640.08	646.83
TV_Planted ~ P90 + thin_status	640.91	647.66
TV_Planted ~ P95 + thin_status	641.40	648.16
TV_Planted ~ P99 + thin_status	642.44	649.20

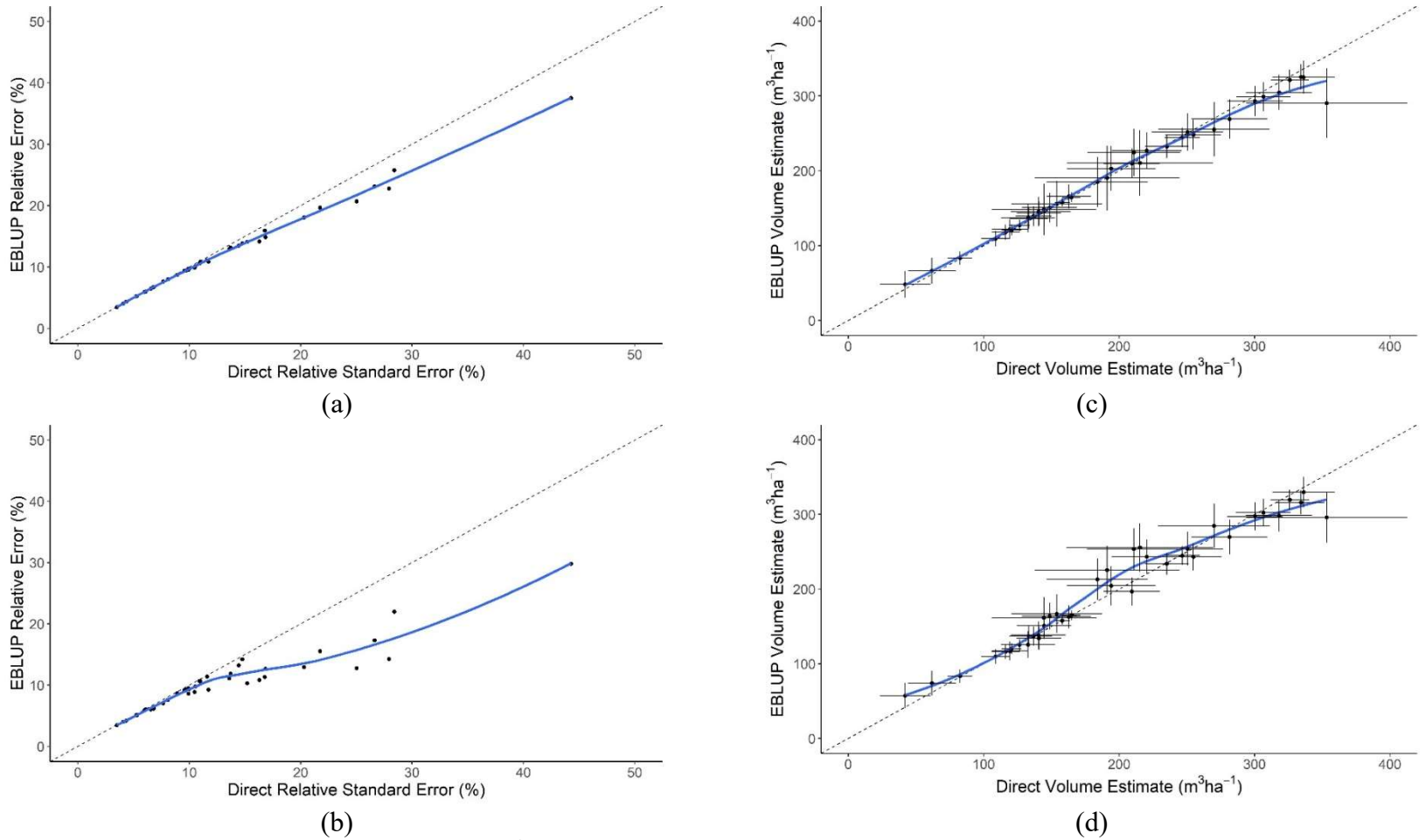

Figure 3-5. Area-level SAE results. (a) Model with lidar 80th height percentile as only auxiliary information relative error comparison and (b) model with lidar 80th height percentile and thinning status as auxiliary information relative error comparison. (c) Estimate comparison for model with lidar 80th height percentile as only auxiliary information and (d) estimate comparison for model with lidar 80th height percentile and thinning status as auxiliary information. Smoothing lines are for visual interpretation only and are not representative of the SAE model fit. Error bars represent one standard error in the x direction and the root mean squared error in the y direction.

3.4.2. Unit-level SAE

Unit-level SAE models were evaluated using lidar height percentiles alone and with thinning status included. The unit-level approach resulted in large increases in precision for some of the stands evaluated; however, a decrease in precision of estimates was observed for some stands, especially those with low variability in the direct estimate (Figure 3-6a). The unit-level models tended to produce estimates that were larger than the associated direct estimates (Figure 3-6c and 3-6d). In addition to the lidar 80^{th} height percentile, the 90^{th}, 95^{th}, and 99^{th} percentiles were evaluated (Table 3-4). Models that used the lidar 80^{th} height percentile exhibited the lowest AIC and BIC values. For consistency, models that use the 80^{th} percentile was used for all figures and further discussion.

Table 3-4. Goodness of fit summaries for unit-level models considered for estimating total volume. Values not calculated directly in the SAE R function. Values calculated from the definitions of AIC and BIC and the log likelihood value calculated with the SAE function.

Model Fit	AIC	BIC
TV_Planted ~ P80	4219.43	4233.67
TV_Planted ~ P90	4237.72	4251.96
TV_Planted ~ P95	4243.65	4257.90
TV_Planted ~ P99	4254.06	4268.31
TV_Planted ~ P80 + thin_status	4140.88	4158.68
TV_Planted ~ P90 + thin_status	4164.39	4182.20
TV_Planted ~ P95 + thin_status	4172.33	4190.14
TV_Planted ~ P99 + thin_status	4186.52	4204.33

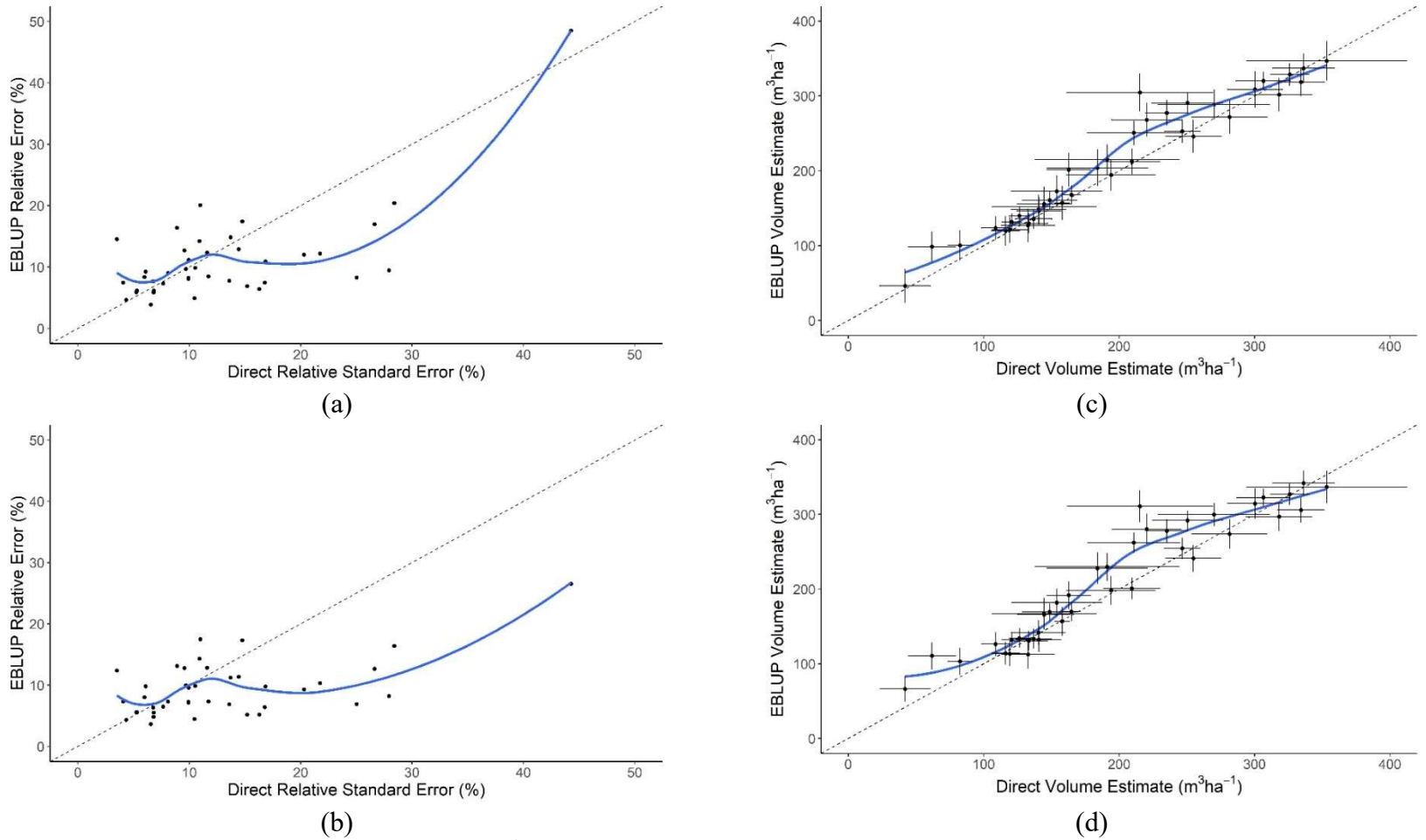

Figure 3-6. Unit-level SAE results. (a) Model with lidar 80th height percentile as only auxiliary information relative error (RE) comparison and (b) best performing model with lidar 80th height percentile and thinning status as auxiliary information RE comparison. (c) Estimate comparison for model with lidar 80th height percentile as only auxiliary information and (d) estimate comparison for best performing model with lidar 80th height percentile and thinning status as auxiliary information. Smoothing lines are for visual interpretation only and are not representative of the SAE model fit. Error bars represent one standard error in the x direction and the root mean squared error in the y direction.

3.4.3. Comparison

Area- and unit-level models are visually compared in Figure 3-7. A comparison was first made between the area- and unit-level models that utilized only the same 80th percentile height as the auxiliary information. As seen in Figure 3-7a, the unit-level model can potentially result in larger gains in precision compared to the area-level model, particularly at some higher levels of variation. The inclusion of thinning status resulted in similar relationships (Figure 3-7b). Despite these potential improvements, the mean RERs were very similar or higher for all model forms evaluated (Table 3-5). Area-level models more often and on average, resulted in larger decreases in uncertainty compared with the unit-level models evaluated.

Table 3-5. Comparison of error ratio means of SAE vs. direct estimates of area- and unit-level models.

Model Fit	Area-level Error Ratio	Unit-level Error Ratio	Count of Stands where Area-level ratio <= Unit-level ratio
TV_Planted ~ P80	0.95	1.09	24
TV_Planted ~ P90	0.95	1.14	24
TV_Planted ~ P95	0.95	1.16	24
TV_Planted ~ P99	0.95	1.18	26
TV_Planted ~ P80 + thin_status	0.89	0.97	21
TV_Planted ~ P90 + thin_status	0.89	1.01	25
TV_Planted ~ P95 + thin_status	0.89	1.04	25
TV_Planted ~ P99 + thin_status	0.89	1.07	26

While estimates were generally similar, the unit-level estimates were consistently higher in most cases compared with the area-level estimates without thinning status included (Figure 3-7c) and when thinning status is incorporated (Figure 3-7d).

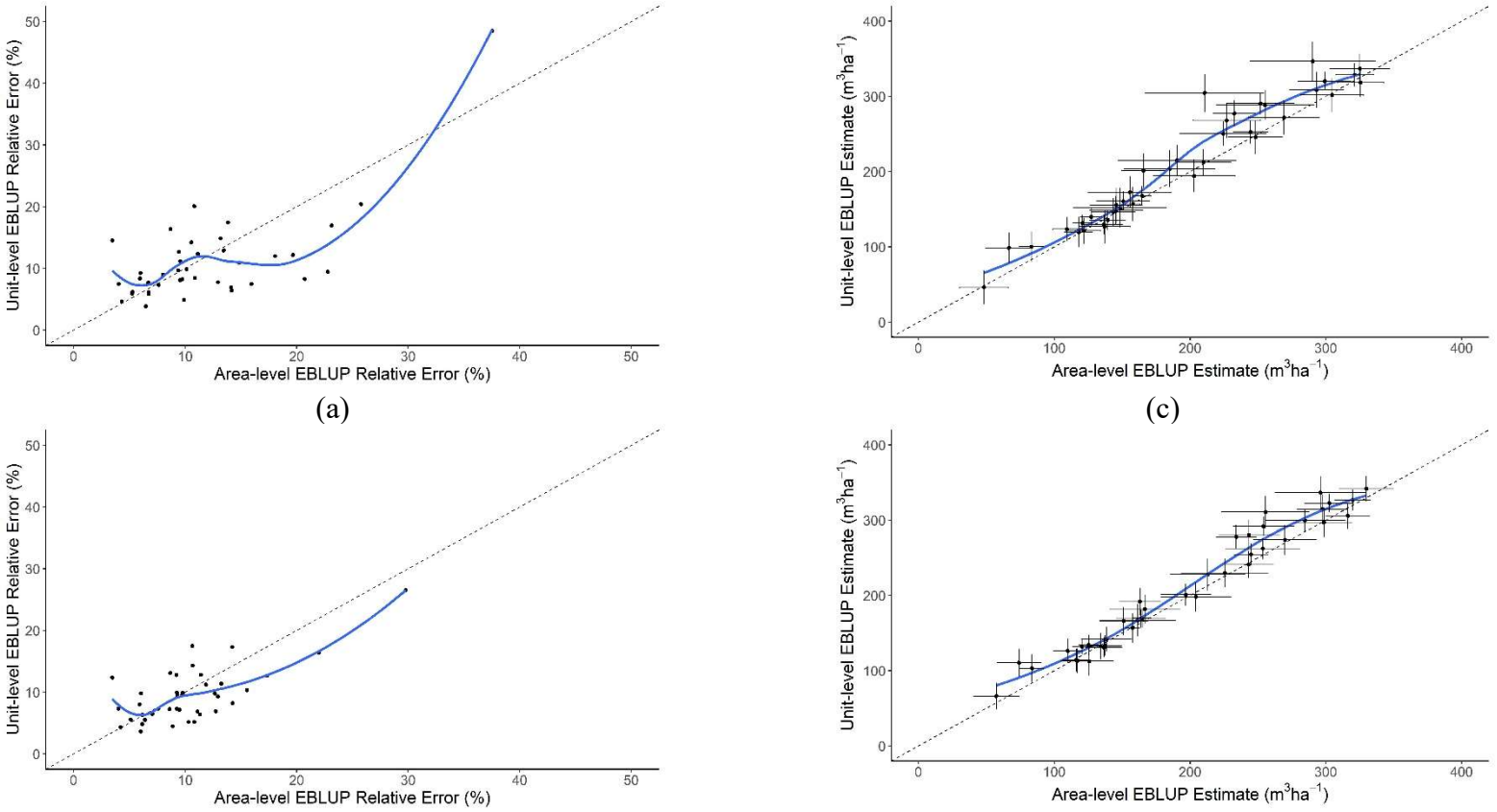

Figure 3-7. Comparison of area- and unit-level SAE models. (a) Relative error (RE) comparison between area- and unit-level models using the lidar 95th percentile height as the only auxiliary variable, (b) RE comparison between area- and unit-level models where the area-level model includes both the lidar 95th percentile height and thinning status as auxiliary information and the unit-level only includes the 95th percentile height as the auxiliary variable, (c) Estimate comparison between area- and unit-level models using the lidar 95th percentile height as the only auxiliary variable and (d) Estimate comparison between area- and unit-level models where the models include both the lidar 95th percentile height and thinning status as auxiliary information. Smoothing lines are for visual interpretation only and are not a representative of the SAE model fit. Error bars represent model RMSE in the x and y directions.

3.5. Discussion

The results of this research have confirmed the potential for reducing volume estimate uncertainty using SAE techniques. Both area and unit-level approached reduced the relative error of the estimate for small areas (stands) compared to less precise direct estimates. Much like Goerndt et al. (2011), Magnussen et al. (2017), and Mauro et al. (2017), lidar was shown to be an effective source of auxiliary information that could be leveraged for use in SAE models. An interesting aspect in this work is that despite the lidar data having been acquired 4-5 years prior to collection of field inventory data, the linear relationship between total planted volume and the auxiliary data was still strong. This follows with McRoberts et al. (2018) in which lidar was found to remain useful in model-assisted estimation many years after collection. If more recent lidar collections were available, additional gains in precision could possibly be achieved, assuming a stronger linear relationship would be found with close temporal matching of lidar and field data collection.

Due to their ability to use finer-scale data, unit-level SAE models can offer greater gains in precision compared with area-level models (Molina and Marhuenda 2015); however, they require precise co-registration of ground sample plots and the associated lidar. High accuracy GPS units are not always readily available, limiting the potential for unit-level estimation in some situations. Variable radius plots pose additional challenges to unit-level methods due to the sample unit's lack of a defined spatial area. Further, some auxiliary information cannot always be summarized at the unit-level. Thinning status is generally a stand-level attribute and cannot easily be incorporated into the unit-level framework unless recorded at the plot level as it was in this study. Despite these limitations, the unit-level models did provide improvements in precision in this work when compared with area-level analysis for some stands, especially those that exhibited large direct estimate variances. The incorporation of both lidar height percentiles and thinning status did offer improvements in precision to both the area- and unit-level analysis. Unit-level model estimates on average, generally had higher variance than direct or area-based estimates and produced estimates that exceeded both the direct and area-level estimates. While unit-level models are unbiased, the

EBLUP estimator requires the true population values for the covariates to be known. In this analysis, there were discrepancies between the stand estimates derived from the area-level gridded lidar metrics and the averages from the unit-level cloud metrics. The unit-level 80th percentile height estimates were, on average, approximately 0.5 meters lower than the gridded area-level heights. This is likely due to a combination of spatial grid smoothing and edge effects from overlapping neighboring tree crowns that were not completely accounted for by filtering gridded area-level outliers. Additionally, differences may have arisen due to the two methods used to summarize the lidar point clouds. Finally, despite using a GPS capable of submeter accuracy, location error likely resulted in auxiliary information being summarized for locations different than the areas measured. Future investigations should focus on refining methods to remediate this disparity.

An important assumption when applying SAE techniques is a linear relationship between the auxiliary data and the variable of interest (Rao and Molina 2015). For this work, we chose to consider a limited set of auxiliary variables that have a theoretical basis for their relationships with our variable of interest total volume. The 80th, 90th, 95th, and 99th height percentiles are of the most interest due to the linear relationship with height and total volume at similar basal areas Burkhart et al. (2019) and in closed canopy stands (Yanli et al. 2019). While height growth has been found to be significantly affected by density in some studies, within the ranges of densities commonly planted (~741 – 2223 tph) differences in height due to density have been found to be either non-significant (Zhao et al. 2011) or of relatively minor differences (e.g. Sharma et al. 2002, Antón-Fernández et al. 2011). Despite the relationship between height and total volume, density is important to consider. The inclusion of stand-level thinning status as auxiliary information, in effect, served as a proxy for density and helped "adjust" the volume estimate rather than using lidar-derived height metrics alone. As evident in figure 3-4, much of the additional unexplained variation in the linear relationship between the auxiliary data and total planted volume is due to the lidar and thinning status not fully taking stand density into account. In most cases, unthinned planted volume that was underestimated by the linear relationship had higher estimated planted stem density than those overestimated by the linear relationship. While lidar metrics have been used to

successfully predict stem density, the relationships are generally not as strong as other stand characteristics (Næsset and Bjerknes 2001; Næsset 2002; Noordermeer et al. 2019). For this reason, we chose to not include lidar estimates of stand density in this work.

SAE was shown to reliably improve estimate precision in this study; however, these models have limitations. The SAE methods evaluated are not applicable when a direct estimate is not available (Goerndt et al. 2011). In these cases, a model-based, synthetic estimate would be required. Further, it is assumed that sample variances ($\widehat{\Psi}_i$) are known without error. While this is often an improbable assumption, it is required for area-level models (Magnussen et al. 2017). Unit-level models are generally more restrictive and not applicable in cases where fine-scale, sample unit data are not available (Magnussen et al. 2017).

3.6. Conclusions

This work has successfully demonstrated the potential for incorporating SAE techniques into operational forest inventory in loblolly pine plantations. Using both lidar and thinning status, the uncertainty of total planted volume estimates was reduced in many cases. To specifically answer our research questions outlined: 1) Area-level SAE methods improved the precision compared with direct estimates for all lidar height percentiles evaluated, 2) Unit-level SAE methods improved the precision of estimates in some stands, particularly when the direct estimates exhibited high variability for all lidar height percentiles evaluated, 3) Unit-level models demonstrated increased precision in some cases compared with area-level methods; however, the average error ratios were lower for area-level methods, and 4) The incorporation of additional auxiliary information, in this case thinning status, improved estimation precision in both model formulations. The results of this study should be of interest to forest inventory managers who regularly conduct forest inventory in southern pine plantations. With the increased importance of enhancing and monitoring the productivity of loblolly pine for both commercial and ecological interests such as carbon sequestration (Zhao et al. 2016), accurate and precise estimates of stand volume are essential. Using the methods outlined in this study, the precision of inventory estimates can be improved leading to more confidence when making management and planning decisions. The area-level SAE

methods evaluated are broadly applicable to many cases in which linearly related covariates are available. Additional gains in precision can be realized if ancillary information can be coupled with data from fixed-area plots with highly accurate center locations under the unit-level SAE framework; however, these methods did not result in precision increases in all stands.

3.7. References

Andreu, M.G., Zobrist, K., Hinckley, T., 2008. Management practices to support increased biodiversity in managed loblolly pine plantations. Pub. FOR183. Gainesville, FL. University of Florida IFAS Extension.

Antón-Fernández, C., Burkhart, H.E., Strub, M., Amateis, R.L., 2011. Effects of initial spacing on height development of loblolly pine. For. Sci. 57(3), 201-211.

Battese, G.E., Harter, R.M., Fuller, W.A., 1988. An error-components model for prediction of county crop areas using survey and satellite data. J. Am. Stat. Assoc. 83(401), 28-36.

Bivand, R., Keitt, T., Rowlingson, B., 2019. rgdal: Bindings for the 'Geospatial' Data Abstraction Library. R package version 1.4-3. https://CRAN.R-project.org/package=rgdal

Bivand, R.S., Pebesma, E., Gomez-Rubio, V., 2013. Applied spatial data analysis with R, Second edition. Springer, NY. http://www.asdar-book.org/

Breidenbach, J., Astrup, R., 2012. Small area estimation of forest attributes in the Norwegian National Forest Inventory. Eur. J. For. Res. 131(4), 1255-1267. https://doi.org/10.1007/s10342-012-0596-7

Breidenbach, J., Magnussen, S., Rahlf, J., Astrup, R., 2018. Unit-level and area-level small area estimation under heteroscedasticity using digital aerial photogrammetry data. Remote Sens. Environ. 212, 199-211.

Burkhart, H.E., Avery, T.E. and Bullock, B.P., 2019. Forest measurements 6th ed. Waveland Press, Long Grove, IL. pp 434.

Campbell, J.B., Wynne, R.H., 2011. Introduction to remote sensing 5th ed. Guilford Press, New York, NY. pp 667.

Clark, Alexander, III; Phillips, Douglas R.; Frederick, Douglas J. 1986. Weight, Volume, and Physical Properties of Major Hardwood Species in the Piedmont. Res. Pap. SE-255. Asheville, NC: U.S. Department of Agriculture, Forest Service, Southeastern Forest Experiment Station. 84 p.

Datta, G.S., Lahiri, P., 2000. A unified measure of uncertainty of estimated best linear unbiased predictors in small area estimation problems. Statistica Sinica 10, 613-627.

Dragulescu, A. A., Arendt, C., 2018. xlsx: Read, Write, Format Excel 2007 and Excel 97/2000/XP/2003 Files. R package version 0.6.1. https://CRAN.R-project.org/package=xlsx

Fay III, R.E., Herriot, R.A., 1979. Estimates of income for small places: an application of James-Stein procedures to census data. J. Am. Stat. Assoc. 74(366a), 269-277.

Fox, T.R., Jokela, E.J., Allen, H.L., 2007. The development of pine plantation silviculture in the southern United States. J. For. 105(7), 337-347.

Goerndt, M.E., Monleon, V.J., Temesgen, H., 2011. A comparison of small-area estimation techniques to estimate selected stand attributes using LiDAR-derived auxiliary variables. Can. J. For. Res. 41, 1189-1201. https://doi.org/10.1139/x11-033

Goerndt, M.E., Monleon, V.J., Temesgen, H., 2013. Small-area estimation of county-level forest attributes using ground data and remote sensed auxiliary information. For. Sci. 59(5), 536-548. https://doi.org/10.5849/forsci.12-073

González-Manteiga, W., Lombardía, M.J., Molina, I., Morales, D., Santamaría, L., 2008. Bootstrap mean squared error of a small-area EBLUP. J. Stat. Comput. Simul. *78*(5), 443-462.

Gyawali, N., Burkhart, H.E., 2015. General response functions to silvicultural treatments in loblolly pine plantations. Can. J. For. Res. 45, 252-265.

Hijmans, R.J., 2019. raster: Geographic Data Analysis and Modeling. R package version 2.8-19. https://CRAN.R-project.org/package=raster

Holmgren, J., 2004. Prediction of tree height, basal area and stem volume in forest stands using airborne laser scanning. Scand. J. For. Res. 19, 543-553.

Jokela, E.J., Martin, T.A., Vogel, J.G., 2010. Twenty-five years of intensive forest management with southern pines: important lessons learned. J. For. 108(7), 338-347.

Johnsen, K.H., Wear, D., Oren, R., Teskey, R.O., Sanchez, F., Will, R., Butnor, J., Markewitz, D., Richter, D., Rials, T., Allen, H.L., 2001. Meeting global policy commitments: carbon sequestration and southern pine forests. J. For. 99(4), 14-21.

LAStools, "Efficient LiDAR Processing Software" (version 180620, academic), obtained from http://rapidlasso.com/LAStools

Magnussen, S., Mauro, F., Breidenbach, J., Lanz, A., Kändler, G., 2017. Area-level analysis of forest inventory variables. Eur. J. For. Res. 136, 839-855.

Maltamo, M., Næsset, E., Vauhkonen, J., 2014. Forestry applications of airborne laser scanning. *Concepts and case studies.* Manag. For. Ecosys. 27. pp 460.

Mauro, F., Monleon, V.J., Temesgen, H., Ford, K.R., 2017. Analysis of area level and unit level models for small area estimation in forest inventories assisted with LiDAR auxiliary information. PloS one, 12(12), p.e0189401. https://doi.org/10.1371/journal.pone.0189401

McCombs, J.W., Roberts, S.D., Evans, D.L., 2003. Influence of fusing lidar and multispectral imagery on remotely sensed estimates of stand density and mean tree height in a managed loblolly pine plantation. For. Sci. 49(3), 457-466.

McGaughey, R., 2018. FUSION/LDV: Software for lidar data analysis and visualization. FUSION version 3.80. Available online at: http://forsys.cfr.washington.edu/fusion/fusion_overview.html

McRoberts, R.E., Chen, Q., Gormanson, D.D., Walters, B.F., 2018. The shelf-life of airborne laser scanning data for enhancing forest inventory inferences. Remote Sens. Environ. 206, 254-259.

Means, J., Acker, S., Fitt, B., Renslow, M., Emerson, L., Hendrix C.J., 2000. Predicting forest stand characteristics with airborne scanning lidar. Photo. Eng. Rem. Sens. 66(11), 1367-1371.

Militino, A.F., Ugarte, M.D., Goicoa, T., González-Audícana, M., 2006. Using small area models to estimate the total area occupied by olive trees. Journal of Agricultural, Biological, and Environmental Statistics 11(3), 450-461.

Molina, I., Marhuenda, Y., 2015. sae: An R Package for Small Area Estimation. The R Journal **7**(1), 81–98. https://journal.r-project.org/archive/2015/RJ-2015-007/RJ-2015-007.pdf.

Næsset, E., 1997a. Determination of mean tree height of forest stands using airborne laser scanning data. ISPRS J. Photo. Rem. Sens. 52, 49-56.

Næsset, E., 1997b. Estimating timber volumes of forest stands using airborne laser scanner data. Remote Sens. Environ. 61, 246-253.

Næsset, E., Bjerknes, K-O., 2001. Estimating tree heights and number of stems in young forest stands using airborne laser scanning data. Remote Sens. Environ. 78, 328-340.

Næsset, E., 2002. Predicting forest stand characteristics with airborne scanning laser using a practical two-stage procedure and field data. Remote Sens. Environ. 80, 88-99.

Næsset, E., 2004a. Practical large-scale forest stand inventory using a small-footprint airborne scanning laser. Scand. J. For. Res. 19, 164-179.

Næsset, E., 2004b. Accuracy of forest inventory using airborne laser scanning: evaluating the first Nordic full-scale operational project. Scand. J. For. Res. 19, 554-557.

Næsset, E., 2007. Airborne laser scanning as a method in operational forest inventory: status of accuracy assessments accomplished in Scandinavia. Scand. J. For. Res. 22, 433-442.

Nelson, R., Krabill, W., Maclean, G., 1984. Determining forest canopy characteristics using airborne laser data. Remote Sens. Environ. 15, 201-212.

Nelson, R., Krabill, W., Tonelli, J., 1988. Estimating forest biomass and volume using airborne laser data. Remote Sens. Environ. 24, 247-267.

Noordermeer, L., Bollandsås, O.M., Økra, H.O., Næsset, E, Gobakken, T., 2019. Comparing the accuracies of forest attributes predicted from airborne laser scanning and digital aerial photogrammetry in operational forest inventories. Remote Sens. Environ. 226, 26-37.

Pebesma, E.J., R.S. Bivand., 2005. Classes and methods for spatial data in R. R News 5 (2), https://cran.r-project.org/doc/Rnews/.

Popescu, S.C., Wynne, R.H., 2004. Seeing the trees in the forest: Using lidar and multispectral data fusion with local filtering and variable window size for estimating tree height. Photo. Eng. Rem. Sens. 70(5), 589-604.

Popescu, S.C., Wynne, R.H., Nelson, R.F., 2003. Measuring individual tree crown diameter with lidar and assessing its influence on estimating forest volume and biomass. Can. J. Rem. Sens. 29(5), 564-577.

QGIS Development Team (2019). QGIS Geographic Information System. Open Source Geospatial Foundation Project. http://qgis.osgeo.org

R Core Team, 2018. R: a language and environment for statistical computing [online]. R Foundation for Statistical Computing, Vienna, Austria. Available from http://www.R-project.org/

Rao, J.N.K., Molina, I., 2015. Small Area Estimation. John Wiley & Sons, Inc. pp 441.

Sharma, M., Burkhart, H.E., Amateis, R.L., 2002. Modeling the effect of density on the growth of loblolly pine trees. South. J. Appl. For. 26(3), 124-133.

Schultz, R.P., 1999. Loblolly--the pine for the twenty-first century. New For. 17(1-3), 71-88.

Tasissa, G., Burkhart, H.E., Amateis, R.L., 1997. Volume and taper equations for thinned and unthinned loblolly pine trees in cutover, site-prepared plantations. South. J. Appl. For. 21(3), 146-152.

Tukey, J.W., 1977. Exploratory data analysis. Addison-Wesley.

U.S. Geological Survey, 2017a, 1 meter Digital Elevation Models (DEMs) - USGS National Map 3DEP Downloadable Data Collection: U.S. Geological Survey.

U.S. Geological Survey, 2017b, lidar Point Cloud - USGS National Map 3DEP Downloadable Data Collection: U.S. Geological Survey.

van Aardt, J.A., Wynne, R.H., Oderwald, R.G., 2006. Forest volume and biomass estimation using small-footprint lidar-distributional parameters on a per-segment basis. For. Sci. 52(6), 636-649.

Warner, J.R., Goebel, N.B., 1963. Total and bark volume tables for small diameter Loblolly, Shortleaf, and Virginia Pine in the upper South Carolina Piedmont. Department of Forestry, South Carolina Agricultural Experiment Station, Clemson, South Carolina. Forest Research Series No. 9.

Wickham, H., 2007. Reshaping Data with the reshape Package. Journal of Statistical Software, 21(12), 1-20. URL http://www.jstatsoft.org/v21/i12/.

Wickham, H., 2016 ggplot2: Elegant Graphics for Data Analysis. Springer-Verlag New York.

Yanli, X., Chao, L., Zhichao, S., Lichun, J., Jingyun, F., 2019. Tree height explains stand volume of closed-canopy stands: Evidence from forest inventory data of China. For. Ecol. Manage. 438, 51-56.

Yu, X., Hyyppä, J., Holopainen, M., Vastaranta, M., 2010. Comparison of area-based and individual tree-based methods for predicting plot-level forest attributes. Rem. Sens. 2, 1481-1495.

Zhao, D., Kane, M., Borders, B.E., 2011. Growth responses to planting density and management intensity in loblolly pine plantations in the southeastern USA Lower Coastal Plain. Ann. For. Sci. 68(3), 625-635.

Zhao, D., Kane, M., Teskey R., Fox, T.R., Albaugh, T.J., Allen, H.L., and Rubilar, R., 2016. Maximum response of loblolly pine plantations to silvicultural management in the southern United States. For. Ecol. Manage. 375, 105-111.

Chapter 4 Small area estimation in loblolly pine (*Pinus taeda* L.) plantations: A follow up

4.1. Abstract

In forest inventory, traditional ground-based resource assessments are often expensive and time-consuming forcing managers to reduce sample sizes to meet budgetary and logistical constraints. Small area estimation (SAE) is a class of statistical estimators that uses a combination of traditional survey data and linearly related auxiliary information to improve estimate precision. These techniques have been shown to improve the precision of stand-level inventory estimates in loblolly pine plantations using lidar height percentiles and thinning status as covariates. In this study, the effects of reduced lidar point cloud density and lower digital elevation model (DEM) spatial resolution were investigated for total planted volume estimates using area-level SAE models. Additionally, individual tree detection estimates of stem density were evaluated. Finally, the stability of the observed estimates and precision was investigated. In the conditions evaluated, lower lidar point cloud densities and DEM spatial resolutions were found to have minimal effects on estimates and precision. Density estimates from individual tree detection provided minimal improvements and are not recommended for use in predicting total planted pine volume with area-level SAE models. The observed relationships between the direct estimates and precision and the associated model estimates and precision were found to be similar across 1000 bootstrapped samples. The results of this study are promising to those interested in incorporating SAE methods into forest inventory programs.

4.2. Introduction

Accurate, precise, and up-to-date forest resource assessments are important for informed management decisions. Foresters have often relied on design-based surveys using fixed- and variable-radius sample plots to estimate parameters for the areas of interest (Burkhart et al. 2019). Traditional, ground-based forest inventory provides reliable, unbiased estimates assuming a fully executed, valid sample design. In many cases, however, budgets and logistical issues limit the sample intensity leading to an estimate that does not meet the precision specified in the original design. In the southeastern United States, loblolly pine (*Pinus taeda* L.) is the most widely planted and intensively managed commercial tree species (Baker et al. 1990). With increasing frequency of land ownership changes (Fox et al. 2007; Jokela et al. 2010) and interest in estimating stand characteristics for both commercial and ecological (Andreu et al. 2008; Zhao et al. 2016) reasons, improving the efficiency and reliability of forest inventories in loblolly pine plantations is important to managers. In recent years, advances in remote sensing products, computing capability, and statistical methods have afforded many new options for resource evaluation (Coops 2015). Small area estimation (SAE) is a class of statistical estimators that can leverage auxiliary information derived from, for example, remote sensing products to be used in a composite estimator with ground-based samples for increasing inventory precision. For areas where loblolly pine is grown for commercial use, auxiliary data are often available that can be used with SAE techniques.

4.2.1. Point Cloud Elevation Products

Point clouds are three-dimensional spatial products that characterize an area both horizontally and vertically. Point clouds are generated with active remote sensors including light detection and ranging (lidar) and active microwave (Campbell and Wynne 2011). Advances in software and computing resources have made point clouds generated through photogrammetric techniques operationally possible and comparable to lidar (Goodbody et al. 2019).

The use of point clouds requires a ground elevation model to normalize the canopy characterized by the three-dimensional data. Generally, elevation models generated from lidar have been found to be highly accurate compared with other standard

models such as the United States Geological Survey (USGS) 30- and 10-meter products (e.g. Reutebuch et al., 2003, Hodgson and Bresnahan, 2004) and well suited to use in forest inventory applications (e.g. Tinkham et al., 2012). To our knowledge, no study has assessed the effects of elevation model spatial resolution for normalizing lidar point clouds when used as auxiliary data in SAE.

Point clouds vary in density depending on acquisition parameters such as flight altitude and sensor specifications. There have been multiple reports in the literature that lower point density lidar results in similar estimates as higher density point clouds in area-based analysis (ABA). Holmgren (2004) found small differences in prediction errors for tree height, basal area, and stem volume using lidar with point densities ranging from 0.10 pulses m^{-2} to 4.29 pulses m^{-2}. Similar results were found in an investigation of plot-level volumes with point densities ranging from 0.13 pulses m^{-2} to 12.7 pulses m^{-2} (Maltamo et al., 2006). In a model-assisted framework, Strunk et al. (2012) found minimal losses in estimate precision with point densities as low as 0.13 pulses m^{-2} compared with 3 pulses m^{-2}. In a study investigating a variety of stand variables in *Pinus radiata* D. Don, point densities ranging from 0.5 pulses m^{-2} to 9 pulses m^{-2} were found to provide comparable model precision (González-Ferreiro et al. 2012). Gobakken and Næsset (2008) found that the point density required for an operational inventory in Sweden could be reduced to as low as 0.25 pulses m^{-2} without a significant loss of inventory quality. Some studies have pointed to reduced precision with thinned point clouds. Magnussen et al. (2010) found reliability ratios decreased for common inventory attributes when predicted with progressively more thinned point clouds. In a study investigating the effects of plot size and point density, the prediction of forest structure attributes was found to be highest with the denser point clouds; however, plot size was found to have more impact on predictions (Ruiz et al. 2014).

While characteristics such as height and volume are reliably measured and estimated with active remote sensing, stem density is more challenging to estimate. Due to the variability in crown architecture, the cover metrics used in ABA and the algorithms in individual tree detection (ITD) often have significant error. Despite these challenges, density has been successfully estimated using ABA (Næsset and Bjerknes 2001; Næsset 2002; Noordermeer et al. 2019) and ITD methods (Popescu and Wynne 2004).

4.2.2. Small Area Estimation

SAE models can be broadly classified as either "area-level" or "unit-level". Area-level models relate estimates of the area of interest to area-level covariates derived from the auxiliary data. Unit-level models relate sample unit direct estimates to the corresponding sample unit auxiliary data (Rao and Molina 2015). SAE has been demonstrated to improve inventory precision in the forestry literature through both area-level (Goerndt et al., 2011; Magnussen et al., 2017; Coulston et al., *in prep*; and Green et al. 2019) and unit-level (Breidenbach and Astrup, 2012; Goerndt et al., 2013, Green et al. 2019) approaches. Comparisons between the two SAE methods have found that while unit-level models offer similar or greater increases in precision (Mauro et al., 2017 and Breidenbach et al., 2018), area-level models are flexible and can be widely applied using a variety of data sources (Breidenbach et al. 2018).

4.2.3. Research Objectives and Questions

The overall objective of this work was to expand the investigations into the area-level SAE methods used by Green et al. (2019). Specific follow-up research objectives and questions include the following:

1. What are the impacts on area-level SAE derived estimates and precision using digital elevation models (DEMs) with lower spatial resolution than those derived from lidar?
2. What are the impacts on area-level SAE derived estimates and precision using lidar point clouds with reduced point density?
3. Do stem density estimates from ITD provide additional estimate precision with area-level SAE models?
4. How stable are the relationships between direct estimates and SAE model-based estimates and precision?

4.3. Data and Methods

4.3.1. Study Locations

This study focused on investigating the effects of auxiliary data precision in areas that loblolly pine is grown commercially. Forty managed loblolly pine plantations located

in three Virginia State Forests were used for this study (Figure 4-1). These stands are managed with silvicultural prescriptions common for the region with the goal of sustainably producing a mixture of fiber and solid wood products. Stands ranged in age from 9-43 years old. Of the 40 stands, 14 had been operationally thinned at least once. The selected stands cover a wide range of growing conditions and management scenarios typical for the region. For additional detail regarding the management and spatial distribution of the stands evaluated, readers are directed to Green et al. (2019).

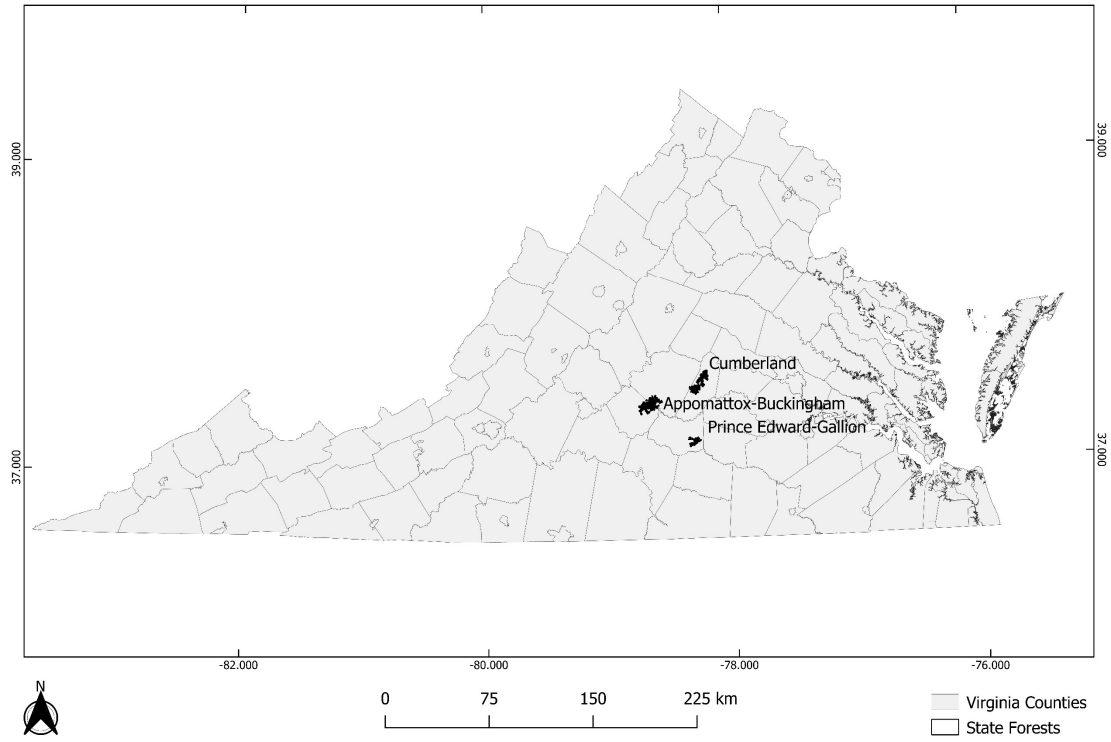

Figure 4-1. Locations of State Forests used for study.

4.3.2. Ground Data

In the winter and early spring of 2019, temporary inventory plots were installed in every stand. One sample unit per 1.2 hectares with a minimum distance of approximately 70-80 meters between plot centers was used to produce an assumed equal probability, simple random sample. Time constraints limited the sample intensity in some stands. 0.13 hectare fixed-radius plots were used in unthinned stands and 0.02 hectare fixed-radius

plots were used in thinned stands. Unthinned stands with excessive natural regeneration were sampled using 0.01 hectare fixed-radius plots.

On each sample unit, every living, planted stem was tallied and diameter at breast height (DBH) was measured using a diameter tape. A subset of trees per plot were measured for total height using either a laser hypsometer or an electronic clinometer. Height trees were selected across the diameter distribution and at least one height per plot was measured. A minimum of 25 height trees per stand was targeted. All living natural trees with DBH >= 7.62 cm were tallied and measured for DBH. A subset of heights across the diameter distribution was measured for natural loblolly pine, Virginia pine (*Pinus virginiana*), and shortleaf pine (*Pinus echinata*). In addition, a subset of hardwood heights was measured. All pine (both planted and natural) heights not measured in the field were predicted using the model form in equation 4-1. Heights of planted pines were predicted using stand-level relationships while natural pine heights used a pooled, "region-wide" relationship developed from all the field measured total heights.

$$\ln(\mathrm{Ht}) = b_0 + b_1(\mathrm{DBH}^{-1}) \qquad \text{Equation 4-1}$$

Plot-level information including thinning status, competing vegetation and other notes were also recorded. For all trees, volume was estimated using the allometric equations presented in Table 4-1. All ground data processing was performed using R (R Core Team 2018). Additional packages used include the following: xlsx (Dragulescu and Arendt 2018) and reshape2 (Wickham 2007).

Table 4-1. Sources of allometric equations used to estimate total stem volume. (Table adapted from Green et al. 2019)

Species or Species Group	Source
Planted *Pinus taeda*	Tasissa et al. 1997 (unthinned coefficients)
Natural *Pinus taeda*, *Pinus virginiana*, and *Pinus echinata* >= 5" DBH	Tasissa et a. 1997 (unthinned coefficients)
Natural *Pinus taeda*, *Pinus virginiana*, and *Pinus echinata* < 5" DBH	Warner and Goebel 1963
Hardwoods with no measured total height	Clark et al. 1986 (coefficients from table 10)
Hardwoods with measured total height	Clark et al. 1986 (coefficients from table 14)

4.3.3. Auxiliary Information

For the entire study area, lidar and the associated 1-m digital elevation models (DEMs) are available from the United States Geological Survey (USGS). The 2015 "Chesapeake Bay" lidar collection encompassed Appomattox-Buckingham (ABSF) and Cumberland (CUSF) State Forests while the 2014 "Sandy" collection covers the Prince Edward-Gallion State Forest (PESF). Details of the lidar collections are summarized in Table 4-2.

Table 4-2. Lidar specifications for the Chesapeake Bay and Sandy projects. (Table adapted from Green et al. 2019)

	Chesapeake Bay Project	Sandy Project
Lidar Collection Dates	Nov. 15, 2015 – Mar. 30, 2016	Mar. 24, 2014 – Apr. 21, 2014
Lidar Sensor	Riegl 680i	Leica ALS60 or Leica ALS70
Scan Angle (degrees)	60	unreported
Lidar Density ($pulses * m^{-2}$)	2.3	unreported
Nominal Pulse Spacing (m)	0.66	0.7
Flight Line Overlaps	55%	30% (ALS60) or 20% (ALS70)
Pulse Rates (kHz)	200	154.3 (ALS60) or 301.6 (ALS70)

Lidar and the associated DEM processing was performed with a combination of R (R Core Team 2018), FUSION (McGaughey 2018), and LAStools (LAStools 2018). Additional R packages used for spatial data processing include: Raster (Hijmans 2019), sp (Pebesma and Riband 2005, Bivand et al., 2013), and rgdal (Bivand et al. 2019). This study evaluated, the impact of three levels of reduced density point clouds. Using the lasthin function in the LAStools suite, the original point clouds were randomly sampled once to 50%, 10%, and 1% of the original point density using the "keep_random_fraction" argument. ITD was performed using two methods in FUSION: 1) A combination of the "CanopyModel" and "TreeSeg" tools and 2) A combination of the "CanopyModel" and "CanopyMaxima" tools. Three canopy height model (CHM) grid sizes (0.5m, 1.0m, and 1.5m) and three height thresholds (1.52m, 3.05m, and 4.57m)

were investigated for the individual tree segmentation algorithms. The elevation products (USGS 2017c) and associated lidar used to generated them (USGS 2017d) are distributed through the USGS National Map (as of July, 2019: https://viewer.nationalmap.gov/basic/).

In addition to lidar derived auxiliary data, stand thinning status was used as a covariate in the SAE models. Thinning status was obtained from stand records and confirmed during field visits. No distinction was made between stands that received one thinning treatment and those that had received multiple.

4.3.4. Additional USGS Elevation Products

In place of lidar derived, 1-meter DEMs, this study evaluated the effects of using lower resolution elevation models. The USGS distributes both 30 m (USGS 2017a) and 10 m elevation data (USGS 2017b) for the entire continental United States. These data are also available on the USGS National Map and are produced from a variety of sources. The same preprocessing tools and steps used for the 1-meter DEM were used for these lower resolution elevation models.

4.3.5. Small Area Estimators

The SAE model considered for this work (equation 4-2), was first described by Fay and Herriot (1979)

$$\hat{\theta}_i = \boldsymbol{z}_i^T \boldsymbol{\beta} + b_i v_i + e_i \qquad \text{Equation 4-2}$$

where $\boldsymbol{z}_i$ is a vector of area-specific covariates, $\boldsymbol{\beta}$ is the vector of regression coefficients, b_i are positive constants (assumed equal 1 in this study), v_i are area-specific random effects assumed iid $N(0, \sigma_v^2)$ and e_i are individual random errors iid $N(0, \Psi_i)$.

The empirical best linear unbiased predictor (EBLUP) is a weighted estimate based on the sampling estimate variance ($\widehat{\Psi}_i$) and the random error variance ($\widehat{\sigma_v^2}$). As the direct estimate (i.e. the ground sample), becomes more reliable, the estimate is weighted towards it. Conversely, the EBLUP weights more towards the synthetic estimate for unreliable (i.e. relatively high sample variance) samples. The form of the estimator utilized is:

$$\hat{\theta}_i^H = \gamma \hat{\theta}_i + (1 - \gamma) \boldsymbol{z}_i^T \hat{\beta} \qquad \text{Equation 4-3}$$

where γ is the weight that uses both sources of error (Ψ_i and σ_v^2) and is given by equation 4-4.

$$\gamma_i = \widehat{\sigma_v^2}/(\widehat{\sigma_v^2} + \widehat{\Psi_i}) \quad \text{Equation 4-4}$$

The area-level SAE models were fit using the SAE package in R (Molina and Marhuenda 2015) using the "mseFH" function. The REML method was used with all default parameters. Details of the REML procedure can be found in Rao and Molina (2015). Additionally, Datta and Lahiri (2000) provide a detailed description of the MSE estimation.

4.3.6. Candidate Models

Using area-based lidar metrics, stand thinning status, and tree counts from both the watershed and canopy maxima individual tree segmentations, a list of candidate SAE models was developed. The list was divided into three groups: 1) Model forms that contained only area-based lidar metrics and thinning status, 2) model forms that included a combination of area-based and watershed derived individual tree-based metrics and, 3) model forms that included a combination of area- and canopy maxima derived individual tree-based metrics. Area-level metrics evaluated included the normalized 80th, 90th, 95th, and 99th height percentiles and thinning status. The individual tree metrics included only the stem counts summarized to a stem count per hectare. The list of candidate predictors is shown in table 4-3. The effects of reduced density point clouds and lower resolution DEMs were evaluated using only model forms that contained the area-based lidar metrics and thinning status (group 1).

Table 4-3. Groups of predictors evaluated.

Area-Level Metrics	Area- and Ind. Tree Metrics Watershed Approach	Area- and Ind. Tree Metrics Canopy Maxima Approach
TV_Planted ~ P80	TV_Planted ~ P80 + TPH	TV_Planted ~ P80 + TPH
TV_Planted ~ P90	TV_Planted ~ P90 + TPH	TV_Planted ~ P90 + TPH
TV_Planted ~ P95	TV_Planted ~ P95 + TPH	TV_Planted ~ P95 + TPH
TV_Planted ~ P99	TV_Planted ~ P99 + TPH	TV_Planted ~ P99 + TPH
TV_Planted ~ P80 + thin_status	TV_Planted ~ P80 + thin_status + TPH	TV_Planted ~ P80 + thin_status + TPH
TV_Planted ~ P90 + thin_status	TV_Planted ~ P90 + thin_status + TPH	TV_Planted ~ P90 + thin_status + TPH
TV_Planted ~ P95 + thin_status	TV_Planted ~ P95 + thin_status + TPH	TV_Planted ~ P95 + thin_status + TPH
TV_Planted ~ P99 + thin_status	TV_Planted ~ P99 + thin_status + TPH	TV_Planted ~ P99 + thin_status + TPH

4.3.7. Model Sensitivity Analysis

To examine the stability of the relationships between small area estimates and precision and the direct estimates, bootstrapped samples were drawn from the 40 stands

evaluated. One thousand samples of 40 were drawn with replacement using the R "sample" function. Each bootstrap sample was used to fit the area-level SAE to the list of model forms evaluated using area-based lidar with and without thinning status. Model sensitivity analysis was only conducted for models that contained the area-based lidar metrics and thinning status. Only full density point clouds and the associated 1-meter DEMs were used.

4.4. Results

The stands evaluated covered a wide range of conditions encountered in operational forest inventory in the southeastern United States in managed loblolly pine plantations (Table 4-4). It is common for the first operational inventory to occur at the time of crown-closure (~10 years old) followed by an inventory immediately pre- and post-thinning (~14-20 years old for first thinning and any subsequent thinning). A final inventory is common at the time preceding final harvest (usually >= 25 years old).

Table 4-4. Direct estimate summary for the 40 stands evaluated

Stand Parameter	Min	Max	Mean	Std.Dev.
Planted Trees per Hectare	177.9	2693.4	899.0	511.7
Planted Basal Area ($m^2 * ha^{-1}$)	8.7	46.8	26.4	9.9
Planted Total Volume ($m^3 * ha^{-1}$)	42.0	353.2	194.4	81.4
Planted Dominant Height (m)	9.3	25.2	15.9	3.6

For the comparisons between the precision of models and direct estimates, 1-1 scatterplots of relative error ratios (RER), were constructed. Any point falling below the 1-1 line indicates greater precision (i.e. smaller variation) for the RER on the y-axis. For SAE models the RER for small area i is

$$RER_i\ (\%) = \frac{\sqrt{MSE(eblup_i)}}{EBLUP_i} * 100 \qquad \text{Equation 4-5}$$

and the RER for the direct estimate is

$$RER_i\ (\%) = \frac{\sqrt{Var(\hat{\theta}_i)}}{\bar{y}_i} * 100 \qquad \text{Equation 4-6}$$

where

$$\hat{\theta}_i = \bar{y}_i = n_i^{-1} \sum_{j=1}^{n_i} y_{ij} \qquad \text{Equation 4-7}$$

and

$$\hat{\Psi}_i = Var(\hat{\theta}_i) = n_i^{-1} \frac{\sum (y_{ij} - \bar{y}_i)^2}{n_i - 1} \qquad \text{Equation 4-8}$$

In addition, estimates were compared using 1-1 scatterplots. Points falling below the 1-1 relationship indicate a lower y-axis estimate compared with the x-axis estimate. Points falling above the 1-1 line indicate a higher y-axis estimate compared with the x-axis estimate.

The lidar height percentiles evaluated resulted in very similar SAE models. Due to the similarities, only results using the 80th percentile lidar height are presented. As reported in Green et al. (2019), area-level SAE models using both lidar and thinning status improved the total volume estimate precision in many cases (Figure 4-2a). While bias cannot be directly assessed because the true population values are not known, there are no patterns suggesting a systematic under or over prediction by the SAE model evaluated (Figure 4-2b).

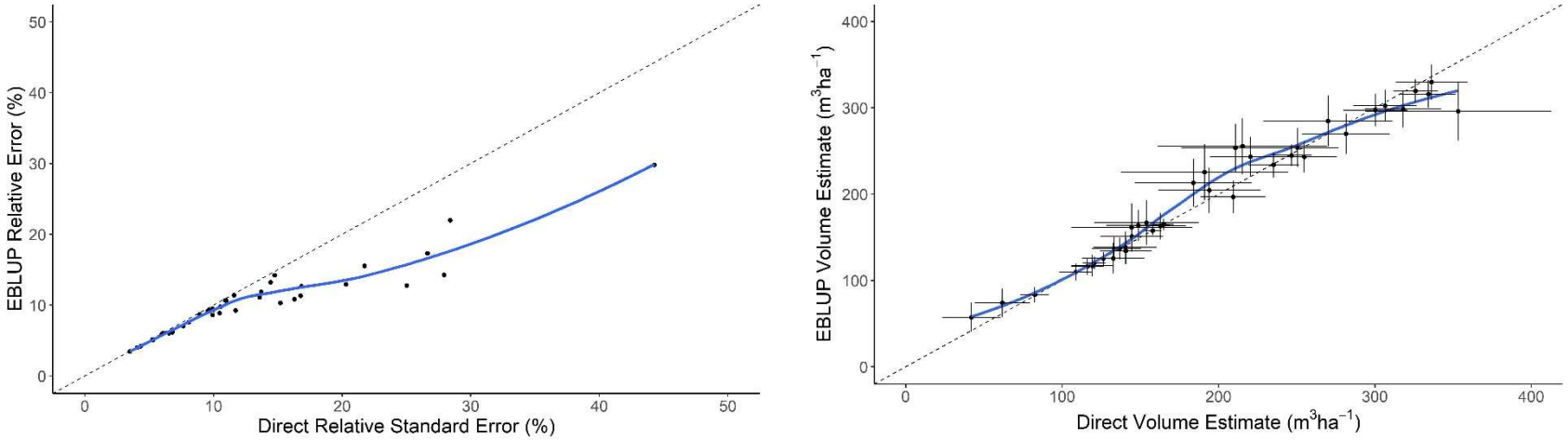

(a) (b)

Figure 4-2. Area-level SAE results. (a) Model with lidar 80th height percentile and thinning status as auxiliary information relative error comparison and (b) estimate comparison with lidar 80th height percentile and thinning status as auxiliary information. Smoothing lines are for visual interpretation only and are not representative of the SAE model fit. Error bars represent one standard error in the x direction and the root mean squared error in the y direction. (Figure adapted from Green et al. 2019)

The effects on the total volume estimate and its precision from reducing the spatial resolution of the DEM were minimal. As can be seen in Figure 4-3a and 4-3b, both the 30- and 10-meter DEM resolutions resulted in very similar precision compared to the lidar derived 1-meter DEM when using the original, unthinned point cloud. In addition, the estimates are essentially unchanged using either the 30-meter (Figure 4-4a) or 10-meter (Figure 4-4b) DEM. When compared to the full point cloud using the 1-meter DEM, thinned point clouds using either the 30- or 10-meter DEM resulted in similar or slightly improved precision in most cases (Figure 4-3c – 4-4h). In addition, the estimate remained similar in most cases (Figure 4-4c – 4-4h).

The inclusion of density estimates using both the watershed segmentation and canopy maxima methods had minimal influence on the SAE fits. For all combinations of model forms, canopy height model resolutions, and height thresholds, similar results were found. Due to the similarity, only the model fits that use the 1m canopy height model with a 4.57m height threshold and include the lidar 80th percentile, thinning status, and a density estimate are shown. As seen in figure 4-5, the relationships between the direct estimate relative standard error and the model relative error remained essentially unchanged when compared to the model that only included the lidar 80th percentile and thinning status as auxiliary data.

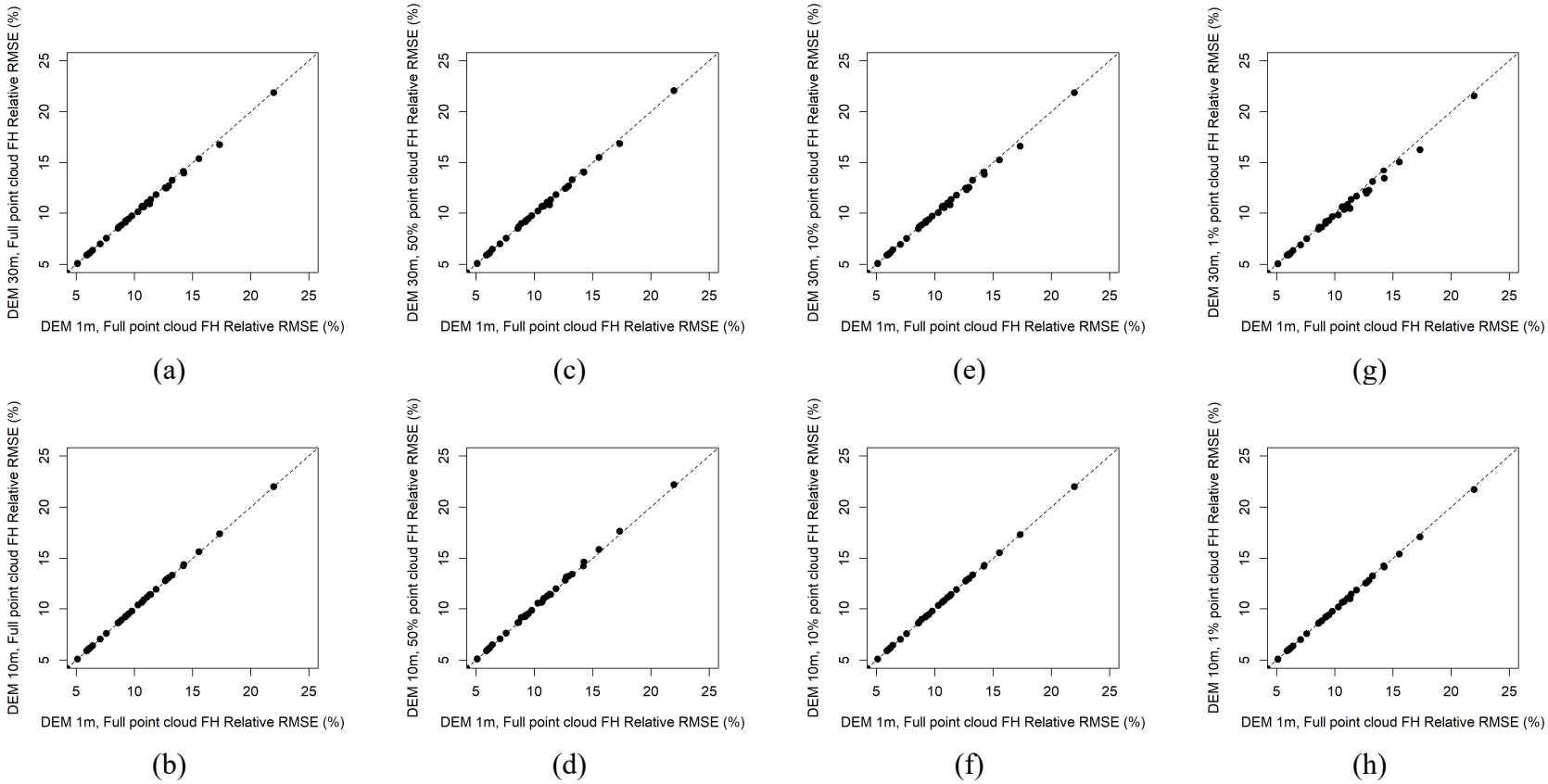

Figure 4-3. Relative root mean squared error (RMSE) comparison between (a) 1m DEM with full point cloud and 30m DEM with full point cloud, (b) 1m DEM with full point cloud and 10m DEM with full point cloud, (c) 1m DEM with full point cloud and 30m DEM with 50% point cloud, (d) 1m DEM with full point cloud and 10m DEM with 50% point cloud, (e) 1m DEM with full point cloud and 30m DEM with 10% point cloud, (f) 1m DEM with full point cloud and 10m DEM with 10% point cloud, (g) 1m DEM with full point cloud and 30m DEM with 1% point cloud, and (h) 1m DEM with full point cloud and 10m DEM with 1% point cloud. Relative RMSE is calculated as: 100*(RMSE/EBLUP) where RMSE is the root mean squared error for the model estimate and EBLUP is the model estimate.

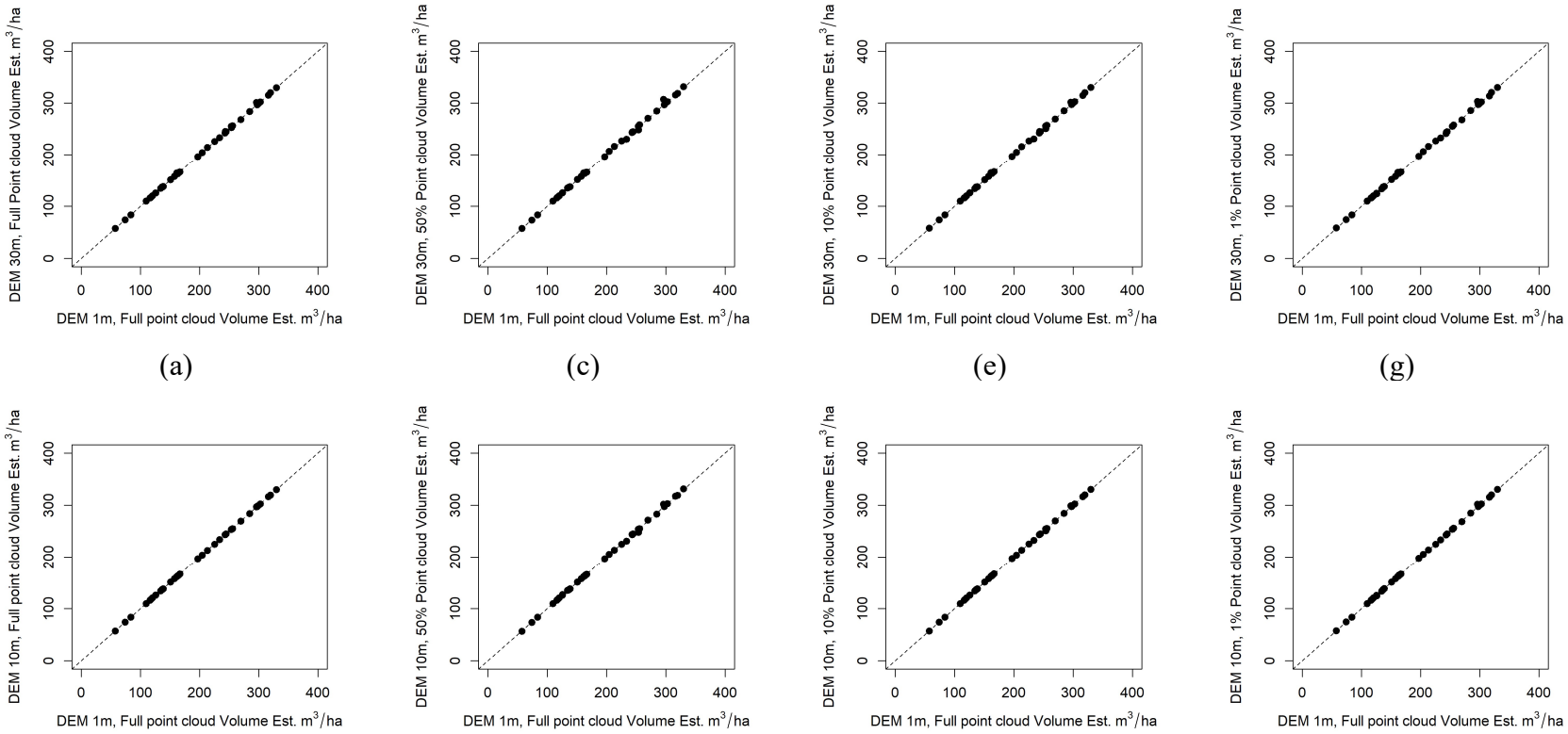

Figure 4-4. Estimate comparison between (a) 1m DEM with full point cloud and 30m DEM with full point cloud, (b) 1m DEM with full point cloud and 10m DEM with full point cloud, (c) 1m DEM with full point cloud and 30m DEM with 50% point cloud, (d) 1m DEM with full point cloud and 10m DEM with 50% point cloud, (e) 1m DEM with full point cloud and 30m DEM with 10% point cloud, (f) 1m DEM with full point cloud and 10m DEM with 10% point cloud, (g) 1m DEM with full point cloud and 30m DEM with 1% point cloud, and (h) 1m DEM with full point cloud and 10m DEM with 1% point cloud.

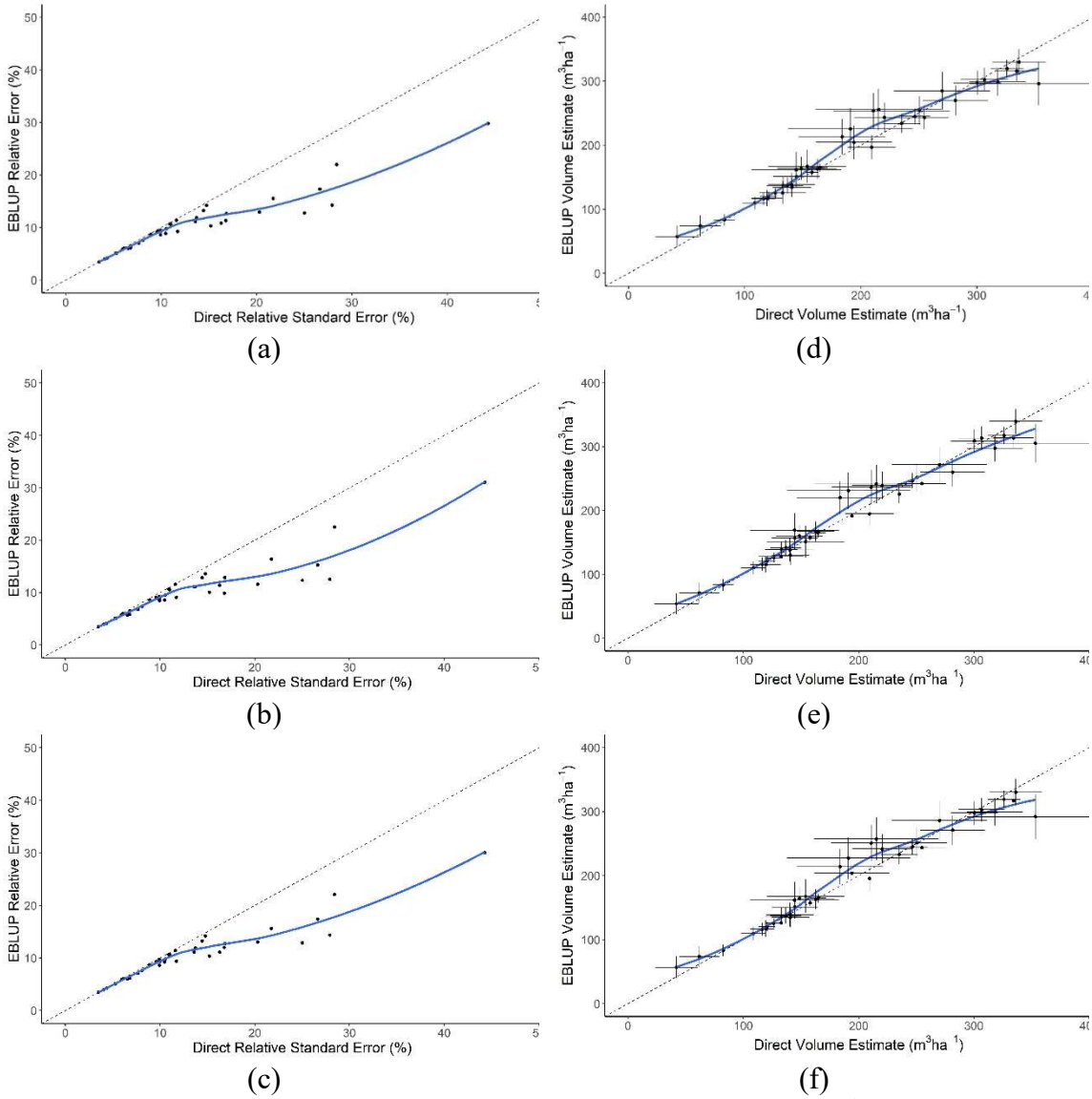

Figure 4-5. (a) Area-level SAE error ratio comparison between model using lidar 80th percentile, thinning status, and no individual tree estimate, (b) lidar 80th percentile, thinning status, and individual tree estimate using the watershed approach, (c) and lidar 80th percentile, thinning status, and individual tree estimate using the canopy maxima approach. Figures d-f are the corresponding estimate comparisons. In all figures, the smoothing lines are for visual interpretation only and are not representative of the SAE model fit. Error bars represent one standard error in the x direction and the root mean squared error in the y direction. For the models including individual tree detection, a 1m resolution canopy height model with a 4.57m height threshold was used. (Figure a and d adapted from Green et al. 2019).

The observed trends of increased estimate precision are consistent with the bootstrapped model fits. Over 1000 repeated samples, there is noticeable RER variation for individual stands (Figure 4-6); however, the general trend resembles that in figure 4-2a. Similarly, the stand volume model estimates vary but follow the 1-1 relationship with the direct estimate. Similar relationships were found with the other lidar height percentiles and only the model form with the 80^{th} height percentile and thinning status are shown.

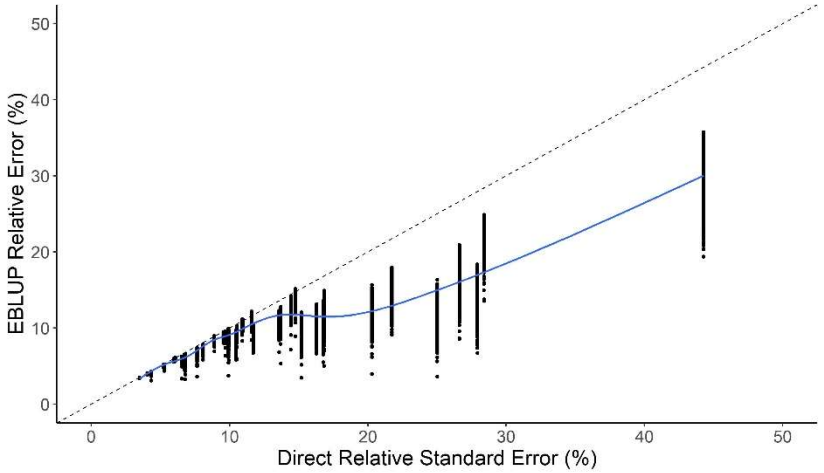

(a)

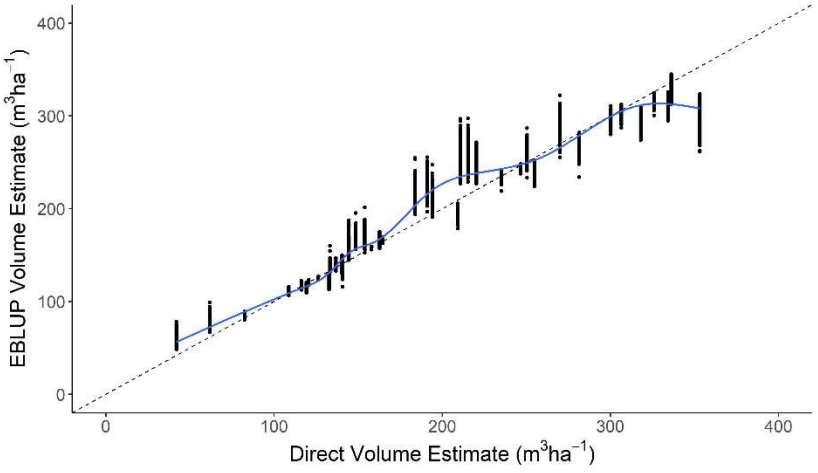

(b)

Figure 4-6. Bootstrapped, area-level SAE results. (a) Model with lidar 80th height percentile and thinning status as auxiliary information relative error comparison and (b) estimate comparison with lidar 80th height percentile and thinning status as auxiliary information. Smoothing lines are for visual interpretation only and are not representative of the SAE model fit.

4.5. Discussion

The similar estimate precision using thinned point clouds does not agree with our initial expectation of lower estimate precision with lower density point clouds. The findings of this study are promising for the future of using point-cloud data from a variety of sources in area-based forest inventory. A common difficulty with using lidar in operational forest inventory is the cost of acquisition (McRoberts et al., 2018). Point-clouds derived from DAP have emerged as a promising, lower cost alternative with a growing body of literature demonstrating the potential (e.g. White et al., 2013 and Goodbody et al., 2019). DAP generates point clouds that characterize the outer canopy envelope necessitating the need for an elevation model generated from other sources. It has been commonly assumed that lidar derived DEMs were necessary to effectively use DAP point clouds in operational settings (White et al., 2013). The results of this work suggest that in areas such as the southeastern United States Piedmont or Coastal Plain, a DEM with lower spatial resolution will generate similar estimates with similar precision in the SAE framework. Further, the results from this work suggest sparse point clouds are useful for improving the precision of inventory estimates. This is not to suggest that lower resolution point clouds are "better", rather, they provide very similar results using the methods described in the conditions evaluated. In planning future lidar missions, common constraints such as cost could be reduced by higher collection altitudes. It is unlikely that similar results would be found if individual tree detection methods were utilized. Increased point cloud density has been shown to be important for accurate tree delineation and calculation of lidar cover metrics (Jakubowski et al., 2013).

An essential requirement when using SAE is a sufficient linear relationship between the variable of interest and the ancillary information (Rao and Molina 2015). The strength of this relationship based on the coefficient of variation (R^2), was found to remain similar, or even slightly improve, as auxiliary data resolution decreased (Table 4-5). The strength of these linear relationships are major contributors to the similar SAE results found amongst the data evaluated.

Table 4-5. Comparison of strength of linear relationship between levels of auxiliary data precision and total planted volume using linear model form that includes the lidar 80th height percentile and thinning status.

Auxiliary Data	R^2
1-meter DEM, full point cloud	0.64
10-meter DEM, 50% of original point cloud	0.63
10-meter DEM, 10% of original point cloud	0.65
10-meter DEM, 1% of original point cloud	0.69
30-meter DEM, 50% of original point cloud	0.64
30-meter DEM, 10% of original point cloud	0.66
30-meter DEM, 1% of original point cloud	0.69

Based on the results of this study, the inclusion of density estimates using the individual tree detection methods evaluated are not recommended. The density estimates are highly sensitive to function parameters and provided minimal improvements in estimate precision compared to lidar height percentiles and thinning status. Delineating individual tree crowns in relatively dense plantations proved ineffective. Depending the spatial resolution of the CHM and the height threshold for the tree detection methods, individual tree crowns were either grouped, leading to an undercount, or separated, leading to an overcount. Further, the delineation errors were not consistently biased, leading to weak linear relationships between the observed and predicted densities.

The results of the bootstrap refitting indicate the observed relationships between direct estimate and model RERs are similar across repeated samples. The trend of increasing model precision for higher levels of direct estimate variation appears stable and was not simply a result of the one sample collected for this study.

4.6. Conclusions

This work has demonstrated the effects of using lower resolution elevation models and lower density lidar point clouds as covariates in loblolly pine plantations SAE models. To specifically address our research objectives and questions: 1) DEM resolution had minimal effects on the precision and estimates using the SAE methods evaluated, 2) Reduced lidar point cloud densities resulted in similar total volume estimate precision and estimates. Lower density point clouds were at worst, as useful as the full density point clouds evaluated, 3) The inclusion of stem density estimates from lidar individual tree detection contributed minimally to the effectiveness of SAE models in improving total volume estimate precision, and 4) The general observed trends between the direct estimates and their precision were stable across repeated bootstrapped samples.

The results from this work are promising to inventory managers interested in using SAE techniques in loblolly pine plantations and indicate that lower resolution auxiliary information can be utilized with confidence in area-based SAE applications for the conditions included in this study.

4.7. References

Andreu, M.G., Zobrist, K., Hinckley, T., 2008. Management practices to support increased biodiversity in managed loblolly pine plantations. University of Florida Extension, IFAS Extension.

Bivand, R., Keitt, T., Rowlingson, B. 2019. rgdal: Bindings for the 'Geospatial' Data Abstraction Library. R package version 1.4-3. https://CRAN.R-project.org/package=rgdal

Bivand, R.S., Pebesma, E., Gomez-Rubio, V. 2013. Applied spatial data analysis with R, Second edition. Springer, NY. http://www.asdar-book.org/

Breidenbach, J., Astrup, R., 2012. Small area estimation of forest attributes in the Norwegian National Forest Inventory. Eur. J. For. Res. 131(4), 1255-1267. https://doi.org/10.1007/s10342-012-0596-7

Breidenbach, J., Magnussen, S., Rahlf, J., Astrup, R., 2018. Unit-level and area-level small area estimation under heteroscedasticity using digital aerial photogrammetry data. Remote Sens. Environ. 212, 199-211.

Burkhart, H.E., Avery, T.E., Bullock, B.P., 2019. Forest measurements 6th ed. Waveland Press. pp 434.

Baker, James B.; Langdon, O. Gordon. 1990. Pinus taeda L. loblolly pine. In: Burns, Russell M.; Honkala, Barbara H., technical coordinators. Silvics of North America. Volume 1. Conifers. Agric. Handb. 654. Washington, DC: U.S. Department of Agriculture, Forest Service: 497-512.

Campbell, J.B., Wynne, R.H., 2011. Introduction to remote sensing 5th ed. Guilford Press. pp 667.

Clark, Alexander, III; Phillips, Douglas R.; Frederick, Douglas J. 1986. Weight, Volume, and Physical Properties of Major Hardwood Species in the Piedmont. Res. Pap. SE-255. Asheville, NC: U.S. Department of Agriculture, Forest Service, Southeastern Forest Experiment Station. 84 p.

Coops, N.C., 2015. Characterizing forest growth and productivity using remotely sensed data. Curr. Forestry Rep. 1, 195-205.

Coulston, J.W., Green, P.C., Radtke, P.J., Prisely, S., Burkhart, H.E., Thomas, V., Wynne, R. Small area estimates of forest removals. *In preparation*.

Datta, G.S., Lahiri, P., 2000. A unified measure of uncertainty of estimated best linear unbiased predictors in small area estimation problems. Statistica Sinica 10, 613-627.

Dragulescu, A. A., Arendt, C. 2018. xlsx: Read, Write, Format Excel 2007 and Excel 97/2000/XP/2003 Files. R package version 0.6.1. https://CRAN.R-project.org/package=xlsx

Fay III, R.E., Herriot, R.A., 1979. Estimates of income for small places: an application of James-Stein procedures to census data. J. Am. Stat. Assoc. 74(366a), 269-277.

Fox, T.R., Jokela, E.J., Allen, H.L., 2007. The development of pine plantation silviculture in the southern United States. J. For. 105(7), 337-347.

Gobakken, T., Næsset, E., 2008. Assessing effects of laser point density, ground sampling intensity, and field sample plot size on biophysical stand properties derived from airborne laser scanner data. Can. J. For. Res. 38(5), 1095-1109.

Goerndt, M.E., Monleon, V.J., Temesgen, H. 2011. A comparison of small-area estimation techniques to estimate selected stand attributes using LiDAR-derived auxiliary variables. Can. J. For. Res. 41: 1189-1201. https://doi.org/10.1139/x11-033

Goerndt, M.E., Monleon, V.J., Temesgen, H., 2013. Small-area estimation of county-level forest attributes using ground data and remote sensed auxiliary information. For. Sci. 59(5), 536-548. https://doi.org/10.5849/forsci.12-073

González-Ferreiro, E., Diéguez-Aranda, U., Miranda, D., 2012. Estimation of stand variables in *Pinus radiata* D. Don plantations using different lidar pulse densities. Forestry. 85(2), 281-292.

Goodbody, T.R.H., Coops, N.C., White, J.C., 2019. Digital aerial photogrammetry for updating area-based forest inventories: a review of opportunities, challenges, and future directions. Curr. For. Rep. 5, 55-75.

Green, P.C., Burkhart, H.E., Coulston, J.W., Radtke, P.J., 2019. Small area estimation in support of plantation loblolly pine (*Pinus taeda* L.) forest inventory. *In review*

Hijmans, R.J., 2019. raster: Geographic Data Analysis and Modeling. R package version 2.8-19. https://CRAN.R-project.org/package=raster

Holmgren, J. 2004. Prediction of tree height, basal area and stem volume in forest stands using airborne laser scanning. Scand. J. For. Res. 19(6), 543-553.

Hodgson, M.E., Bresnahan, P. 2004. Accuracy of airborne lidar-derived elevation. Photo. Eng. Rem. Sens. 70(3), 331-339.

Jakubowski, M.K., Guo, Q., Kelly, M., 2013. Tradeoffs between lidar pulse density and forest measurement accuracy. Remote Sens. Environ. 130, 245-253.

Jokela, E.J., Martin, T.A., Vogel, J.G., 2010. Twenty-five years of intensive forest management with southern pines: important lessons learned. J. For. 108(7), 338-347.

LAStools, "Efficient LiDAR Processing Software" (version 180620, academic), obtained from http://rapidlasso.com/LAStools

Magnussen, S., Mauro, F., Breidenbach, J., Lanz, A., Kändler, G., 2017. Area-level analysis of forest inventory variables. Eur. J. For. Res. 136, 839-855.

Magnussen, S., Næsset, E., Gobakken, T., 2010. Reliability of LiDAR derived predictors of forest inventory attributes: A case study with Norway spruce. Remote Sens. Environ. 114(4), 700-712.

Maltamo, M., Eerikäinen, K., Packalén, P., Hyyppä, J., 2006. Estimation of stem volume using laser scanning-based canopy height metrics. Forestry, 79(2), 217-229.

Mauro, F., Monleon, V.J., Temesgen, H., Ford, K.R., 2017. Analysis of area level and unit level models for small area estimation in forest inventories assisted with LiDAR auxiliary information. PloS one, 12(12), p.e0189401. https://doi.org/10.1371/journal.pone.0189401

McGaughey, R., 2018. FUSION/LDV: Software for Lidar data analysis and visualization. FUSION version 3.80. Available online at: http://forsys.cfr.washington.edu/fusion/fusion_overview.html

McRoberts, R.E., Chen, Q., Gormanson, D.D., Walters, B.F., 2018. The shelf-life of airborne laser scanning data for enhancing forest inventory inferences. Remote Sens. Environ. 206, 254-259.

Molina I., Marhuenda Y., 2015. sae: An R Package for Small Area Estimation. The R Journal, 7(1), 81–98. https://journal.r-project.org/archive/2015/RJ-2015-007/RJ-2015-007.pdf.

Næsset, E., Bjerknes, K-O., 2001. Estimating tree heights and number of stems in young forest stands using airborne laser scanning data. Remote Sens. Environ. 78, 328-340.

Næsset, E., 2002. Predicting forest stand characteristics with airborne scanning laser using a practical two-stage procedure and field data. Remote Sens. Environ. 80, 88-99.

Noordermeer, L., Bollandsås, O.M., Økra, H.O., Næsset, E, Gobakken, T., 2019. Comparing the accuracies of forest attributes predicted from airborne laser scanning and digital aerial photogrammetry in operational forest inventories. Remote Sens. Environ. 226, 26-37.

Pebesma, E.J., R.S. Bivand. 2005. Classes and methods for spatial data in R. R News 5 (2), https://cran.r-project.org/doc/Rnews/.

Popescu, S.C., Wynne, R.H., 2004. Seeing the trees in the forest: Using lidar and multispectral data fusion with local filtering and variable window size for estimating tree height. Photo. Eng. Rem. Sens. 70(5), 589-604.

R Core Team, 2018. R: a language and environment for statistical computing [online]. R Foundation for Statistical Computing, Vienna, Austria. Available from http://www.R-project.org/

Rao, J.N.K., Molina, I., 2015. Small Area Estimation. John Wiley & Sons, Inc. pp 441.

Reutebuch, S.E., McGaughey, R.J., Andersen, H.E., Carson, W.W., 2003. Accuracy of a high-resolution lidar terrain model under a conifer forest canopy. Can. J. Rem. Sens. 29(5), 527-535.

Ruiz, L.A., Hermosilla, T., Mauro, F., Godino, M., 2014. Analysis of the influence of plot size and LiDAR density on forest structure attribute estimates. Forests. 5, 936-951.

Strunk, J., Temesgen, H., Andersen, H.E., Flewelling, J.P., Madsen, L., 2012. Effects of lidar pulse density and sample size on a model-assisted approach to estimate forest inventory variables. Can. J. Rem. Sens. 38(5), 644-654.

Tasissa, G., Burkhart, H.E., Amateis, R.L., 1997. Volume and taper equations for thinned and unthinned loblolly pine trees in cutover, site-prepared plantations. South. J. Appl. For. 21(3), 146-152.

Tinkham, W.T., Smith, A.M., Hoffman, C., Hudak, A.T., Falkowski, M.J., Swanson, M.E., Gessler, P.E., 2012. Investigating the influence of LiDAR ground surface errors on the utility of derived forest inventories. Can. J. For. Res. 42(3), 413-422.

U.S. Geological Survey, 2017a, 1 Arc-second Digital Elevation Models (DEMs) - USGS National Map 3DEP Downloadable Data Collection: U.S. Geological Survey.

U.S. Geological Survey, 2017b, 1/3rd arc-second Digital Elevation Models (DEMs) - USGS National Map 3DEP Downloadable Data Collection: U.S. Geological Survey.

U.S. Geological Survey, 2017c, 1 meter Digital Elevation Models (DEMs) - USGS National Map 3DEP Downloadable Data Collection: U.S. Geological Survey.

U.S. Geological Survey, 2017d, Lidar Point Cloud - USGS National Map 3DEP Downloadable Data Collection: U.S. Geological Survey.

Warner, J.R., Goebel, N.B., 1963. Total and bark volume tables for small diameter Loblolly, Shortleaf, and Virginia Pine in the upper South Carolina Piedmont. Department of Forestry, South Carolina Agricultural Experiment Station, Clemson, South Carolina. Forest Research Series No. 9.

White, J., Wulder, M., Vastaranta, M., Coops, N., Pitt, D., Woods, M., 2013. The utility of image-based point clouds for forest inventory: A comparison with airborne laser scanning. Forests, 4(3), 518-536.

Wickham, H. 2007. Reshaping Data with the reshape Package. Journal of Statistical Software, 21(12), 1-20. URL http://www.jstatsoft.org/v21/i12/.

Zhao, D., Kane, M., Teskey R., Fox, T.R., Albaugh, T.J., Allen, H.L., and Rubilar, R., 2016. Maximum response of loblolly pine plantations to silvicultural management in the southern United States. For. Ecol. Manage. 375, 105-111

Chapter 5 Comparison of plot-level and stand-level projections of simulated loblolly pine (*Pinus taeda* L.) stands[3]

5.1. Abstract

Estimating current stand conditions and value is often required for making management decisions. However, costs and logistical constraints make yearly inventory impractical in most settings necessitating the use of growth and yield models. Projection of plots aggregated within stands, denoted as stand-level projection, and aggregation of individual projected plots within stands, denoted as plot-level projection, are two strategies to predict stand parameters at future times. This study investigated the differences in the two projection strategies under differing levels of spatial heterogeneity and stand development. Simulated mapped stands and samples, along with three whole stand models, were utilized to perform the comparisons.

The results indicated that the two methods produced similar projections in terms of dominant height, basal area, and stems per hectare under most situations. As spatial heterogeneity increased, the stand-level projection indicated a significant bias of predicted total volume compared with the plot-level projection regardless of plot size as indicated by Jensen's Inequality. The model used made a noticeable impact on the differences, while thinning did not alter the patterns of observed differences. When implementing projections at the whole-stand level, careful consideration of stand heterogeneity and the growth and yield model is recommended.

[3] This chapter has been published by NRC Research Press as: Green, P.C., Yang, S., Burkhart, H.E. 2019. Comparison of plot- and stand-level projections of simulated loblolly pine (*Pinus taeda*) stands. Can. J. For. Res. 49, 692-100. DOI: dx.doi.org/10.1139/cjfr-2018-0208. The permission to use this publication as a chapter in this dissertation is acknowledged. Green, P.C., Yang, S., and Burkhart, H.E. contributed to the design and ideas for the work. Green, P.C., and Yang, S. contributed to the analysis and writing.

5.2. Introduction

An accurate, up-to-date understanding of forest stand conditions is essential for informed management decisions. The two primary tools commonly utilized to estimate stand parameters are forest inventory and growth and yield models. Common inventory procedure involves using either fixed or variable radius sample plots established at some established intensity and spatial distribution. Data collected at each sample unit varies but typically consists of species, diameter at breast height (DBH), total height (H) and tree quality information (Burkhart et al. 2019). Ultimately, the purpose of many inventories is to assess both volumetric yields and monetary values. Costs and logistical constraints make yearly inventory impractical in most settings necessitating the use of growth and yield models to estimate both current and future conditions. Growth and yield models can be generalized into two broad classes, whole stand and tree level models. The two categories can differ greatly in complexity, data requirements and use; however, they both have found successful use in forest modeling (Clutter et al. 1983; Burkhart and Tomé 2012).

Spatial variation of forest attributes exists at some level in both natural and managed stands. The degree of variation in managed systems depends on many factors; however, patterns of spatial heterogeneity can be classified as regular, random or aggregated (Li and Reynolds 1994; Hou et al. 2015). Stratification is commonly used to improve the precision of volume estimates when strata boundaries can be reliably determined (Shiver and Borders 1996). When growth projections are of primary interest, measurements such as density and/or site index are generally used in lieu of volume (Smith and Burkhart 1984). Barriers with stratification include determining locations of the strata boundaries, and if spatial variation is large enough to justify the effort to locate, digitize, and measure strata sizes. Due to these challenges, individual stands are often inventoried under the assumption that they are sufficiently spatially homogeneous to forgo stratification.

Loblolly pine (*Pinus taeda* L.) is the most widely planted plantation species in the southeastern United States. Ground based inventory is typically conducted at several stages in stand development including: (i) early stand survival counts (~1-2 years old),

(ii) crown closure (~9-11 years old), (iii) immediate pre- and post-first thinning (~ 12-17 years old), (iv) pre- and post-additional thinning, and (v) prior to final harvest (~ 25 years old). Despite the multiple inventory entry points, reliable estimates of stand conditions and value are needed every year. Further, estimates of standing conditions and value are often required for management decisions, financial planning and fiduciary reporting requirements. Common practice following inventory is to project a single aggregate of the sample plot estimates to future times, denoted as stand-level projection. Alternatively, a stand-level parameter estimate can be obtained by aggregating projected plot estimates at future times, denoted as plot-level projection. The aggregation of sample units x with mean $\bar{x}$ and variance > 0, followed by projection with a non-linear function $f(x)$ results in $f(\bar{x})$. This result does not equal the projection of the x sample units with the same non-linear function $f(x)$ followed by aggregation $\overline{f(x)}$. This mathematical property is known as Jensen's Inequality (Jensen 1906) and is important to consider when examining the effects of variation in natural systems (Ruel and Ayres 1999). Bias of estimates was noted by Moeur and Ek (1981) with stand-level aggregation projections compared with plot-level projections. The magnitude of the differences observed is dependent on the projection model and the levels of spatial heterogeneity (Smith and Burkhart 1984). A method for approximation of the magnitude of mathematical bias encountered with stand level aggregations was proposed by Duursma and Robinson (2003); however, the differences induced from stand-level projection of forest inventories under various stand conditions or sampling designs has not been extensively examined. Therefore, in this study we compared stand parameter estimates in simulated loblolly pine plantations when using the stand-level projection compared with the mathematically unbiased, plot-level projection strategy. The overall objective was to evaluate the magnitude of differences encountered from the two projection strategies under (i) four different levels of spatial heterogeneity (two for thinned stands), (ii) three example whole stand projection models, (iii) two plot sizes, and (iv) the presence or absence of thinning. The use of simulated data allowed for known initial stand parameters, control over levels of spatial heterogeneity, control over thinning treatments, and repeated sampling with different sample plot sizes. Repeated simple random sampling from simulated stands was utilized

to accomplish the objectives. Parameter estimates of interest include dominant height, basal area per hectare, trees per hectare and total volume per hectare.

5.3. Data and methods

5.3.1. Simulated plantations with varying levels of spatial variability

The PTAEDA growth and yield model (Daniels and Burkhart 1975) was used to generate the simulated loblolly pine plantations. In PTAEDA, individual trees located in an x-y grid are grown as a function of age (years since planting), site quality, intraspecific competition, and management treatments. Annual diameter and height increment are predicted for each tree through the years unless it succumbs to mortality or is removed in a thinning treatment. Evolution of major data, model components and software used in PTAEDA were detailed in Amateis and Burkhart (2016).

Four simulated loblolly pine stands, denoted basemaps, were generated from PTAEDA 4.1. Each basemap occupied 37.63 ha (93 ac); an initial planting density of 1235 tree per ha (500 trees per ac) was specified in all cases, and the average site index (SI) was 21 m (70 ft) for all scenarios.

To simulate different levels of spatial heterogeneity, each basemap was evenly divided into 6×6 patches, and a site index was assigned to each patch (see Fig. 5-1). Specifically,

(1) homogeneous stand with a single site index of 21 m (Fig. 5-1a)
(2) heterogeneous stand, 22 of 36 patches assigned to a site index of 21 m while the remaining 14 patches were randomly and equally assigned by site indices of 24 m and 18 m (Fig. 5-1b)
(3) heterogeneous stand, site indices of 24 m, 21 m and 18 m were systematically and equally assigned to one third of all patches (Fig 5-1c).
(4) heterogeneous stand, site indices of 24 m and 18 m were systematically and equally assigned to one half of all patches (Fig. 5-1d)

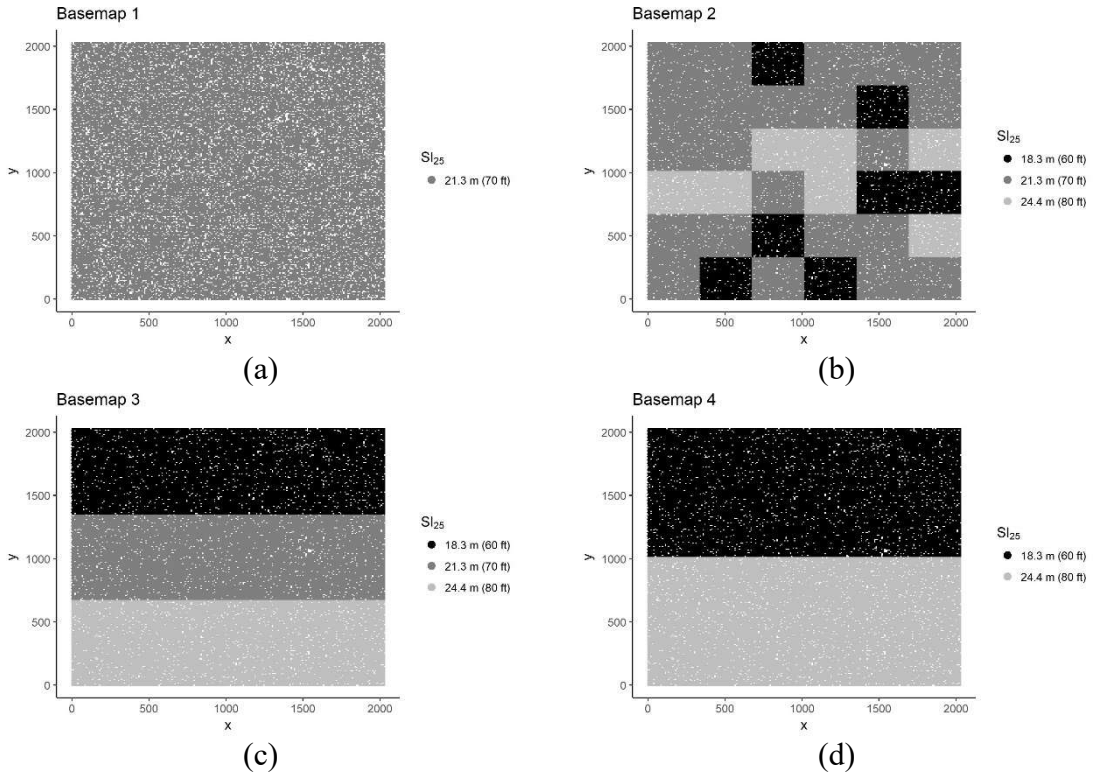

Figure 5-1. Spatial arrangement of PTAEDA generated basemaps utilized in this study. (a) Pure SI 21.3 m (70 ft), (b) random, uneven SI 24.4 m (80 ft), 21.3 m (70 ft), and 18.3 m (60 ft) with more 21.3 m (70 ft), (c) Even, systematic SI 24.4 m (80 ft), 21.3 m (70 ft), and 18.3 m (60 ft) and (d) Even systematic SI 24.4 m (80 ft), 18.3 m (60 ft). Small white patches are due to individual tree mortality.

The four basemaps with varying levels of spatial heterogeneity were generated at age 10, denoted as unthinned basemaps. Basemaps 1 and 2 were grown to age 15 and a thinning treatment was applied. Thus, there are four unthinned basemaps at age 10 and two thinned basemaps at age 15. Stands subject to the thinning treatment were thinned to approximately 16 m^2ha^{-1} (70 ft^2ac^{-1}) using a third-row removal plus selective thinning from below to meet the basal area target. Approximately 12.5 - 13 m^2ha^{-1} (55-57 ft^2ac^{-1}) were removed. This thinning treatment was chosen to simulate a non-intensive operational first thinning treatment common to loblolly pine plantations.

5.3.2. Sampling simulator and samples

Tree attributes and coordinates generated by PTAEDA 4.1 were used when simulating forest sampling plans using the FMRC sampling simulator[4]. Since one plot per

[4] A copy of the user's guide for the sampling simulator is available upon request.

three acres in a commonly used sampling intensity for pine plantation timber inventory, 30 circular plots were randomly selected for each scenario. A plot size of 0.02 ha (20^{th} ac) or 0.01 ha (40^{th} ac) was used. 100 repeated samples were drawn from each basemap using the FMRC sampling simulator. CV of stand basal area among sample plots was calculated to quantify the magnitude of spatial heterogeneity for each basemap

5.3.3. Growth and yield projection and prediction

To analyze the effect of growth model choice, simulations were conducted with the three growth models: FASTLOB, TAUYIELD (Amateis et al. 2016), and PMRC 1996-1 (Harrison and Borders 1996) (denoted PMRC in the following). The three stand projection models are composed of a set of stand growth and yield equations, and all have been widely applied in the southeastern US. Sources for the model forms for estimating stand parameters evaluated are provided in Table 5-1.

Table 5-1. Model form sources utilized for projections

Model	Stand Parameter	Model Form Source
PMRC	H_d projection	Harrison and Borders (1996)
	SI prediction	Harrison and Borders (1996)
	Unthinned Basal Area Projection (G)	Harrison and Borders (1996)
	Basal Area Prediction (G)	Harrison and Borders (1996)
	Competition Index	Pienaar (1979)
	Thinned Basal Area Projection (G)	Pienaar (1979)
	Survival (N)	Harrison and Borders (1996)
	Volume (V)	Harrison and Borders (1996)
FASTLOB	H_d (or SI)	Bailey and Clutter (1974)
	Basal Area Projection (G)	Hasenauer et al. (1997)
	Survival (N)	Amateis et al. (1997)
	Volume (V)	$Y = b_0 + b_1 BA(HD)$
TAUYIELD	H_d (or SI)	Diéguez-Aranda et al. (2006)
	Basal Area Projection (G)	Amateis et al. (2016)
	Survival (N)	Gyawali and Burkhart (2014)
	Volume (V)	Amateis et al. (2016)

Dominant height, survival (i.e number of trees per unit area) and basal area were projected from age 10 to age 25 in the unthinned stands and from age 15 to age 25 in the thinned stands (thinning was implemented at age 15). Dominant height was defined as all trees in the top 80 percent of heights per plot. In the United States, the generally accepted definition of dominant height for estimating site index is the average height of dominant and codominant trees (Burkhart et al. 2019). Since crown class is not a tree attribute that is available in simulated stands used in this research, an alternative definition of average height of dominant and codominant trees was needed. An analysis of region-wide data from loblolly pine plantations in which crown class was assigned to all measured trees showed that the height of the top 80 percent of trees closely approximated the mean height of trees classified in the dominant or codominant crown class[5]. This definition was used when estimating site index from tree heights on simulated plots.

5.3.4. Stand-level and plot-level projections

The stand-level and plot-level projections were implemented as follows:

(1) For stand-level projection, initial stand conditions, which were averaged over all plots located in the same stand, were used for projection. That is, for a given stand

[5] Protocol for Computing Site Index for Loblolly Pine Plantations in the Tier I Data Sets in PINEMAP, unpublished project report

variable, a single average of the initial plot conditions was used to project the future growth and yield of a stand.

(2) For plot-level projection, each plot was treated as a "stand", and each "stand" was projected individually based on its own initial conditions. The stand parameters were then calculated by averaging the projected stand variables from all plots at future ages.

For example, thirty plots are sampled in a stand. For stand-level projection, the stand parameters are projected under the initial stand conditions, which are calculated by averaging over the thirty plots. For plot-level projection, stand parameter estimates on each plot are first projected followed by averaging of the thirty projected values to obtain the whole stand parameter estimate. At a given age, the projected average stand parameters are used to predict total yield.

The value of zero was assigned to all stand parameters for the plots with no sampled trees. A one percent per year constant rate of mortality was applied for the PMRC survival model when initial density was less than 247 stems per hectare (100 stems per acre). Bootstrapping one hundred repeated samples 1000 times was used to construct 95% confidence intervals of the projected stand variables for stand- and plot-level projections, respectively. For each scenario, stand- and plot-level projections were significantly different if the two 95% confidence intervals were not overlapping. This method of statistical hypothesis testing was chosen to provide flexibility in the interpretation of results. Due to the data being in the form of a paired series of projected sample distributions, it was decided that a confidence interval comparison between the two methods would effectively test for significant differences at each step of the projection period instead of a single test of statistical significance for the entire projection period.

For all models, sample unit size, and levels of spatial heterogeneity combinations, a ratio of the estimate projected at plot-level to the estimate projected at stand-level was calculated, and the mean of the ratios was computed by averaging over one hundred samples. If these values were determined to be statistically significantly different from 1 (non-overlapping confidence intervals). This implies that the stand-level projection strategy deviated significantly from the plot-level method.

Violin plots were constructed for each year of the projection period to compare the stand- and plot-level projections. The shape of the violin is a kernel-density plot fit around the sampling distribution. The 95% bootstrapped confidence intervals are plotted to indicate if the distributions are significantly different at each time interval. All projections, predictions and analyses were conducted in R (R Core Team 2013; Wickham 2009; Wickham 2011; Wickham et al. 2017; Wickham 2018).

5.4. Results and discussion

5.4.1. Impact of spatial heterogeneity on projections

Although the three models showed differences in predicted total volume between the two projection methods in varying degrees, the general trends of the impact of the four levels of spatial heterogeneity on total volume estimates are consistent among the models (see Figs. 5-2 and 5-3). In the homogeneous, consistent SI 21 m stand (basemap 1), total volume predicted by plot-level-projected variables is statistically similar to that predicted by stand-level-projected variables (ratio of means ~1.01-1.02); however, in the three stands with heterogeneity introduced, the predicted total volume between the two projection methods is noticeably different, especially for stands with systematically-distributed patches (basemaps 3 and 4). Ratio of means vary from ~1.04 -1.13 (see Table 5-2). This indicates that characteristics of stands, such as spatial arrangement, influence the stand volume prediction between the two methods of projection.

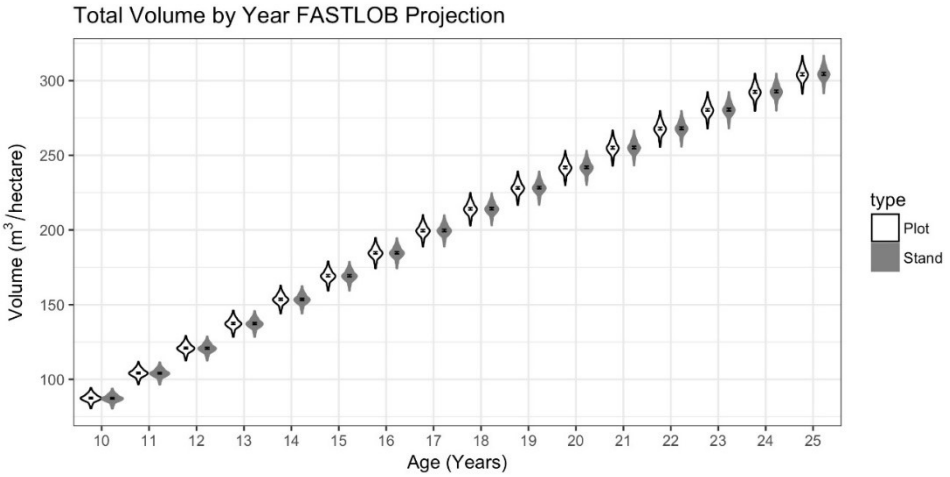

(a)

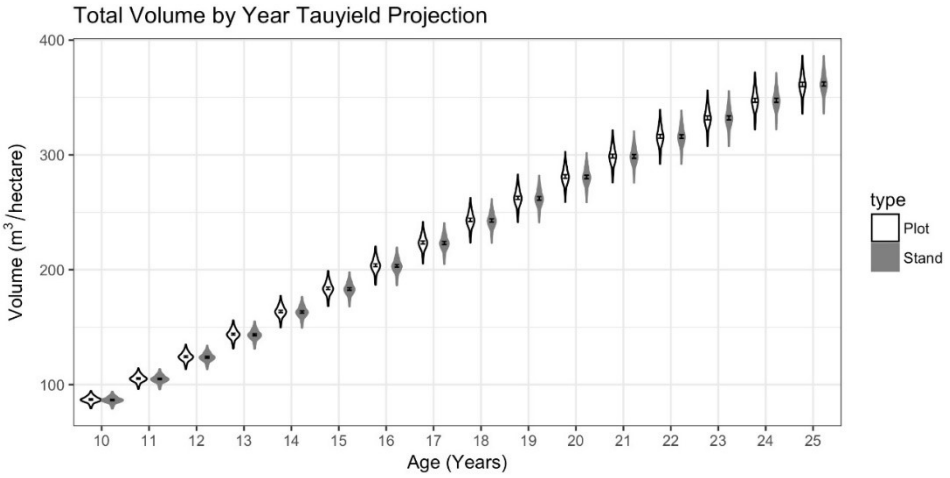

(b)

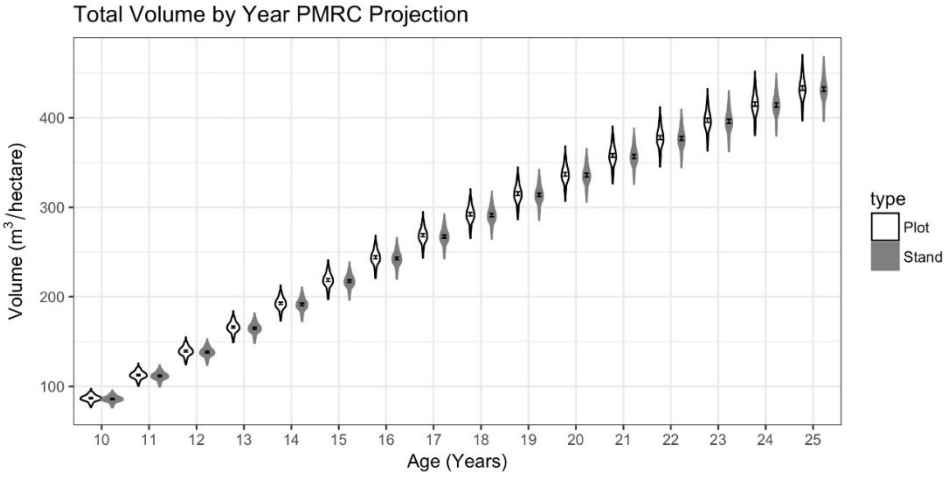

(c)

Figure 5-2. Pure SI 21.3 m (70 ft) base age 25 unthinned total volume projections for 0.02 ha sample plots and three projection models. Kernel density (violin plots) distributions of the repeated samples and 95% confidence intervals of the mean bars (inside of the violins). The projection type is indicated with the fill of the violins.

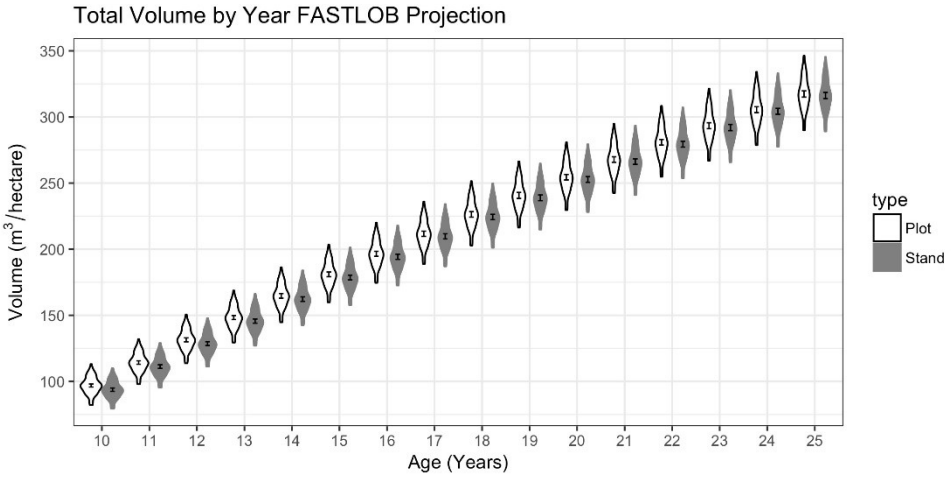

(a)

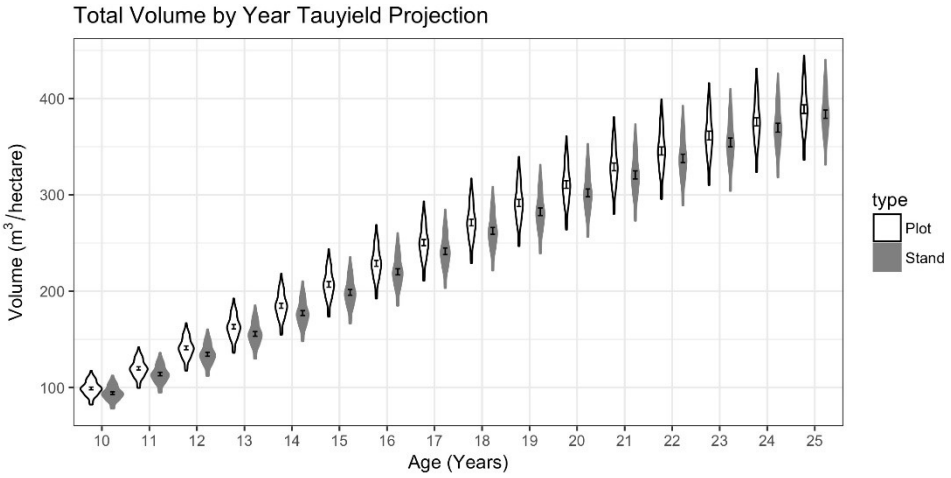

(b)

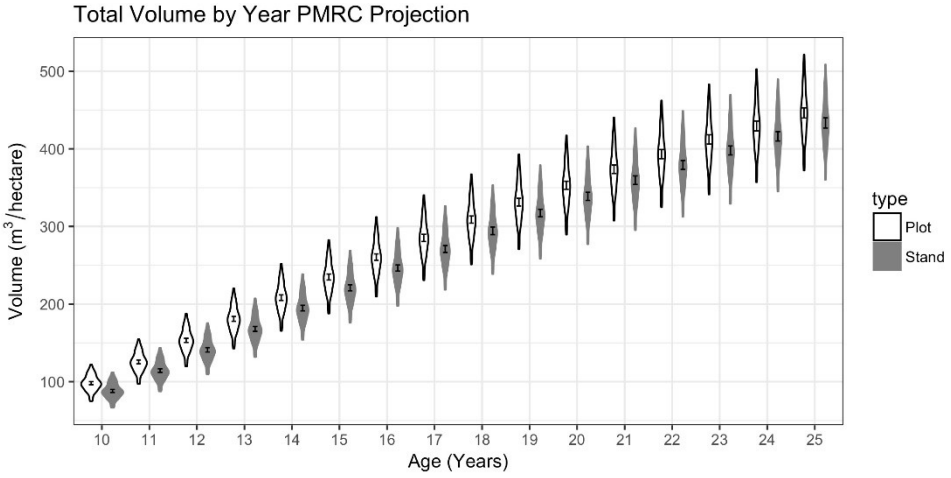

(c)

Figure 5-3. Even systematic SI 24.4 m (80 ft), 18.3 m (60 ft) base age 25 unthinned total volume projections for 0.02 ha sample plots and three projection models. Kernel density (violin plots) distributions of the repeated samples and 95% confidence intervals of the mean bars (inside of the violins). The projection type is indicated with the fill of the violins.

Table 5-2. Mean ratios between plot and stand level projections. Highlighted and bold values indicate the ratio is statistically significantly different from 1 at 95% confidence level.

Mean of ratios btwn plot and stand lv proj.			Dominant Ht.				No. of Trees				Basal Area				Total Vol.			
			Age				Age				Age				Age			
Basemap	Plot Size (ha)	Model	10	15	20	25	10	15	20	25	10	15	20	25	10	15	20	25
Stand 1	0.02	FAST.	1.00	1.00	1.00	1.00	1.00	1.00	1.00	1.00	1.00	1.00	1.00	1.00	1.01	1.00	1.00	1.00
		TAUY.	1.00	1.00	1.00	1.00	1.00	1.00	1.00	1.00	1.00	1.00	1.00	1.00	1.01	1.00	1.00	1.00
		PMRC	1.00	1.00	1.00	1.00	1.00	1.00	1.00	1.00	1.00	1.00	1.00	1.00	1.01	1.00	1.00	1.00
	0.01	FAST.	1.00	1.00	1.00	1.00	1.00	1.00	1.00	1.00	1.00	1.00	1.00	0.99	1.01	1.01	1.00	1.00
		TAUY.	1.00	1.00	1.00	1.00	1.00	1.00	1.00	1.00	1.00	1.00	1.00	1.00	1.01	1.01	1.00	1.00
		PMRC	1.00	1.00	1.00	1.00	1.00	1.00	1.00	1.00	1.00	1.00	1.00	1.00	1.02	1.01	1.01	1.00
Stand 2	0.02	FAST.	1.00	1.00	1.00	1.00	1.00	1.00	1.00	1.00	1.00	1.00	1.00	0.99	1.03	1.02	1.01	1.01
		TAUY.	1.00	1.00	1.00	1.00	1.00	1.00	1.00	1.00	1.00	1.00	1.00	0.99	1.03	1.02	1.01	1.01
		PMRC	1.00	1.00	1.00	1.00	1.00	1.00	1.00	1.00	1.00	1.00	1.00	1.00	**1.05**	**1.03**	1.02	1.01
	0.01	FAST.	1.00	1.00	1.00	1.00	1.00	1.00	1.00	1.00	1.00	1.00	1.00	0.99	1.03	1.02	1.01	1.01
		TAUY.	1.00	1.00	1.00	1.00	1.00	1.00	1.00	1.00	1.00	1.00	1.00	0.99	**1.03**	1.02	1.01	1.01
		PMRC	1.00	1.00	1.00	1.00	1.00	1.00	1.00	1.00	1.00	1.00	1.00	0.99	**1.06**	**1.04**	1.03	1.02
Stand 3	0.02	FAST.	1.00	1.00	1.00	1.00	1.00	1.00	1.00	1.00	1.00	1.00	1.00	0.99	**1.04**	1.03	1.02	1.01
		TAUY.	1.00	1.00	1.00	1.00	1.00	1.00	1.00	1.00	1.00	1.00	1.00	0.99	**1.04**	**1.03**	1.02	1.01
		PMRC	1.00	1.00	1.00	1.00	1.00	1.00	1.00	1.00	1.00	1.00	1.00	0.99	**1.08**	**1.04**	**1.03**	1.02
	0.01	FAST.	1.00	1.00	1.00	1.00	1.00	1.00	1.00	1.00	1.00	1.00	0.99	0.99	**1.04**	1.03	1.02	1.01
		TAUY.	1.00	1.00	1.00	1.00	1.00	1.00	1.00	1.00	1.00	1.00	0.99	**0.99**	**1.04**	**1.03**	1.02	1.01
		PMRC	1.00	1.00	1.00	1.00	1.00	1.00	1.00	1.00	1.00	1.00	0.99	0.99	**1.10**	**1.05**	**1.04**	**1.03**
Stand 4	0.02	FAST.	1.00	1.00	1.00	1.00	1.00	1.00	1.00	1.00	1.00	1.00	0.99	0.99	**1.06**	1.05	1.03	1.02
		TAUY.	1.00	1.00	1.00	1.00	1.00	1.00	1.00	1.00	1.00	1.00	0.99	**0.99**	**1.06**	**1.05**	**1.03**	1.02
		PMRC	1.00	1.00	1.00	1.00	1.00	1.00	1.00	1.00	1.00	1.00	0.99	0.99	**1.11**	**1.06**	**1.04**	**1.03**
	0.01	FAST.	1.00	1.00	1.00	1.00	1.00	1.00	1.00	1.00	1.00	1.00	0.99	0.98	**1.06**	1.05	1.03	1.02
		TAUY.	1.00	1.00	1.00	1.00	1.00	1.00	1.00	1.00	1.00	1.00	0.99	**0.98**	**1.06**	**1.05**	**1.03**	1.02
		PMRC	1.00	1.00	1.00	1.00	1.00	1.00	1.00	1.00	1.00	0.99	0.99	0.99	**1.13**	**1.07**	**1.05**	**1.04**

Often spatial heterogeneity is not considered when inventories are conducted at the stand level. That is, individual stands are not stratified by a measure of productivity such as site index. A goal of this study was to assess the impact of conducting and projecting a forest inventory under the common assumption that site index is homogeneous across a stand. In short, with the increase of stand variability the predicted total volume varies between plot- and stand-level projections. These results implied that it is necessary to consider stand variability following an inventory when projecting stand parameters. In this study, we were able to manipulate and control stand variability using the simulated plantations. The four basemaps represent four levels of spatial heterogeneity. The CV of basal area among the samples for each model is shown in Figure 5-4. As the CV increases, it is assumed that the stand is more heterogeneous in terms of productivity due to the strong correlation of loblolly pine basal area and volume. Calculating CV of stand basal area among sample plots as in this work or using remote sensing data as auxiliary information can be helpful for forest managers to assess stand variability in practice. If heterogeneity is determined to be severe enough to result in stand-level projections statistically deviating from the plot-level projection method, a stratified inventory, followed by stand-level projection, is an alternative method to reduce the magnitude of these differences in the projections.

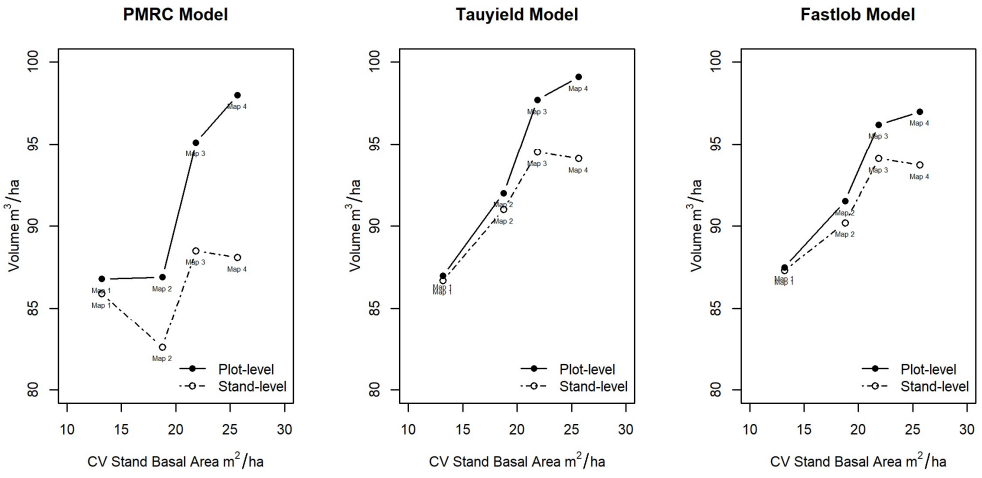

Figure 5-4. Comparison of predicted total volume at age 10 using samples. CV of stand basal area calculated from the 100 independent samples of 30 0.02 ha plots. (Map 1) Pure SI 21.3 m (70 ft), (Map 2) random, uneven SI 24.4 m (80 ft), 21.3 m (70 ft), and 18.3 m (60 ft) with more 21.3 m (70 ft), (Map 3) Even, systematic SI 24.4 m (80 ft), 21.3 m (70 ft), and 18.3 m (60 ft), and (Map 4) Even systematic SI 24.4 m (80 ft), 18.3 m (60 ft).

5.4.2. Impact of whole-stand growth and yield models

The three stand growth and yield models evaluated are commonly used in the southeastern United States for the management of loblolly pine. All three models were constructed with region-wide data and were designed with sensible biological constraints. Despite their similarities, the models have unique, non-linear forms. The different forms and levels of non-linearity affected the observed differences between the two projection strategies, especially for total volume. The difference between the mean of a nonlinear function and the function evaluated at the mean (Jensen's Inequality) has been studied extensively (e.g. Duursma and Robinson 2003), but growth and yield models consist of numerous interacting components of varying degrees of nonlinearity. Hence, analytical approximations of the overall model differences can become intractable. However, a useful empirical approximation of expected differences between the two estimation approaches may be obtained for a variety of stand conditions and models through a simulation approach. The FASTLOB model exhibited the fewest differences while the PMRC model exhibited both the largest and greatest number of significant differences (Table 5-2, Figures 5-2 and 5-3, supplemental figures 5-1 - 5-4). For example, in the most heterogeneous stand (basemap 4), the FASTLOB model ratio of means at age 10 was 1.06 while the PMRC model ranged from 1.11 – 1.13 at age 10. Due to the increased variability of parameter estimates from single plots, unusual conditions required exceptions to be made for certain components of the growth and yield models. Specifically, sample plots with no trees could not be projected. An exception was required so that the plots with no volume remained as part of the overall average. Additionally, the PMRC survival function required an initial density of at least 247 stems per hectare (100 stems per acre). Below this threshold, a constant rate of mortality had to be assumed according to the recommendation of the model developers. For this study, a one percent constant mortality rate was assumed; however, this value may not be valid under different circumstances.

5.4.3. Impact of sample unit size

In general, the two plot sizes evaluated in this study (0.02 and 0.01 hectares) resulted in similar trends in projected differences. The larger plot size did not alleviate

the significant differences found when using the stand level projections. The larger plot size did slightly decrease the difference in the values between the two projection methods in some instances (Table 5-2). However, significant differences occurred with both plot sizes. The PMRC model exhibited the greatest difference in the ratio of means (0.02) at age 10 for the stands with systematic heterogeneity. Due to the similarities, only results for the larger plot size (0.02 ha) are shown in Figures 2 and 3 and supplemental figures 5-1 - 5-4.

5.4.4. Impact of thinning on projections

The two basemaps with higher levels of heterogeneity (Figure 5-1c and 5-1d) were excluded from thinning treatments. Operationally, stands with these patterns and levels of heterogeneity would likely have separate thinning treatments applied at different ages. The thinning treatment imposed increased the CV of stand basal area from 11.48% to 22.01% in basemap 1 and increased the CV for basemap 2 from 18.77% to 29.66%. Despite the increase in variation after thinning, the difference in basal area CV between the stands remained similar. While thinning dramatically altered the stand conditions, the basemaps with thinning imposed exhibited non-significant differences between the two projection methods as compared with the unthinned counterparts (Supplementary Figures 5-3 and 5-4). Due to the lack of significant differences in the projection period as seen from the confidence interval bars, mean ratios are not presented for the thinning treatments.

5.4.5. Further discussion

Aggregation error has been studied extensively in ecological literature (e.g. Cale et al. 1983; Iwasa et al. 1987; Ruel and Ayres 1999). However, to the best of our knowledge, there has been little research into this topic for the aggregation and projection of plantation pine inventory data. As with the aggregation study by Moeur and Ek (1981), differences were noted with stand-level aggregation projections compared to plot-level projections. This study demonstrated that as spatial heterogeneity increased, the differences between the two aggregation strategies increased as indicated by Jensen's Inequality for all three models, especially for total volume. Other parameters including height, stems per hectare, and in most cases basal area, were not significantly different.

This is likely due to these parameters being first estimated directly from the sample data, followed by projection. The initial condition at each subsequent age for stand volume was predicted. The non-linear models used to predict volume produced significantly different estimates depending on the aggregation strategy utilized. Figure 5-4 demonstrates that the differences of volume predicted at age 10 volume following sampling increases as the CV of basal area increases for all models. Despite the differences, both the stand- and plot-level projection methods have advantages and disadvantages. Stand-level projection is more computationally efficient, but it is not unbiased for non-linear model forms and the bias becomes larger with higher levels of stand heterogeneity. Plot-level projection preserves more information concerning variance, but it is more computationally intensive and more subject to issues such as model limitations. Unlike Moeur and Ek (1981), this study utilized simulated stands and samples. The use of simulated data allowed for known stand establishment parameters, control over levels of heterogeneity, control over thinning treatments, and repeated sampling with different sample plot sizes. While the basemaps generated in PTAEDA and the samples drawn with the sample simulator are not "real" data, they are representative of common conditions. It is important to mention that this study is not comparing projected inventories to known population parameters. PTAEDA basemaps are "established" with known parameters and then sampled using a sample simulator. These samples are then projected to future dates and compared against each other, not the basemap. If the projected values were compared to a projected basemap, this would involve comparing the three whole-stand models to another model projection, that of the PTAEDA simulator. The objective of the study was to evaluate the magnitude of differences between the two aggregation-projection strategies, not compare the effectiveness of model forms to estimate overall population parameters at specified points in stand development. These maps, in conjunction with the sampling simulator, provide a means to assess sample projection questions such as those in this study. The four stand parameters considered are commonly utilized for management decisions. Of these values, total volume is often of greatest interest as it is most correlated with important characteristics such as monetary value or biomass.

5.5. Conclusions

In summary, stand spatial heterogeneity and the growth and yield model used made noticeable impacts on the differences of predicted total volume in two projection methods. The general trends of predicted total volume over time in the two projection methods were similar among the three models across four basemaps. In this study, however, plot size and thinning treatment did little to affect the patterns of observed differences.

Except for total volume and in several cases basal area, the projected stand parameters in stand- and plot-level projections are not statistically different. Either projection method can be used interchangeably to estimate future growth and yield when spatial heterogeneity is not severe. The difficulties, such as the definition of dominant height and no tally plots, need to be addressed when implementing plot-level projections.

The results of this work should provide guidance for forest managers who regularly conduct and project forest inventories at the whole stand level. Carefully evaluating the growth and yield systems and their performance under differing levels of spatial heterogeneity before applying projection is recommended.

5.6. References

Amateis, R.L. and Burkhart, H.E., 2016. Simulating the effects of site index variation within loblolly pine plantations using an individual tree growth and yield model. In Proceedings of the 18th Biennial Southern Silvicultural Research Conference. Knoxville, TN., 2-5 March 2015. *Edited by* Callie Jo Schweitzer, Wayne K. Clatterbuck, and Christopher M. Oswalt, USDA Forest Service e-Gen. Tech. Report SRS-212, pp. 245-251.

Amateis, R.L., Burkhart, H.E. and Liu, J., 1997. Modeling survival in juvenile and mature loblolly pine plantations. For. Ecol. and Manage. 90(1), 51-58.

Amateis, R.L., Radtke, P.J. and Burkhart, H.E., 2016. TAUYIELD: a stand-level growth and yield model for thinned and unthinned loblolly pine plantations. Version 3.0. Dep. For. Res. Env. Cons. Virginia Tech. Available online: https://www.fmrc.frec.vt.edu/documents/TAUYIELD3.0.pdf.

Bailey, R.L. and Clutter, J.L., 1974. Base-age invariant polymorphic site curves. For. Sci. 20(2), 155-159.

Burkhart, H.E., Avery, T.E. and Bullock, B.P., 2019. Forest measurements 6th ed. Waveland Press. pp 434.

Burkhart, H.E. and Tomé, M., 2012. Modeling forest trees and stands. Springer, Dordrecht, Netherlands. pp. 457.

Cale, W.G., O'Neill, R.V. and Gardner, R.H. 1983. Aggregation error in nonlinear ecological models. J. of Theor. Biol. 100(3), 539-550.

Clutter, J.L., Fortson, J.C., Pienaar, L.V., Brister, G.H. and Bailey, R.L. 1983. Timber management a quantitative approach. Krieger Publishing Company, Malabar, FL. pp. 88-139.

Daniels, R.F. and Burkhart, H.E. 1975. Simulation of individual tree growth and stand development in managed loblolly pine plantations. Div For. & Wildl. Res., Va. Polytech. Inst. and State Univ. Publ. FWS-5-75. pp. 69.

Diéguez-Aranda, U., Burkhart, H.E. and Amateis, R.L., 2006. Dynamic site model for loblolly pine (Pinus taeda L.) plantations in the United States. For. Sci. 52(3), 262-272.

Duursma, R.A. and Robinson, A.P., 2003. Bias in the mean tree model as a consequence of Jensen's inequality. For. Ecol. and Manage. 186(1-3), 373-380.

Gyawali, N. and Burkhart, H.E., 2014. General response functions to silvicultural treatments in loblolly pine plantations. Can. J. For. Res. 45(3), 252-265.

Harrison, W.M. and Borders, B.E. 1996. Yield prediction and growth projection for site-prepared loblolly pine plantations in the Carolinas, Georgia, Alabama, and Florida. Plantation Management Research Cooperative Tech. Rep. University of Georgia. Athens, GA, USA. Available online: http://pmrc.uga.edu/TR1996-1.pdf

Hasenauer, H., Burkhart, H.E. and Amateis, R.L, 1997. Basal area development in thinned and unthinned loblolly pine plantations. Can. J. For. Res. 27(2), 265-271.

Hou, Z., Xu, Q., Hartikainen, S., Antilla, P., Packalen, T., Maltamo, M. and Tokola, T. 2015. Impact of plot size and spatial pattern of forest attributes on sampling efficacy. For. Sci. 61(5): 847-860. doi: https://doi.org/10.5849/forsci.14-197

Iwasa, Y., Andreasen, V. and Levin, S., 1987. Aggregation in model ecosystems. I. Perfect aggregation. Ecological Modelling. 37(3-4), 287-302.

Jensen, J.L.W.V., 1906. Sur les fonctions convexes et les inégalités entre les valeurs moyennes. Acta mathematica. 30(1), 175-193. (In French)

Li, H. and Reynolds, J.F., 1994. A simulation experiment to quantify spatial heterogeneity in categorical maps. Ecology, 75(8), 2446-2455.

Moeur, M. and Ek, A.R., 1981. Plot, stand, and cover-type aggregation effects on projections with an individual tree based stand growth model. Can. J. For. Res. 11(2), 309-315.

Pienaar, L.V., 1979. An approximation of basal area growth after thinning based on growth in unthinned plantations. For. Sci. 25(2), 223-232.

R Core Team 2013. R: A language and environment for statistical computing. R Foundation for Statistical Computing, Vienna, Austria. URL http://www.R-project.org/.

Ruel, J.J. and Ayres, M.P., 1999. Jensen's inequality predicts effects of environmental variation. Trends Ecol. Evol. 14(9), 361-366.

Shiver, B.D. and Borders, B.E., 1996. Sampling techniques for forest resource inventory. John Wiley & Sons, Inc. New York. pp. 356.

Smith, J.L. and Burkhart, H.E., 1984. A simulation study assessing the effect of sampling for predictor variable values on estimates of yield. Can. J. For. Res. 14(3), 326-330.

Wickham, H., 2009. ggplot2: Elegant Graphics for Data Analysis. Springer-Verlag: New York, NY, USA.

Wickham, H., 2011. The split-apply-combine strategy for data analysis. J. Stat. 40(1), 1-29.

Wickham, H., 2018. stringr: simple, consistent wrappers for common string operations. R package version 1.3.0. https://CRAN.R-project.org/package=stringr

Wickham, H., Francois, R., Henry, L. and Müller, K., 2017. dplyr: a grammar of data manipulation. R package version 0.7.4. https://CRAN.R-project.org/package=dplyr

5.7. Supplemental Figures

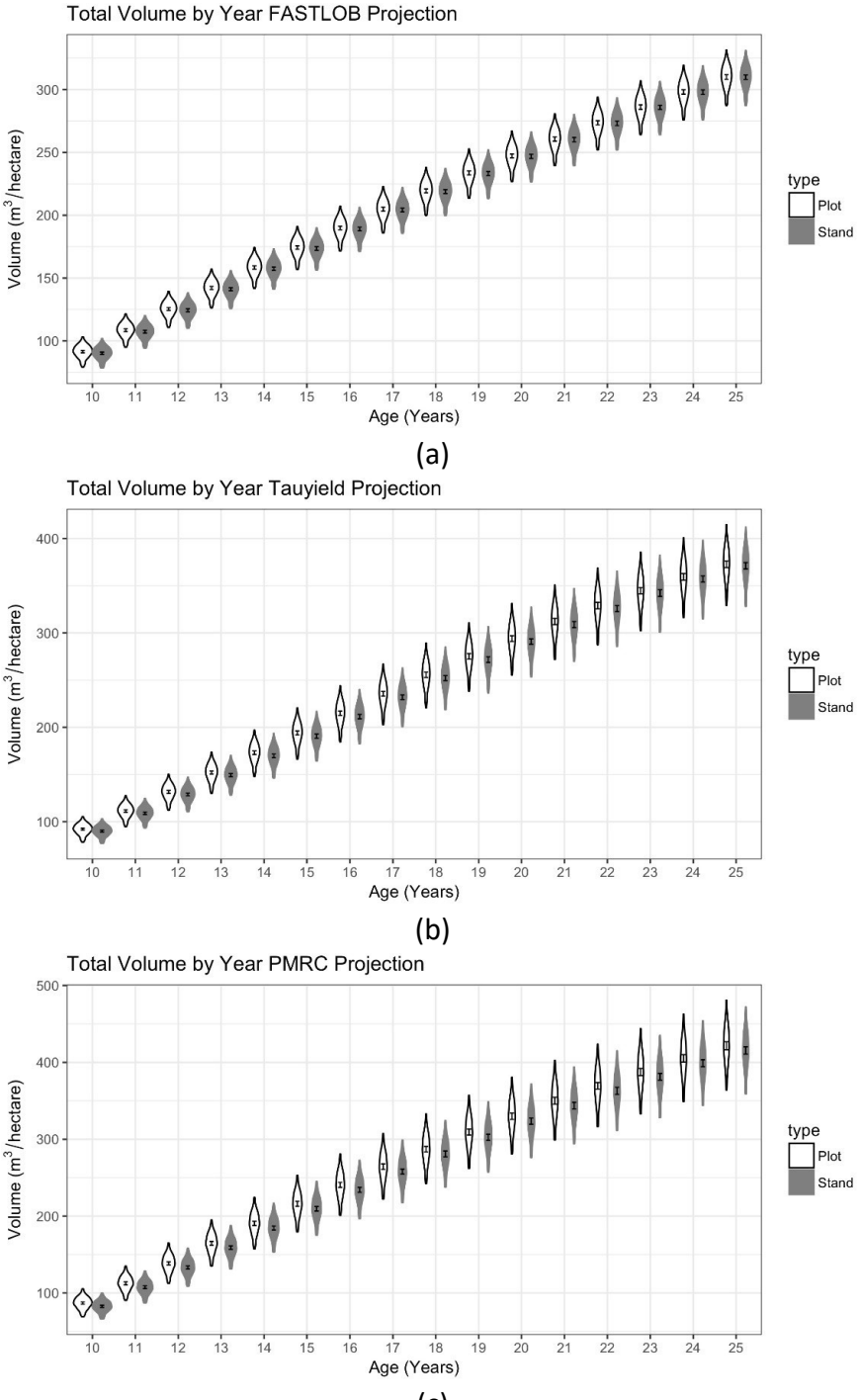

Supplemental Figure 5-1. Uneven random SI 24.4 m (80 ft), 21.3 m (70 ft), 18.3 m (60 ft) more 21.3 m (70 ft) base age 25 unthinned total volume projections for 0.02 ha sample plots and three projection models. Kernel density (violin plots) distributions of the repeated samples and 95% confidence bars (inside of the violins). The projection type is indicated with the fill of the violins.

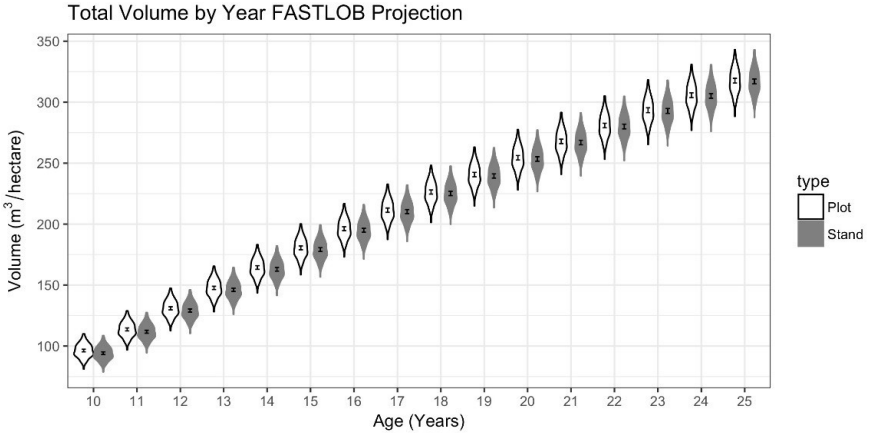

(a)

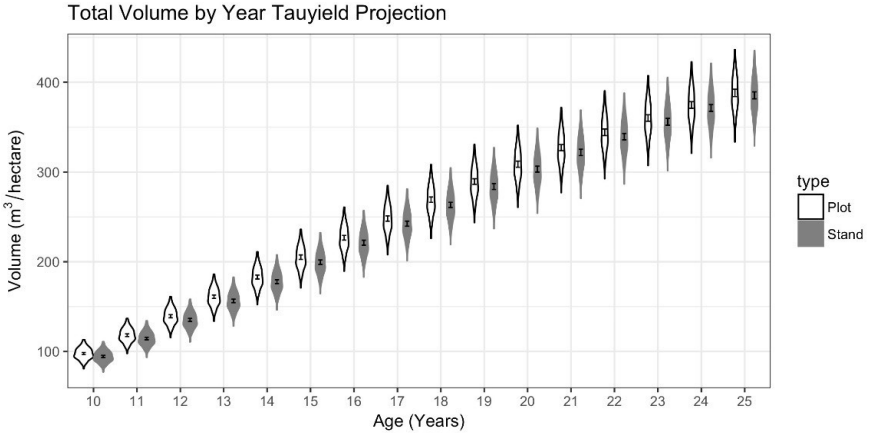

(b)

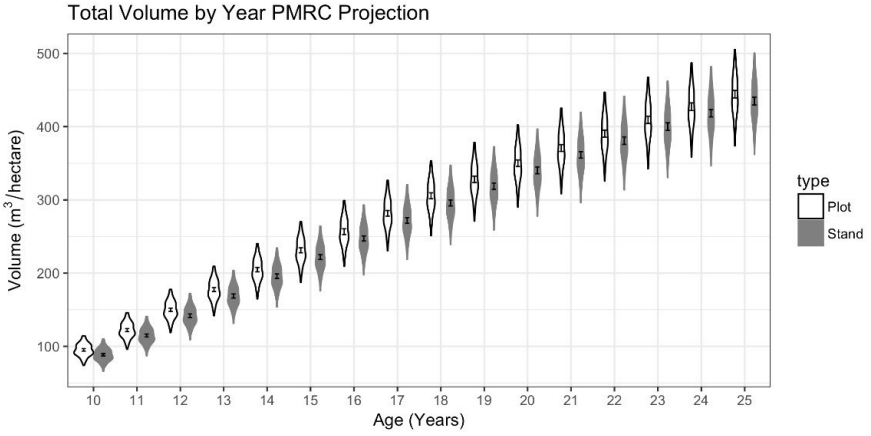

(c)

Supplemental Figure 5-2. Even systematic SI 24.4 m (80 ft), 21.3 m (70 ft), 18.3 m (60 ft) base age 25 unthinned total volume projections for 0.02 ha sample plots and three projection models. Kernel density (violin plots) distributions of the repeated samples and 95% confidence bars (inside of the violins). The projection type is indicated with the fill of the violins.

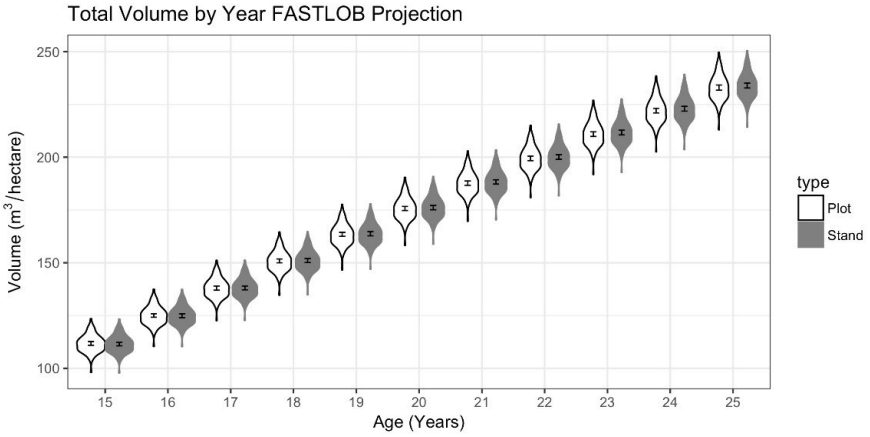

(a)

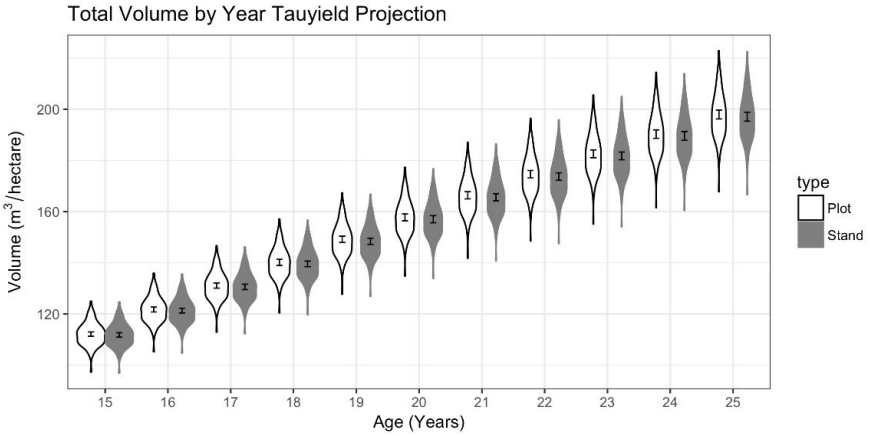

(b)

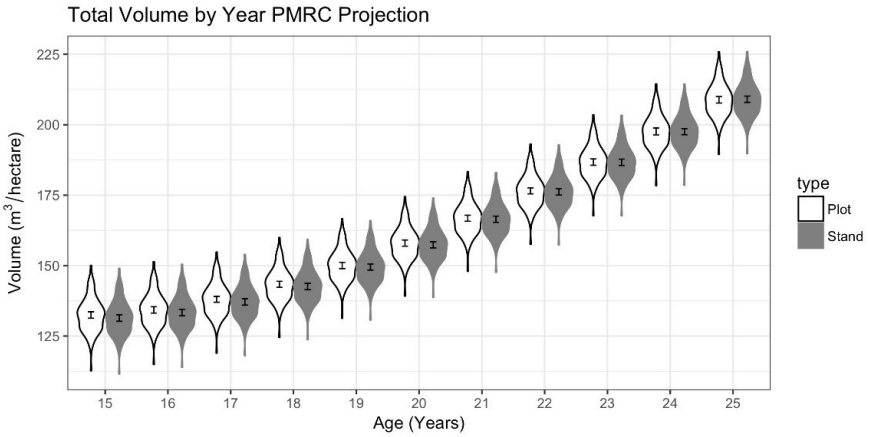

(c)

Supplemental Figure 5-3. Pure SI 21.3 m (70 ft) base age 25 thinned total volume projections for 0.02 ha sample plots and three projection models. Kernel density (violin plots) distributions of the repeated samples and 95% confidence bars (inside of the violins). The projection type is indicated with the fill of the violins.

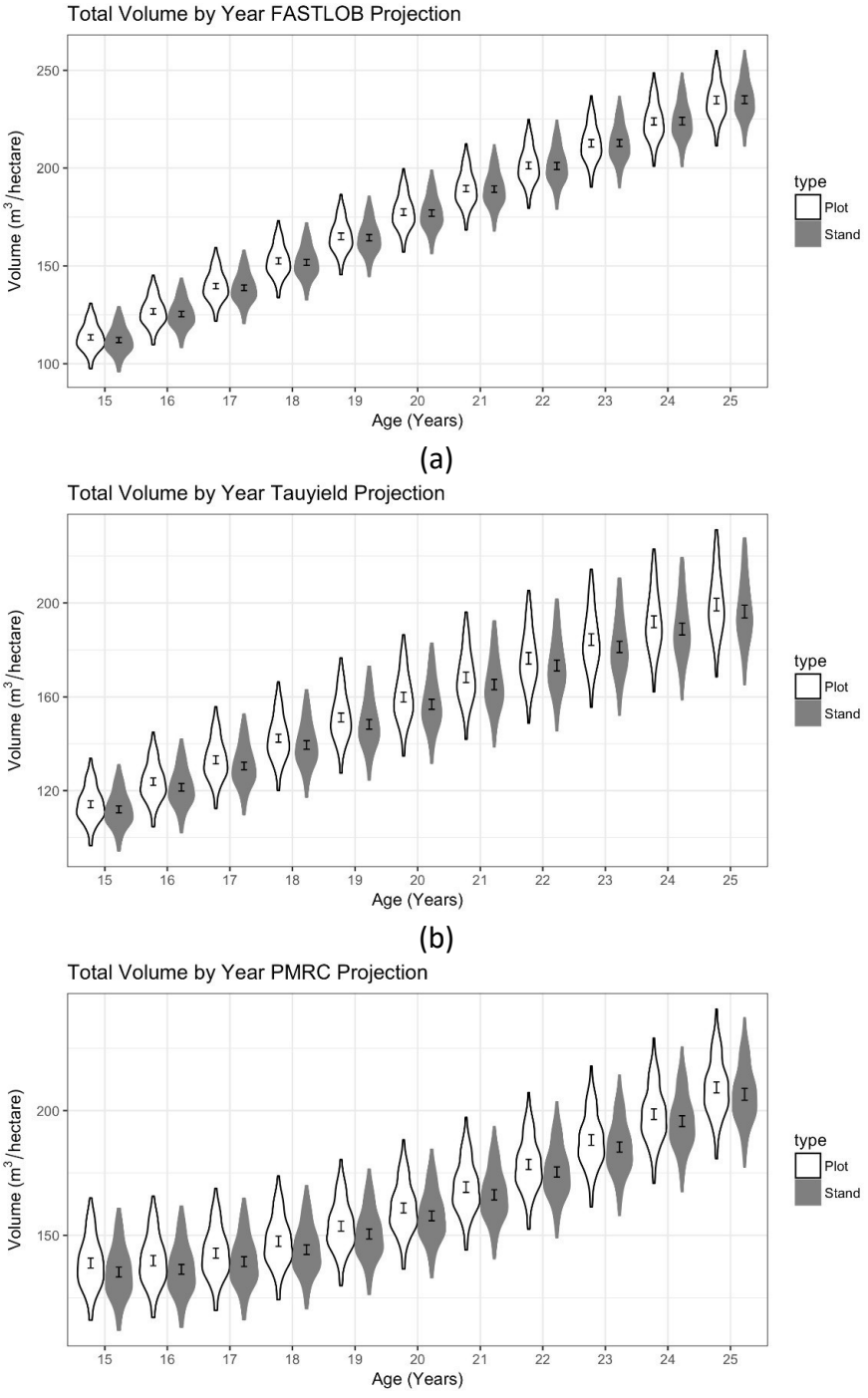

Supplemental Figure 5-4. Uneven random SI 24.4 m (80 ft), 21.3 m (70 ft), 18.3 m (60 ft) more 21.3 (70 ft) base age 25 thinned total volume projections for 0.02 ha sample plots and three projection models. Kernel density (violin plots) distributions of the repeated samples and 95% confidence bars (inside of the violins). The projection type is indicated with the fill of the violins.

Chapter 6 Summary

The results of this work are applicable to those who conduct forest resource assessments and use inventory data to make future predictions and projections of stand conditions. In summary, auxiliary data has broad potential to enhance forest inventory across many of the conditions evaluated. Further, the way in which inventory data are aggregated and used to make future assessments can significantly differ in stands with high levels of spatial heterogeneity. A brief summary of each research objective outlined in the introduction is given below.

1) Unmanned aircraft system (UAS) imagery was found to be unreliable for use in loblolly pine regeneration surveys. While the automated detection methods performed well in some cases, significant natural regeneration, issues with image quality, and inadequate sensors limited the success of the methods evaluated. Recommendations for future studies include the use of cameras with a near infrared band and aircraft GPS capable of real time kinematic positioning for higher location accuracy. Additionally, large visible targets should be installed on all validation sample locations.
2) Using lidar and stand thinning status as auxiliary data, both area and unit-level small area estimation (SAE) models demonstrated potential to improve total volume estimate precision across the conditions evaluated. Area-level methods were found to provide reliable increases in precision and were more broadly applicable than unit-level models.
3) Lidar point cloud density and elevation model spatial resolution had minimal effects on estimates and estimate precision with the area-level SAE models evaluated. In the conditions evaluated, estimates of stand density from lidar were found to provide minimal improvements when incorporated in the SAE models. Finally, the SAE models were found to provide reliable improvements in precision across many repeated samples.
4) Plot and stand-level aggregation strategies resulted in similar estimates of dominant height, stem density, basal area, and total volume for simulate stands with low levels of spatial heterogeneity. At higher levels of spatial heterogeneity,

differences in total volume predictions were significant. Significant differences were noted between model form while plot size and thinning status had minimal effects.

There is opportunity to expand this work in future research. Seedling detection with UAS has the potential to improve using improved aircrafts, cameras, and image processing techniques. New streams of remotely sensed data such as USDA National Agriculture Imagery Program (U.S. Department of Agriculture 2018) imagery and NASA ICESat-2 (NASA 2019) global elevation products have the potential to be used with similar SAE techniques across broad spatial scales. Additionally, the use of SAE for improving the precision of diameter distribution estimation is of interest to growers who require accurate stand tables for management decisions. Finally, the effects of aggregation strategy on stand table projection have yet to be fully explored.

6.1. References

National Aeronautics and Space Administration, Ice, Cloud, and Land Elevation Sattellite-2. Information available online at https://icesat-2.gsfc.nasa.gov/. Last accessed 9/7/2019

U.S. Department of Agriculture, Farm Service Agency. Information available online at https://www.fsa.usda.gov/programs-and-services/aerial-photography/imagery-programs/naip-imagery/index. Last accessed 9/7/2019